National Library of Canada
Canadian Theses Service
Ottawa, Canada
K1A 0N4

Bibliothèque nationale du Canada
Services des thèses canadiennes

CANADIAN THESES

THÈSES CANADIENNES

NOTICE

The quality of this microfiche is heavily dependent upon the quality of the original thesis submitted for microfilming. Every effort has been made to ensure the highest quality of reproduction possible.

If pages are missing, contact the university which granted the degree.

Some pages may have indistinct print especially if the original pages were typed with a poor typewriter ribbon or if the university sent us an inferior photocopy.

Previously copyrighted materials (journal articles, published tests, etc.) are not filmed.

Reproduction in full or in part of this film is governed by the Canadian Copyright Act, R.S.C. 1970, c. C-30. Please read the authorization forms which accompany this thesis.

AVIS

La qualité de cette microfiche dépend grandement de la qualité de la thèse soumise au microfilmage. Nous avons tout fait pour assurer une qualité supérieure de reproduction.

S'il manque des pages, veuillez communiquer avec l'université qui a conféré le grade.

La qualité d'impression de certaines pages peut laisser à désirer, surtout si les pages originales ont été dactylographiées à l'aide d'un ruban usé ou si l'université nous a fait parvenir une photocopie de qualité inférieure.

Les documents qui font déjà l'objet d'un droit d'auteur (articles de revue, examens publiés, etc.) ne sont pas microfilmés.

La reproduction, même partielle, de ce microfilm est soumise à la Loi canadienne sur le droit d'auteur, SRC 1970, c. C-30. Veuillez prendre connaissance des formules d'autorisation qui accompagnent cette thèse.

THIS DISSERTATION
HAS BEEN MICROFILMED
EXACTLY AS RECEIVED

LA THÈSE A ÉTÉ
MICROFILMÉE TELLE QUE
NOUS L'AVONS REÇUE

NL 339 (r. 86/01)

Canada

204

0-315-26935-9

National Library of Canada
Canadian Theses Division
Ottawa, Canada
K1A 0N4

Bibliothèque nationale du Canada
Division des thèses canadiennes

PERMISSION TO MICROFILM — AUTORISATION DE MICROFILMER

• Please print or type — Écrire en lettres moulées ou dactylographier

Full Name of Author — Nom complet de l'auteur

DHIRAJ LAL

Date of Birth — Date de naissance	Country of Birth — Lieu de naissance
28 AUGUST 1947	FIJI

Permanent Address — Résidence fixe

8109 - 27 AVENUE
EDMONTON, ALTA
T6K 3C9

Title of Thesis — Titre de la thèse

SOLUBILITY OF GASES IN HEAVY OILS

University — Université

UNIVERTY OF ALBERTA

Degree for which thesis was presented — Grade pour lequel cette thèse fut présentée

MASTER OF SCIENCE IN CHEMICAL ENGINEERING

Year this degree conferred — Année d'obtention de ce grade	Name of Supervisor — Nom du directeur de thèse
1983	DR. F. D. OTTO

Permission is hereby granted to the NATIONAL LIBRARY OF CANADA to microfilm this thesis and to lend or sell copies of the film.

The author reserves other publication rights, and neither the thesis nor extensive extracts from it may be printed or otherwise reproduced without the author's written permission.

L'autorisation est, par la présente, accordée à la BIBLIOTHÈQUE NATIONALE DU CANADA de microfilmer cette thèse et de prêter ou de vendre des exemplaires du film.

L'auteur se réserve les autres droits de publication; ni la thèse ni de longs extraits de celle-ci ne doivent être imprimés ou autrement reproduits sans l'autorisation écrite de l'auteur.

Date	Signature
25 APRIL 1983	Dhiraj Lal

NL-91 (4/77)

THE UNIVERSITY OF ALBERTA

SOLUBILITY OF GASES IN HEAVY OILS

by

(C) DHIRAJ LAL

A THESIS

SUBMITTED TO THE FACULTY OF GRADUATE STUDIES AND RESEARCH

IN PARTIAL FULFILMENT OF THE REQUIREMENTS FOR THE DEGREE

OF MASTER OF SCIENCE

IN

CHEMICAL ENGINEERING

DEPARTMENT OF CHEMICAL ENGINEERING

EDMONTON, ALBERTA

FALL 1983

THE UNIVERSITY OF ALBERTA

RELEASE FORM

NAME OF AUTHOR DHIRAJ LAL

TITLE OF THESIS SOLUBILITY OF GASES IN HEAVY OILS

DEGREE FOR WHICH THESIS WAS PRESENTED MASTER OF SCIENCE

YEAR THIS DEGREE GRANTED FALL 1983

Permission is hereby granted to THE UNIVERSITY OF ALBERTA LIBRARY to reproduce single copies of this thesis and to lend or sell such copies for private, scholarly or scientific research purposes only.

The author reserves other publication rights, and neither the thesis nor extensive extracts from it may be printed or otherwise reproduced without the author's written permission.

(SIGNED) Dhiraj Lal

PERMANENT ADDRESS:

8109 - 27 Avenue

Edmonton, Alberta

T6K 3C9 CANADA

DATED April 20 1983

THE UNIVERSITY OF ALBERTA

FACULTY OF GRADUATE STUDIES AND RESEARCH

The undersigned certify that they have read, and recommend to the Faculty of Graduate Studies and Research, for acceptance, a thesis entitled SOLUBILITY OF GASES IN HEAVY OILS submitted by DHIRAJ LAL in partial fulfilment of the requirements for the degree of MASTER OF SCIENCE in CHEMICAL ENGINEERING.

.....

Supervisor

.....

.....

Date.....April 20/83.....

Abstract

The solubility of hydrogen in heavy hydrocarbons and coal-heavy oil slurries was measured using a batch autoclave. The solvents ranged from a hydrocracked gas oil product of molecular weight 250 to heavy bitumen residues of molecular weights above 800. The experiments were conducted mainly at 200° and 300°C, and pressures up to 24.8 MPa. Limited carbon dioxide and hydrogen sulphide solubility measurements were also made.

The prediction and correlation of the solubility data by the Peng-Robinson equation and the Grayson-Streed method were attempted. The best result for the correlation of hydrogen solubility data was obtained with the use of either a modified Peng-Robinson or Soave-Redlich-Kwong equation of state.

Acknowledgements

I wish to thank Drs. F.D. Otto and A.E. Mather for their assistance, advice and encouragement given during the course of this work. I would also like to thank the Federal Department of Energy, Mines and Resources who provided financial support and supplied the oil, coal samples and Hempel Distillation data used.

Table of Contents

Chapter	Page
Abstract	iv
Acknowledgements	v
List of Figures	viii
List of Tables	xi
Nomenclature	xiv
1. Introduction	1
2. Literature Survey	6
2.1 Theory	6
2.2 Experimental Techniques	8
2.3 Correlation	17
2.3.1 Grayson-Streed	21
2.3.2 Soave-Redlich-Kwong Method	24
2.3.3 Penn-State-Soave Method	26
2.3.4 Peng-Robinson	28
2.3.5 Modified Soave-Redlich-Kwong	31
2.4 Characterization of Mixtures	32
2.4.1 Cavett Method	35
2.4.2 API Data Book Method	36
2.4.3 PNA Analysis	37
3. Solubility Experiments	40
3.1 Reagents and Materials	40
3.2 Experimental Procedure	41
4. Results and Discussion	50
4.1 Solubility of Hydrogen in Bitumens	50
4.2 Solubility of Hydrogen in Slurries	65

4.3 Solubility of H_2S and CO_2 in Bitumens 72

5. Correlation and Fraction Characterization 79

5.1 Results and Discussion 79

5.1.1 Modified Soave-Redlich-Kwong Method 80

5.1.2 Peng-Robinson Method 87

5.1.3 Grayson-Streed Method 97

5.1.4 Correlation of CO_2 and H_2S Systems 98

5.1.5 Fraction Characterization 105

6. Summary and Conclusions 108

7. References 110

8. Appendix I 116

9. Appendix II 145

10. Appendix III 160

List of Figures

No.		page
1	Schematic Diagram of Canmet Pilot Plant	3
2	Schematic Diagram of the Apparatus	48
3	H_2 Solubility in Mesitylene at 204°C	52
4	Solubility of H_2 in Athabasca Bitumen	53
5	Solubility of H_2 in Cold Lake Bitumen	54
6	Solubility of H_2 in Lloydminster Residue	55
7	Solubility of H_2 in 650°F+ Topped Athabasca Bitumen	56
8	Solubility of H_2 in 800°F+ Topped Athabasca Bitumen	57
9	Solubility of H_2 in 650°F+ Topped Cold Lake Bitumen	58
10	Solubility of H_2 in 800°F+ Topped Cold Lake Bitumen	59
11	Solubility of H_2 in Lloydminster Residues	60
12	Solubility of H_2 in Amoco Feed	61
13	Solubility of H_2 in 60% Conversion Heavy End	62
14	Solubility of H_2 in 74.7% Conversion Heavy End	63
15	Solubility of H_2 in 84.3% Conversion Heavy End	64
16	Effect of Solvent Molecular Weight on Apparent Henry's Constant	67
17	Hydrogen Solubility in 10 wt % Sub-Bituminous Coal/Bitumen Slurry	68
18	Hydrogen Solubility in 40 wt % Sub-Bituminous Coal/Bitumen Slurry	69

19	Hydrogen Solubility in 40 wt % Lignite Coal/Bitumen Slurry	70
20	Hydrogen Solubility in 25 wt % Sub-Bituminous Coal/Bitumen Slurry	71
21	Solubility of H_2S in Athabasca Bitumen	74
22	Solubility of H_2S in 84.3% Conversion Heavy End	75
23	Solubility of H_2S in EMR Gas Oil	76
24	Solubility of CO_2 in Athabasca Bitumen	77
25	Solubility of CO_2 in EMR Gas Oil	78
26	Hydrogen K-Value vs Pressure for Bicyclohexyl (Sebastian et al. (56))	82
27	Hydrogen K-Value vs Pressure for Bicyclohexyl (Sebastian et al. (56))	89
28	Hydrogen K-Value vs Pressure for Athabasca Bitumen	93
29	Hydrogen K-Value vs Pressure for EMR Gas Oil	94
30	Binary Parameter E_{Hj} in Modified Peng-Robinson Equation of State	95
31	Hydrogen K-Value vs Pressure for Bicyclohexyl (Sebastian et al. (56))	96
32	Carbon Dioxide K-Value vs Pressure for Tetralin (Sebastian et al. (57))	100
33	Carbon Dioxide K-Value vs Pressure for Athabasca Bitumen	101
34	Carbon Dioxide K-Value vs Pressure for EMR Gas Oil	102

35 Hydrogen Sulphide K-Value vs Pressure for Athabasca Bitumen 103

36 Hydrogen Sulphide K-Value vs Pressure for EMR Gas Oil 104

List of Tables

Table		Page
1	Properties of Components Required for PR, SRK and Grayson-Streed Methods	33
2	Properties of Cold Lake Bitumen and Conventional Oil	42
3	Properties of Athabasca Bitumen	43
4	Properties of Lloydminster Residue and Amoco Feed	44
5	Boiling Point Distribution for Topped Athabasca Bitumen (2-AB-77)	45
6	Boiling Point Distribution for Lloydminster Residue (3-LL-78)	45
7	Boiling Point Distribution for Amoco Feed	45
8	Molecular Weights of Selected Solvents	46
9	Effect of Molecular Weights on Apparent Henry's Constants	66
10	Interaction Parameters Required in PR, Modified PR and Modified SRK Methods	83
11	Comparison of Absolute Average Deviations	85
12	Solubility of H_2 in Mesitylene	117
13	Solubility of H_2 in Athabasca Bitumen (4-AB-77)	118
14	Solubility of H_2 in Cold Lake Bitumen (1-CL-37)	120
15	Solubility of H_2 in Lloydminster Residue (3-LL-77)	121
16	Solubility of H_2 in 650°F+ Topped Athabasca Bitumen (2-AB-77)	122

17	Solubility of H_2 in 800°F+ Topped Athabasca Bitumen (36-1)	123
18	Solubility of H_2 in 650°F+ Topped Cold Lake Bitumen (37-1)	124
19	Solubility of H_2 in 800°F+ Topped Cold Lake Bitumen (6-CL-77)	125
20	Solubility of H_2 in 650°F+ Lloydminster Residue (3-LL-78)	126
21	Solubility of H_2 in 760°F+ Lloydminster Residue (1-LL-78)	127
22	Solubility of H_2 in Amoco Feed (4-AM-78)	128
23	Solubility of H_2 in EMR Gas Oil	129
24	Solubility of H_2 in Heavy Ends (91-1-1)	130
25	Solubility of H_2 in Heavy Ends (78-T-22)	131
26	Solubility of H_2 in Heavy Ends (78-T-23)	132
27	Solubility of H_2 in Heavy Ends (78-T-24)	133
28	Solubility of H_2 in Coal/Bitumen Slurry	134
29	Solubility of H_2 in Coal/Bitumen Slurry	135
30	Solubility of H_2 in Coal/Bitumen Slurry	137
31	Solubility of H_2 in Coal/Bitumen Slurry	138
32	Solubility of H_2S in Athabasca Bitumen (4-AB-77)	139
33	Solubility of H_2S in Heavy Ends (78-T-24)	141
34	Solubility of H_2S in EMR Gas Oil	142
35	Solubility of CO_2 in Athabasca Bitumen (4-AB-77)	143
36	Solubility of CO_2 in EMR Gas Oil	144

37	Vapor-Liquid Equilibrium Data for H_2-Bicyclohexyl (56)	146
38	Vapor-Liquid Equilibrium Data for H_2-Bicyclohexyl (56)	147
39	Vapor-Liquid Equilibrium Data for H_2-Tetralin (61)	148
40	Vapor-Liquid Equilibrium Data for H_2-Tetralin (61)	149
41	Vapor-Liquid Equilibrium Data for H_2-Athabasca Bitumen (4-AB-77)	150
42	Vapor-Liquid Equilibrium Data for H_2-EMR Gas Oil	151
43	Vapor-Liquid Equilibrium Data for CO_2-Tetralin (57)	152
44	Vapor-Liquid Equilibrium Data for CO_2-Athabasca Bitumen (4-AB-77)	154
45	Vapor-Liquid Equilibrium Data for CO_2-EMR Gas Oil	156
46	Vapor-Liquid Equilibrium Data for H_2S-Athabasca Bitumen (4-AB-77)	158
47	Vapor-Liquid Equilibrium Data for H_2S-EMR Gas Oil	159
48	Hempel Distillation of Topped Athabasca Bitumen (2-AB-77)	161
49	Hempel Distillation of Lloydminster Residue (3-LL-78)	162
50	Hempel Distillation of Amoco Feed (2-AM-78)	163

Nomenclature

A	constant defined by eqn. (4.28)
a	attraction parameter
B	constant defined by eqn. (4.29)
b	van der Waals covolume factor
C	interaction coefficient in the SRK equation
E	binary parameter in the modified SRK equation and the modified PR equation
f	fugacity
H	apparent Henry's constant
i	component i
j	component j
K	equilibrium ratio
k	interaction coefficient in the Chueh-Prausnitz equation
n	moles
P	pressure
R	gas constant
S	characteristic constant in the SRK equation
T	temperature
v	molar volume
x	mole fraction in the liquid phase
y	mole fraction in the vapor phase
z	compressibility factor

Greek Letters

α	scaling factor in the PR and Soave equations
γ	activity coefficient
δ	interaction coefficient in the PR equation
κ	characteristic constant in the PR equation
ϕ	fugacity coefficient
ω	acentric factor

Superscripts

P	Peng-Robinson
S	SRK

Subscripts

A	attraction
b	boiling point parameter
c	critical property
H	hydrogen in the modified SRK equation and the modified PR equation
HC	hydrocarbon
R	repulsion
r	reduced property
i	component identification
j	component identification
k	component identification

1. Introduction

Solubility data for gases in hydrocarbon solvents are useful in the petroleum industry. The effect of temperature on gas solubilities is of practical importance because of the wide range of temperatures encountered in chemical processes. The measurement and correlation of phase equilibrium data provide important information needed in the design of chemical processing equipment.

Recent interest in the recovery and processing of shale oil, coal liquids and oil-sands bitumens has created a need for solubility data for hydrogen, carbon dioxide and hydrogen sulphide, at elevated temperatures and pressures, in heavy hydrocarbons quite different from the normal petroleum mixtures. These systems contain mono-nuclear and poly-nuclear aromatics, naphthenes, high boiling paraffins and ring compounds containing N, S and O. As well, the need to increase recovery of distillates from petroleum residues has demanded accurate vapor-liquid equilibrium data for hydrogen in heavy petroleum mixtures.

In hydrotreating applications hydrogen coexists with carbon dioxide, hydrogen sulphide and light hydrocarbon gases in hydrocarbon liquids. The design of reformers, hydrocrackers, hydrotreaters and scrubbing units requires accurate knowledge of solubilities of these gases.

The Canada Centre for Mineral and Energy Technology (CANMET) of the Department of Energy, Mines and Resources has developed a hydrocracking process, operable at high

pressure and producing low pitch and high distillate yields from bitumen fractions. Figure 1 presents a simplified flow scheme of a one-barrel per day CANMET hydrocracking pilot plant simulating a commercial process. A mixture of hydrogen and topped bitumen is preheated and pumped into a 4.5 litre reactor vessel where the bitumen is cracked and hydrogenated to form low molecular weight distillate and residual pitch. The reactor effluent is cooled in two stages giving a heavy oil and a light oil. The hydrogen-rich gas stream is scrubbed to remove gaseous hydrocarbons and hydrogen sulphide, mixed with make-up hydrogen and recycled back to the reactor. Because of the high sulphur content in bitumen, substantial hydrogen sulphide is formed during hydrocracking. The process is capable of handling a wide variety of feedstocks. The pitch conversion can be altered, as desired.

Hydrogen exists in equilibrium with the feed and products at the high temperature required in the CANMET hydrocracking process, together with hydrogen sulphide formed by hydrodesulphurisation. Consequently, solubility data for hydrogen and hydrogen sulphide in bitumen feedstocks and cracked products are useful for the design and analysis of commercial bitumen-upgrading processes. As well, these data are required in the kinetic modelling of the complex reactions taking place during the hydrocracking and hydrodesulphurisation. The present work was undertaken to provide data at the temperatures and pressures

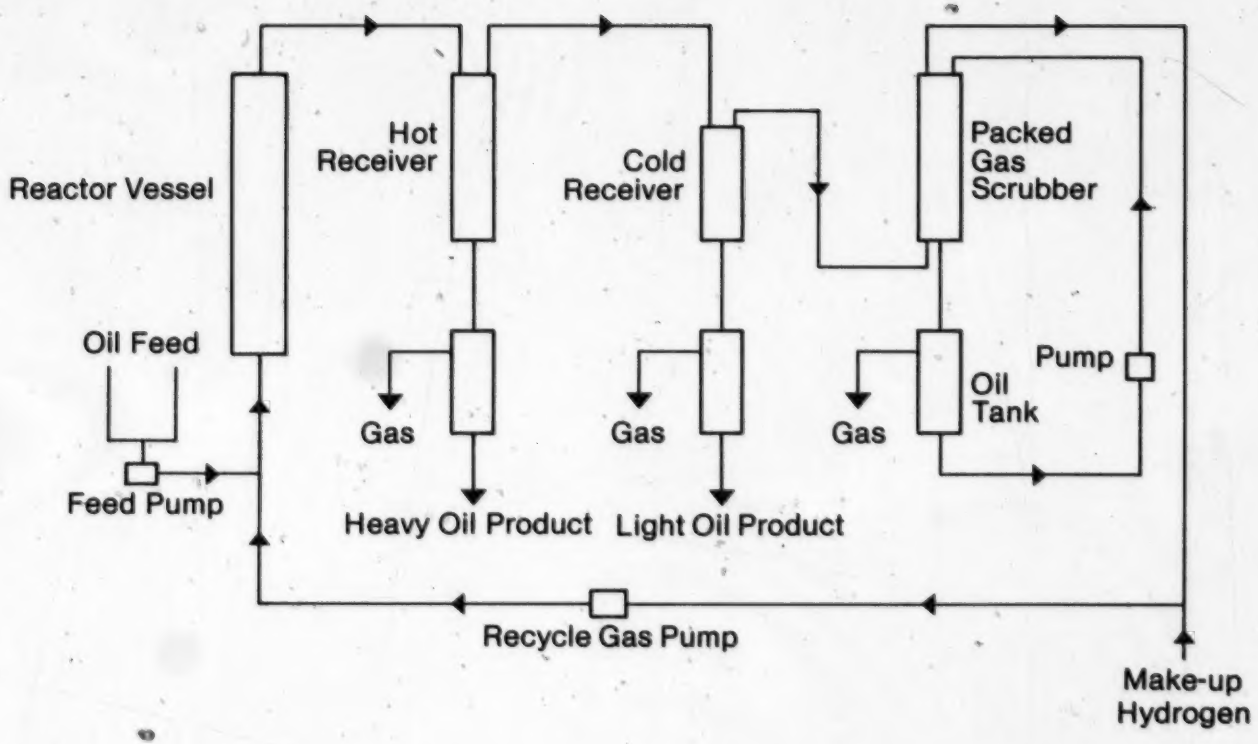

Fig 1 Schematic Diagram of Canmet Pilot Plant

approaching those used in the CANMET hydrocracking process. The solvents used were actual feedstocks and hydrocracked products from the pilot plant.

Coal upgrading can be done in a slurry medium; the solvent used can either donate hydrogen or act as a hydrogen carrier. No data on hydrogen solubility in coal-oil slurries are available. These studies were extended to obtain hydrogen solubility in selected coal-bitumen slurries. The data will be helpful in the analysis of kinetics of coal liquefaction.

As a result of the present shortage of crude oil, there is increased interest in the use of carbon dioxide as a tertiary oil recovery agent, since it promotes swelling of the heavy oils and reduces their viscosity greatly. The knowledge of carbon dioxide solubility in bitumens at reservoir temperatures, as well as at temperatures required to recover the solute gas, is desirable.

In the modelling of hydrocracking and related hydrotreatment processes, thermodynamic correlations are used to calculate the vapor and liquid phase compositions and their properties. The 'dual' model method of Chao-Seader is a technique widely applied in the petroleum industry. The Soave modification of the Redlich-Kwong equation of state and the Peng-Robinson equation of state are more recent methods, and are popular due to their simplicity and accuracy. The reliability of these methods to predict phase equilibrium was tested using experimental data obtained here

and from the literature.

2. Literature Survey

2.1 Theory

For most gases at ordinary temperatures the solubility in a liquid solvent decreases with rising temperature. This is expected because, as temperature rises, the kinetic energy of the gas increases and thus there is a decreasing tendency to condense into a liquid phase. However, the solubilities of some gases increase with temperature while others first decrease and then increase. It appears likely that the solubilities of all gases first decrease, go through a minimum, and then increase if taken over a wide enough temperature. The increase of solubility of some gases with temperature is probably related to the decrease in solvent density as temperature rises (45,69).

The temperature derivative of the solubility, calculated from the Gibbs-Helmholtz equation, is directly related to the partial molar entropy of the gaseous solute in the liquid phase. Therefore, if something can be said about the entropy change of the solution, insight can be gained on the effect of temperature on solubility. Consider the relatively simple case where the solvent is essentially non-volatile and where the solubility is sufficiently small to make the activity coefficient of the solute independent of the mole fraction. With these restrictions it can be shown that

$$\frac{\partial \ln x_2}{\partial \ln T} = \frac{\Delta \bar{s}_2}{R} \qquad (2.1)$$

where x_2 is the mole fraction of gaseous solute at saturation and

$$\Delta \bar{s}_2 = \bar{s}_2(1) - s_2(v) \qquad (2.2)$$

First we consider equation (2.1); if the partial molar entropy of change of the solute is positive, then the solubility increases with rising temperature; otherwise it falls. To understand the significance of the entropy change it is convenient to divide it into two parts:

$$\Delta \bar{s}_2 = (s_2(1) - s_2(v)) + (\bar{s}_2(1) - s_2(1)) \qquad (2.3)$$

where $s_2(1)$ is the entropy of the (hypothetical) pure liquid at the temperature of the solution. The first term on the right-hand side of equation (2.3) is the entropy of condensation of the pure gas and in general this is expected to be negative since the entropy of a liquid is lower than that of a saturated gas at the same temperature. The second term is the partial molar entropy of solution of the condensed solute and, assuming ideal entropy of mixing for the two liquids, it is

$$\bar{s}_2(1) - s_2(1) = - R \ln x_2 \qquad (2.4)$$

Since $x_2 < 1$ the second term in Eq (2.3) is positive and the smaller the solubility, the larger this term becomes. It therefore follows that $\Delta\bar{s}_2$ should be positive for those gases which have very small solubilities and negative for others. Gases which are sparingly soluble show positive temperature coefficients of solubility, whereas gases which are readily soluble show negative temperature coefficients. This is in fact observed.

2.2 Experimental Techniques

Solubility determinations consist essentially in bringing the solvent into equilibrium with the gas at a known total pressure, taking a sample of the liquid phase and determining its composition. Individual methods differ in the manner in which the attainment of equilibrium is accelerated (stirring,shaking,circulating the liquid or bubbling the gas) and as to whether sampling is continuous or intermittent. Chappelow and Prausnitz (5), and Cukor and Prausnitz (8) investigated the solubility of hydrogen at low pressure in bicyclohexyl, diphenylmethane, squalane, *n*-hexadecane and octamethyl-cyclotetrasiloxane. The experimental apparatus consisted of 5 sections: (1) a degassing flask, (2) an equilibrium cell, (3) a reservoir of degassed solvent, (4) a precision gas burette, and (5) a section for pressure measurement. Solvent was continuously circulated through a vapor space containing a measured

quantity of solute. The solubility was determined by making a material balance on the gaseous solute. The precision of their results was about 1%.

The solubilities of hydrogen in isobutane, 2,2,4-trimethylpentane, and in a mixture of isomeric dodecanes were investigated by Dean and Tooke (11).Hydrogen and the liquids were placed in an equilibrium cell mounted in an oil-filled bath in which it was rocked at 30 cycles a minute. At the upper end of the cell one valve was attached with an induction tube for withdrawing liquid phase samples. Another valve was provided for taking vapor phase samples. Solubilities in isobutane were determined for temperatures from 100° to 250°F and pressures from 500 psia to 3000 psia. The solubility of hydrogen in 2,2,4-trimethylpentane was measured for temperatures from 100° to 302.5°F and in the dodecanes for 200° and 300°F with pressures ranging from 500 to 5000 psia. The liquid and vapor samples were analyzed by repeatedly freezing and thawing the samples, resulting in the physical separation of the hydrogen from the hydrocarbon. An Orsat apparatus was also used to analyze the hydrogen-isobutane systems. They showed that hydrogen solubility increased with temperature and pressure and that solubility decreased as solvent molecular weight increased. They also concluded that hydrogen is more soluble in paraffins than in aromatics of similar molecular weight.

Eakin and DeVaney (12) investigated the vapor-liquid equilibrium for hydrogen sulphide-*n*-nonane, hydrogen

sulphide-isopropylcyclohexane, and hydrogen sulphide-mesitylene at 100° to 400°F. Ternary mixtures of hydrogen sulphide-hydrogen-*n*-nonane, hydrogen sulphide-hydrogen-isopropylcyclohexane, and hydrogen sulphide-hydrogen-mesitylene at up to 2000 psia at these same temperatures were also studied. The apparatus consisted of a rocking type equilibrium cell. All samples were analyzed on a Beckman GC-4 chromatograph. The column was a 16 foot long, 1/8 inch OD tube packed with 80-100 mesh Porapak P. The carrier gas was argon.

Frolich et al. (15) determined gas solubility by saturating a liquid with gas at suitable intervals of pressure and measuring the ratio of solute to solvent in a sample drawn off for analysis. To this end a small amount of solvent was introduced into an evacuated steel cylinder of 2 litre capacity. The gas was then forced in at the highest pressure available and the cylinder agitated in a water bath maintained at 25°C. The liquid phase analysis was done by flashing a sample of the liquid and collecting the vapor over mercury in a burette. The total error of this method is such that the results should not be considered accurate to better than ±5%. The liquids studied included: gas oil, heavy naphtha, cyclohexane, octane, and hexane at 25°C and pressures up to 200 atmospheres.

Grove et al. (19) measured the solubility of hydrogen in terphenyl at high temperatures. Their apparatus was made of two cylindrical stainless steel vessels isolated from one

another by means of a stainless steel bellows. A pressure difference between the two vessels caused contraction or expansion of the bellows. The assembly was agitated by a motor at about 320 cycles/min to establish equilibrium. A known weight of terphenyl was placed in one vessel, degassed and pressured with hydrogen, the other vessel being pressured with nitrogen simultaneously so that no large stresses were placed on the bellows. Hydrogen solubilities were calculated by measuring the decrease in the number of moles of gas in the vapor space over the solvent in passing from the initial equilibrium condition when the solvent was solid, to the temperature of measurement.

Ipatieff et al. (21) studied the solubility of hydrogen in benzene, toluene, xylene, mesitylene, gasoline, kerosene, cylinder oil and paraffin mazout. The liquid under investigation was placed in a high pressure bomb. The necessary pressure was applied through an upper valve and the liquid was thoroughly mixed with the gas. Afterwards a sample was taken into a gas burette through a special valve. The volumes of the liquid and the evolved gas were read directly from the burette. Solubilities were reported for temperatures of 25, 40 and 100°C and for pressures up to 319 atmospheres in benzene, toluene, xylene, and mesitylene, and at 25° to 300°C (to a maximum pressure of 300 atmospheres) in gasoline fraction, kerosene, cylinder oil and paraffin mazout oil. They concluded that (i) solubilities increased as temperature increased (ii) solubilities increased

linearly with pressures to 300 atmospheres and (iii) solubilities decreased with the complexity of the composition of the molecule, being the greatest for benzene and gasoline, and the smallest for mesitylene and mazout.

Lachowicz et al. (26) investigated the solubility of hydrogen in *n*-heptane and *n*-octane at 25°, 37.5° and 50°C at pressures between 50 and 300 atmospheres. Their apparatus consisted of (i) a mercury piston compressor, (ii) an equilibrium cell, and (iii) an apparatus for expanding the sample to 1 atm. and analyzing it. The vessel was rocked in a thermostat to attain equilibrium. During the withdrawal of the sample, the pressure in the vessel was maintained within ±0.5 atm. by admitting compressed gas from a gas storage vessel. The liquid sample was expanded into a cooled trap and frozen. The evolved gas was collected in a burette and its volume measured at room temperature and pressure. The liquid sample was weighed after bringing it to room temperature.

Nichols et al. (39) measured the specific volumes of four mixtures of hydrogen-*n*-hexane at eight temperatures between 40 and 460°F, for pressures up to 10000 psi. A mixture sample of known composition and weight was confined in a stainless steel vessel over mercury. The effective volume of this chamber was varied by the introduction and withdrawal of mercury. Mechanical agitation was provided to hasten the attainment of physical equilibrium within and between the phases. The cell was immersed in an agitated

liquid bath. Sample of the gas phase was removed under isobaric-isothermal conditions and passed through a series of weighing bombs maintained at liquid nitrogen temperature. The total quantity of hydrogen in the gas phase was then determined volumetrically. No liquid compositions were reported.

Prather et al. (44) used an Autoclave Engineers 316 stainless steel Magnedrive autoclave with a volume of one US gallon to study the solubility of hydrogen in recycle oil and creosote oil, and in coal-creosote oil slurry. Hydrogen analysis was carried out on a Varian model 920 Aerograph using a 15 ft column packed with 75% molecular sieve 13 X and 25% molecular sieve 5A. The oil was charged into the autoclave and the system was evacuated. The autoclave was then brought to the desired temperature and hydrogen was added. Stirring was carried on at 2000 rpm. Samples of the vapor were withdrawn from the top of the autoclave and analyzed by GC. Liquid samples were withdrawn from the autoclave into a stainless steel bomb. The bomb was then fitted to an evacuated glass rack, in which the volume of the dissolved gases was measured. The gas was withdrawn by action of a Toepler pump, and after volume measurement it was passed to a GC for analysis. Data were provided at temperatures up to 400°C and for 385 psia to 3000 psia hydrogen pressure. These authors concluded that hydrogen solubility in a 3:1 solvent:coal mixture was similar to that in the pure solvent at temperatures high enough for coal to

be thermally decomposed.

Prausnitz and Benson (46) studied the vapor phase solubility of iC_8H_{18}, $C_6H_5CH_3$, and $C_{10}H_{22}$ in compressed hydrogen with a flow system. The gas was dried with silica gel before entering the equilibrium cells. Two equilibrium cells connected in series were used to assure saturation of the gas. The liquid was contained within the cell, in pyrex liners, and the gas was very finely dispersed from a fritted glass sparger (pore size 14 microns) at the bottom of the cells. The equilibrium cells were immersed in a constant -temperature bath, which was controlled to within ±0.05°C. After leaving the second cell the vapor was led to a needle expansion valve. After expansion the vapor mixture entered the condenser. It was assumed that the vapor leaving the condenser was in equilibrium with the condensate. The flow of gas was measured with a wet-test meter. From the amount of condensate collected and hydrogen passed through the wet-test meter, the vapor phase composition was determined.

Simnick et al. (61,62,63,64), Sebastian et al. (53,55,56), Lin (29), and Yao et al. (72) studied the gas-liquid equlibrium for binary mixtures of hydrogen in *m*-cresol, *m*-xylene, tetralin, diphenylmethane, bicyclohexyl, toluene, 1-methylnaphthalene, thianaphthene and quinoline. A flow apparatus was used to reduce the residence time of the fluids in the apparatus. The liquid was pumped in at a rate of 500-2000 cc/h and the hydrogen gas was supplied at a rate of about 5500 cc/min. The two streams were mixed, and heated

in a tubular heater to the desired temperature and then passed into an isothermal cell. The cell effluent was throttled and cooled to ambient conditions. The liquid was trapped and later weighed with an analytical balance and the quantity of hydrogen gas determined volumetrically. The work was later extended to ternary systems of hydrogen -tetralin-diphenylmethane and hydrogen-tetralin-*m*-xylene mixtures.

Sagara et al. (51) determined the vapor-liquid equilibrium relations of the hydrogen-methane, hydrogen-ethylene, hydrogen-ethane, hydrogen-methane-ethylene and hydrogen-ethane-ethylene systems by a static method at several temperatures from -25° to -170°C and at pressures up to 100 atmospheres. The vapor and liquid samples were collected in chambers and analyzed by gas chromatography.

The work which reached the highest temperature was by Grayson and Streed (18) who presented a correlation of K values of hydrogen in heavy oils at 320° to 480°C and pressures to 200 atmospheres. No experimental data were reported.

King et al. (24,25) measured the solubilities of carbon dioxide and hydrogen sulphide as functions of temperature in the *n*-alkanes hexane to hexadecane at normal pressure, and correlated the solubilities at 25°C. A 'falling film' type of apparatus was used. Each solvent was degassed before use by spraying into a continuously evacuated chamber. It was then displaced from this chamber by injecting mercury and

flowed drop by drop over a lip where it passed as a film down the inside wall of a spiral, and finally accumulated in a graduated pipette. A magnetically operated stirrer agitated the gas-liquid interface in the pipette. A known volume of gas was stored in a burette and amount dissolved in a known quantity of solvent was determined by noting the volume of gas expelled from the gas burette.

Low pressure solubilities for hydrogen sulphide in *n*-hexadecane, diphenylmethane, bicyclohexyl, and 1-methylnaphthalene have been studied by Tremper and Prausnitz (69). The experimental apparatus and procedure was essentially the same as those described by Cukor and Prausnitz (9).

Yarborough (73) investigated the vapor-liquid equilibrium for hydrogen sulphide and *n*-decane. An equilibrium cell, sampling valves, and 2 different chromatographs were used for analysis during this study.

Jacoby and Rzasa (22) obtained experimental vaporization K-values for hydrogen sulphide and carbon dioxide in two natural gas-absorber oil mixtures and in two natural gas-crude oil mixtures at temperatures of 100, 150 and 200°F and various pressures in the range 200 to 5000 psia. The pressure cell consisted of a hollow stainless steel cylinder, placed horizontally, and fitted with a piston. The liquid phase was circulated with a magnetic pump. The vapor samples were analyzed directly with a mass spectograph. The liquid samples were flashed and the light

gases were analyzed by the mass spectrograph. The remainder of the samples were fractionated and C_7+ fractions were characterised.

Simon and Graue (66) studied the solubility of carbon dioxide in nine different oils at conditions covering a range of 100 to 250 °F and pressures up to 2300 psia. Known amounts of pure carbon dioxide and crude oil were combined in a visual cell and bubble points of the mixture were measured. Correlations for predicting the solubility, swelling, and viscosity behaviour of these systems were obtained in graphical form.

From the experimental methods described by the various authors, it was concluded that a batch autoclave is suitable for the measurement of hydrogen solubility in heavy bituminous materials and coal-bitumen slurries. This type of equipment is available in different sizes, and operable at high temperatures and pressures. A GC, with either N_2 or Ar as carrier gas, is adequate for both the liquid and vapor phase analyses.

2.3 Correlation

Early attempts to describe the volumetric properties of gases led to the ideal gas law and the van der Waals equation for real gases. Since then systematic efforts have been made to describe the equilibrium properties of real gases. A review of the various equations of state that have been widely used is presented by Tsonopoulos and Prausnitz

(70).

Equations of state serve four purposes : (i) prediction of vapor-liquid equilibria of mixtures at wide ranges of temperatures and pressures, (ii) prediction of gas phase properties of pure fluids and their mixtures, (iii) prediction of liquid phase properties of pure fluids and their mixtures, (iv) interpolation of PVT data, and differentiation and integration of PVT data for estimation of derived properties (e.g. fugacity).

A single equation of state does not satisfactorily achieve all these purposes. The virial equation of state expresses the compressibility factor, z, of a gas by a power series in the density, and is useful only for modest densities (approximately 3/4 of the critical density) when virial coefficients beyond the third are ignored. The virial equation is attractive because of its theoretical basis and of its relation to intermolecular forces. Its usefulness is limited by our incomplete knowledge of virial coefficeients.

Benedict, Webb and Rubin (2) presented an equation of state with eight adjustable parameters. To obtain eight meaningful constants, extensive experimental data are required. Even if such data are available, the constants are not unique. The equation represents satisfactorily volumetric properties of non-polar gases and liquids to densities up to about 1.8 times the critical.

The most successful variation on the van der Waals equation was that proposed by Redlich and Kwong (49), which

uses only two adjustable parameters. The RK equation, while admittedly less accurate than the BWR equation when applied to pure substances, is attractive for mixtures since it does not rely on extensive experimental data. The equation has been applied extensively to vapor mixtures and their properties. A notable application is in the Chao-Seader (4) correlation which applies a 'dual' model approach to calculate the vapor-liquid equilibria. The vapor-phase fugacity coefficient is calculated using the RK equation of state.

Numerous variations on the RK equation have been proposed. Chueh and Prausnitz (6) applied the RK equation assuming a geometric mean mixing rule for the critical temperature of the binary formed by i and j, and introducing the interaction parameter, k_{ij}, to correct for the departure from the geometric mean.

Zudkevitch and Joffe (74) also modified the RK equation, utilising Chueh and Prausnitz's ideas, and introduced the binary interaction parameter to correct for the deviation from the geometric mean in the cross parameter a_{ij}. They applied the RK equation to both the vapor and the liquid phases.

In the Chao-Seader correlation the upper limit for the liquid fugacity coefficient for hydrogen is 260°C. Grayson and Streed (18) used Chao and Seader's experimental data, as well as their own, to modify the Chao-Seader correlation for the K-values in hydrogen-gas oil systems. The correlation is

applicable for temperatures up to 480°C.

Recently, more emphasis has been placed on applying a single equation of state for the calculation of vapor-liquid equilibria, since the same equation can then be used for the fugacity coefficient in both the phases. Soave (67) modified the attraction parameter term in the RK equation, making it temperature dependent, as well as a function of the acentric factor. The SRK equation of state gained acceptance in the hydrocarbon processing industry because of its relative simplicity and its ability to generate reasonably accurate K-values in vapor-liquid equilibrium calculations. However, both the SRK and RK equations fail to generate satisfactory density values for the liquid. Graboski and Daubert (17) recommended improvements to the SRK method to handle hydrogen-containing systems.

Peng and Robinson (41) presented a simple equation of state that gave improved liquid density values as well as accurate vapor pressures and K-values. The PR method assumed the geometric mean mixing rule in the energy parameter, a , for the binary. An interaction coefficient was then applied to correct for the departure from the geometric mean. The one-fluid approximation was used to define the covolume factor, b, for the mixture.

El-Twaty and Prausnitz (14) obtained an improved correlation of K-values for hydrogen-heavy hydrocarbon mixtures by modifying the composition dependence of the covolume factor b in the SRK equation. The modification

introduced a binary interaction parameter E_{Hj} that can be adjusted to fit binary data.

Recently, Sebastian et al. (54) developed a correlation in which the fugacity of dissolved hydrogen at zero pressure was correlated as a function of temperature and solubility parameter. The high pressure fugacity was obtained upon applying a Poynting factor. The new correlation has its basis in the 'regular' solution assumption, and the Chueh-Prausnitz modification of the RK equation of state.

A literature search has shown that many equations of state have been proposed for mixtures containing low molecular weight solvents. Only a few of these have been applied to highly asymmetric mixtures of small molecules, such as hydrogen, and large molecules, such as tetralin. This work considers the applicability of the PR, the modified SRK and the Grayson-Streed methods for predicting solubility of hydrogen in high boiling point hydrocarbon solvents as well in the heavier and more complex feedstocks and products of the CANMET bitumen upgrading process. The ability of the PR equation of state to handle hydrogen sulphide and carbon dioxide in these solvents was also investigated.

2.3.1 Grayson-Streed

The Chao-Seader correlation is limited to a maximum temperature of 260°C for hydrogen systems. New experimental vapor-liquid equilibria data for high temperature, high

pressure hydrogen-hydrocarbon systems were used to extend the temperature range of the Chao-Seader K correlation. The experimental results covered a range of temperature up to 480°C and a range of pressure up to 3000 psia. Modified coefficients for computing the liquid fugacity coefficient at temperatures up to 425°C for hydrogen, methane and heavier hydrocarbons were developed.

In the Chao-Seader correlation K-values are calculated through a combination of three factors:

$$K = y / x = \nu_1 \gamma / \phi \qquad (2.5)$$

The quantity ν_1 is the fugacity coefficient of the pure component in the liquid phase. The quantity γ is the activity coefficient of this component in the liquid mixture. The quantity ϕ is the fugacity coefficient of the component in the vapor mixture.

The upper temperature limits in the Chao-Seader correlation for the liquid fugacity coefficient, ν_1, are:

1. Hydrogen and methane: 260°C
2. Other hydrocarbons: reduced temperature of 1.3.

The liquid activity coefficient and vapor fugacity coefficient correlations remain unchanged from those proposed by Chao-Seader. Liquid activity coefficients are calculated from Hildebrand's equation, assuming 'regular' liquid solutions. Vapor fugacity coefficients are calculated from the Redlich-Kwong equation of state.

The Chao-Seader correlation for liquid fugacity coefficient has been developed within the framework of Curl and Pitzer's modified form of the principle of corresponding states which is presented in equation (2.6):

$$\log \nu_1 = \log \nu_2 + \omega \log \nu_3 \qquad (2.6)$$

The first term on the right-hand side represents the fugacity coefficient of 'simple fluids'. The second term is a correction accounting for the departure of the properties of 'simple fluids'.

The quantity ν_2 is dependent only on reduced temperature and reduced pressure and was fitted with the following function by Chao and Seader:

$$\log \nu_2 = A_0 + A_1/T_r + A_2T_r + A_3T_r^2 + A_4T_r^3 + (A_5 + A_6T_r + A_7T_r^2)P_r + (A_8 + A_9T_r)P_r^2 - \log P_r \qquad (2.7)$$

New coefficients for equation (2.7) were determined to fit Grayson and Streed's experimental high temperature data as well as Chao and Seader's low temperature data. A separate set of coefficients are required for hydrogen, since the typical application temperatures in the hydrotreating processes are far above the critical temperature of hydrogen. These are listed in Grayson and Streed (18). The value of ω, the acentric factor, for hydrogen is then taken as zero in equation (2.6).

The quantity ν_3 is also dependent only on reduced temperature and reduced pressure and was fitted with the following function by Chao and Seader:

$$\log \nu_3 = -4.23893 + 8.65808\, T_r - 1.22060 / T_r - 3.15224\, T_r^3 - 0.025\,(P_r - 0.6) \qquad (2.8)$$

A modification to the limits of this equation is necessary in order to fit the high temperature data. For values of T_r above 1.0, values of ν_3 are set equal to the value at $T_r = 1.0$.

2.3.2 Soave-Redlich-Kwong Method

Soave (67) originally proposed a modification of the Redlich-Kwong equation of state which introduced a third parameter, the acentric factor, and a temperature dependency into the cohesive energy term to account for the effect of non-sphericity on fluid P-V-T properties. The forms of the equation of state for the compressibility factor and fugacity coefficient are given by equations (2.9) and (2.10):

$$z = \frac{v}{v-b} - \frac{a\,\alpha}{RT(v+b)} \qquad (2.9)$$

$$\ln \phi_i = \ln \left(\frac{v}{v+b}\right) + \left(\frac{b_i}{v-b}\right) - \frac{z}{RTb} \sum_j a_{ij} x_j \ln \left(\frac{v+b}{b}\right) + \frac{ab_i}{RTb^2} \left\{ \ln \left(\frac{v+b}{b}\right) - \left(\frac{b}{v+b}\right) \right\} - \ln z \qquad (2.10)$$

For any component, the constants a and b are determined from the universal relationships:

$$a = 0.42747\ R^2\ T_c^{\,2} / P_c \qquad (2.11)$$

$$b = 0.08664\ R\ T_c / P_c \qquad (2.12)$$

For hydrocarbons and certain nonhydrocarbons, the additional constant α is a function of the temperature and the acentric factor:

$$\alpha = \{1 + S(1 - \sqrt{T_r})\}^2 \qquad (2.13)$$

The S parameter was given by Graboski and Daubert (17) as:

$$S = 0.48508 + 1.5517\ \omega - 0.15613\ \omega^2 \qquad (2.14)$$

The equation of state was extended to mixtures by Soave (67) using the combining rules given as:

$$a\alpha = \sum_i \sum_j x_i x_j a_{ij} \alpha_{ij} \qquad (2.15)$$

$$b = \sum_i x_i b_i \qquad (2.16)$$

where

$$a_{ij}\alpha_{ij} = \sqrt{(a_i a_j \alpha_i \alpha_j)}(1 - C_{ij}) \qquad (2.17)$$

Graboski and Daubert (17) computed the interaction coefficients, C_{ij}, using the SRK model, for a number of hydrogen binaries. They restricted the values of the interaction coefficients to $C_{ij} < 1$ and observed that the predicted phase behaviour was insensitive to C_{ij} for heavy hydrocarbons at higher temperatures. However, they found the SRK method fitted the experimental solubility data only with unrealistically large positive and negative values of the interaction coefficients for some of the hydrogen-hydrocarbon systems. In the cases where C_{ij} was greater than 1 physically meaningless $a_{ij} < 0$ resulted. The interaction coefficients were also dependent on temperature. A similar pattern of behavior was observed by El-Twaty and Prausnitz (14).

2.3.3 Penn-State-Soave Method

Graboski and Daubert (17) derived the function for S in equation (2.14), based on a regression of vapor pressure data and applied the result to correlate vapor-liquid equilibria data for hydrocarbon mixtures and for binary mixtures of hydrocarbon with carbon dioxide, hydrogen

sulphide, carbon monoxide and nitrogen. The basic SRK procedure failed to give accurate results for hydrogen K-values. Thus, they proposed the new expression for α of hydrogen as given in equation (2.18):

$$\alpha = 1.202 \exp (- 0.30228\ T_r) \qquad (2.18)$$

This equation can be expected to be accurate for hydrogen at reduced temperatures greater than 2.5. They proposed that the modified α function (for hydrogen) be used directly for hydrogen systems without interaction coefficients. Testing their modified SRK method, called the PSS method, for binary mixtures of hydrogen in 1-methylnaphthalene, bicyclohexyl, tetralin and diphenylmethane they found average deviations to be 18.6% and 10.2% in K-values of hydrogen and the heavy solvent, respectively.

The advantage of SRK over PSS is that the deviations of the calculated results from experimental values for the SRK method do not appear to increase as the molecular weight of the hydrocarbon solvent is increased, and the PSS method fails to represent the K-values of hydrogen in heavy hydrocarbons as accurately as in the lighter solvents (29).

In the case of hydrogen sulphide existing in the mixtures, the relationship (2.13) is valid. The interaction coefficient for hydrogen sulphide and the hydrocarbon is then given by equation (2.19):

$$C_{ij}(H_2S) = 0.0178 + 0.0244\ \Delta\delta \qquad (2.19)$$

where

$$\Delta\delta = |\delta_{HC} - \delta_{H_2S}| \qquad (2.20)$$

δ is the Scatchard-Hildebrand solubility parameter.

2.3.4 Peng-Robinson

The equation of state proposed by Peng and Robinson (41) is of the form

$$P = \frac{RT}{v-b} - \frac{a}{v(v+b)-b(v-b)} \qquad (2.21)$$

Equation (2.21) can be written as

$$z^3 - (1-B)z^2 + (A-3B^2-2B)z - (AB-B^2-B^3) = 0 \qquad (2.22)$$

where

$$A = a\ P\ /\ R^2\ T^2 \qquad (2.23)$$

$$B = b\ P\ /\ R\ T \qquad (2.24)$$

$$z = P\ v\ /\ R\ T \qquad (2.25)$$

Equation (2.22) can be solved analytically to determine the compressibility factor z. The equation yields one or three real roots depending on the number of phases in the system. In the two phase region, the largest root is the compressibility factor of the vapor while the smallest positive root corresponds to that of the liquid.

The fugacity coefficient of any component in a mixture is related to the volumetric behaviour of the vapor phase.

$$\ln \phi_i = \int_0^P (z_i - 1)\, d \ln P \qquad (2.26)$$

Here $z_i = P\bar{v}_i/RT$ and $\bar{v}_i$ is the partial molar volume of the ith component. Applying equation (2.21) to (2.26) the following expression for the fugacity coefficient is obtained:

$$\ln \phi_i = \frac{b_i}{b}(z-1) - \ln (z-b) - \frac{A}{2\sqrt{2}B}\left(\frac{2\Sigma x_i a_{ij}}{a} - \frac{b_i}{b}\right) x \ln \left(\frac{z+2.414B}{z-2.414B}\right) \qquad (2.27)$$

where

$$a = \sum_i \sum_j y_i y_j a_{ij} \qquad (2.28)$$

$$b = \sum_i y_i b_i \qquad (2.29)$$

$$a_{ij} = \sqrt{(a_i a_j)}(1-\delta_{ij}) \qquad (2.30)$$

In equation (2.30) δ_{ij} is an empirically determined binary interaction coefficient characterising the binary formed by the i and j component. It is equivalent to the interaction coefficient C_{ij} in the SRK equation of state.

The constants a and b are related to the critical properties and the acéntric factor of component i, such that

$$a_i(T) = a_i(T_c)\ \alpha_i(T_r, \omega) \qquad (2.31)$$

$$b_i(T) = b_i(T_c) \qquad (2.32)$$

$$a_i(T_c) = 0.45724\ R^2\ T_c^2\ /\ P_c \qquad (2.33)$$

$$b_i(T_c) = 0.07780\ R\ T_c\ /\ P_c \qquad (2.34)$$

$$\alpha = \{1 + \kappa(1 - \sqrt{T_r})\}^2 \qquad (2.35)$$

$$\kappa = 0.37464 + 1.54226\ \omega - 0.26992\ \omega^2 \qquad (2.36)$$

The fugacity coefficient ϕ_i is defined by :

$$\phi_i = f_i\ /\ x_i\ P \qquad (2.37)$$

where f_i is the fugacity. K-values are found from the relation

$$K_i = \phi_i(\text{liquid}) \; / \; \phi_i(\text{vapor}) \qquad (2.38)$$

2.3.5 Modified Soave-Redlich-Kwong

El-Twaty and Prausnitz (14) found that when equation (2.16) was applied to mixtures of hydrogen and heavy hydrocarbons, the experimental data could be fitted only with unrealistic values of C_{ij}. In some cases, it was necessary to use $C_{ij} > 1$, giving meaningless $a_{ij} < 0$. It was shown that calculated vapor-liquid equilibria for hydrogen-containing systems were more sensitive to small changes to b than to large changes to a . Equation (2.16) was replaced by equation (2.39):

$$b = \sum_i x_i b_i + x_H \sum_j x_j E_{Hj} \qquad (2.39)$$

where subscript H stands for hydrogen and the summation over i extends to all components (including hydrogen), and the summation over j extends to all components except hydrogen. When $E_{Hj} = 0.$, equation (2.39) reduces to equation (2.16). Using equations (2.9), (2.15), and (2.39) to find the fugacity coefficient for component i, we obtain:

$$\ln \phi_i = \phi_i^s + \chi_i \{ \frac{1}{v-b} - \frac{a}{RTb^2} (\ln \frac{v+b}{v} - \frac{b}{v+b}) \} \qquad (2.40)$$

where the fugacity coefficient ϕ_i is defined by equation (2.37). ϕ_i^s designates the fugacity coefficient derived from equation (2.10). For hydrogen,

$$\chi_H = (1-x_H) \sum_j x_j E_{Hj} \qquad (2.41)$$

For all other components

$$\chi_i = x_H (E_{Hj} - \sum_k x_k E_{Hk}) \qquad (2.42)$$

where the summation over components k includes all components ($E_{Hk} = 0$ when k is hydrogen).

For temperatures above the critical, the characteristic constant, α, is calculated from equation (2.43):

$$\alpha = \exp \{ 2 S(1 - \sqrt{T_r}) \} \qquad (2.43)$$

Otherwise, equation (2.13) applies.

2.4 Characterization of Mixtures

Table 1 lists the properties needed to calculate the VLE data. The PR, SRK and Grayson-Streed procedures require

TABLE 1

PROPERTIES OF COMPONENTS REQUIRED FOR PR, SRK AND GRAYSON - STREED METHODS

	PR	SRK	GS
Critical Temperature	yes	yes	yes
Critical Pressure	yes	yes	yes
Acentric Factor	yes	yes	yes
Solubility Parameter	no	no	yes
Liquid Molar Volume	no	no	yes
Interaction Parameter	yes	yes	no

that each component of the mixture be characterised by its critical pressure, critical temperature, and acentric factor. In addition, the solubility parameter and the liquid molar volume of each component are used in the 'regular' solution model of Chao-Seader and Grayson-Streed. The values of these parameters for well-defined hydrocarbons are compiled in Reid et al. (50).

Heavier hydrocarbons such as bitumens and gas oils are not pure compounds but contain numerous constituents that would be difficult, if not impossible, to identify. Consequently these hydrocarbons are treated either as:

(i) single pseudo-substances,

(ii) fractions derived from distillation cuts, or

(iii) fractions that are further divided into three different groups, viz., paraffins, naphthenes, and aromatics (PNA).

The GPA-Peng-Robinson Programs (43) have a routine that calculates the critical properties and the acentric factor of heptane-plus fractions by the PNA analysis. This method requires the molecular weight (or the carbon number), weight average or volume average boiling point and the specific gravity of each undefined fraction as inputs. The method of Cavett (3), and that described in the API Data Book (1) are commonly used to characterise petroleum fractions. In these methods the boiling point parameters and the specific gravities are specified. In addition, molecular weights are required in the experimental determination of molar liquid

phase compositions. Detailed descriptions of these three methods follow.

2.4.1 Cavett Method

The pseudocritical temperature T_c (in degrees Rankine) is calculated from equation (2.44):

$$T_c = a_0 + a_1T + a_2T^2 + a_3AT + a_4T^3 + a_5AT^2 + a_6A^2T^2 \qquad (2.44)$$

where T = molal average boiling point, °F

A = °API

Constants a_0, a_1,..., a_6 are listed in Cavett (3).

The pseudocritical pressure P_c (in psia) is calculated using equation (2.45):

$$\log P_c = b_0 + b_1T + b_2T^2 + b_3AT + b_4T^3 + b_5AT^2 + b_6A^2T + b_7A^2T^2 \qquad (2.45)$$

where T = mean average boiling point, °F

Constants b_0, b_1,..., b_7 are listed in Cavett (3).

The acentric factor ω is derived from the following relationship:

$$\omega = -\log_{10} P_r - 1.0 \qquad (2.46)$$

where P_r is reduced vapor pressure at reduced temperature of 0.7.

In the absence of vapor pressure data, equation (2.47) proposed by Edmister (13) is used:

$$\omega = \frac{3 \ln P_c}{7(T_c/T - 1)} - 1 \qquad (2.47)$$

where T_c and P_c are calculated from equations (2.44) and (2.45), respectively. T is the mean average boiling point.

2.4.2 API Data Book Method

The boiling point data of each fraction is converted to ASTM D 86 temperatures using Figure 3A1.1 of Technical Data Book-Petroleum Refining (1). The molal average boiling point and mean average boiling point are obtained from Figure 2B1.1. The pseudocritical temperature and pressure are obtained from Figure 4D4.1. Figure 2B2.1, redrawn from the Winn nomograph, is used to calculate the molecular weight, given specific gravity and mean average boiling point. The acentric factor is obtained from Figure 2B2.3. The solubility parameter is derived from chart developed by Kesler and included in Chap. 8 of the Data Book.

The Winn nomograph was represented analytically by Sim and Daubert (60).

2.4.3 PNA Analysis

In this method it is assumed that the fractions can be divided into three groups, namely, *n*-alkanes, *n*-alkyl-cyclohexanes, and *n*-alkyl-benzenes, based on their molecular structures.

The normal boiling point temperatures have been fitted to an equation of the form:

$$\ln T_b = \sum_i C_i \, (n-6)^{i-1} \qquad (2.48)$$

for each of the hydrocarbon groups. T_b is the normal boiling point temperature (K) and n is the number of carbon atoms in the molecule. Constants C_i are listed in Table 1 of Peng and Robinson (42).

To generate the critical pressure values for the fractions a group contribution correlation of Lydersen (32) is used:

$$P_c = \frac{14.026n+\gamma}{(0.227n+\beta)^2} \qquad (2.49)$$

where P_c is in atmospheres. The coefficients β and γ are listed in Table 1 of (42).

Assuming a linear function between acentric factor and carbon number the following equation is derived:

$$\omega = f\, n + g \qquad (2.50)$$

where f and g, coefficients for all three groups, are listed in Table 1 of (42).

The critical temperature T_c is calculated from Edmister's equation (13), which rearranged gives:

$$T_c = S\, T_b \left\{1 + \frac{3 \ln P_c}{7(1+\omega)}\right\} \qquad (2.51)$$

where S is a correction factor given by equation (2.52):

$$S = 0.996704 + 0.00043155\, n \qquad (2.52)$$

The overall parameters for each cut can be calculated according to the following equations:

$$T_c = \sum_i x_i\, T_{ci} \qquad (2.53)$$

$$P_c = \sum_i x_i\, P_{ci} \qquad (2.54)$$

$$\omega = -\log\left\{\frac{\sum_i x_i P_{ci}\, 10^{-(1+\omega_i)}}{P_c} - 1\right\} \qquad (2.55)$$

where subscript i stands for paraffin, naphthenic, and aromatic.

In the GPA-Peng-Robinson Programs (43), the following options are permitted in order to characterise the undefined

components:

1. average carbon number (or molecular weight), specific gravity and boiling point for the entire fraction are specified,
2. carbon number (or molecular weight) and the PNA analysis are specified,
3. carbon number, weight average boiling point, and molecular weight are specified,
4. carbon number (or molecular weight), volume average boiling point, and specific gravity are provided, or
5. similar to (ii) except that the PNA analysis is given in terms of volume fractions instead of mole fractions.

Other methods exist that characterise particular groups of hydrocarbons and are restricted to fractions whose molecular weights and boiling points are far below those of bitumens. Recently Wilson et al. (71) proposed correlations predicting the critical properties of aromatic fractions.

It has become evident from recent studies that the correlation of hydrogen-hydrocarbon systems is not handled well by the SRK equation of state, particularly at conditions of high temperatures and pressures. The modified SRK and the PR equations were used to correlate the experimental hydrogen-heavy hydrocarbon VLE data. The results were compared with the Grayson-Streed predictions.

3. Solubility Experiments

3.1 Reagents and Materials

The samples of bitumens and hydrocracked fractions used in this study were obtained from the Department of Energy, Mines and Resources, and were received with the following notations:

1. 1-CL-77 Cold Lake Bitumen
2. 4-AB-77 Athabasca Bitumen
3. 3-LL-77 Lloydminster Residue
4. 2-AB-77 650°F+ Topped Athabasca Bitumen
5. 36-1 800°F+ Topped Athabasca Bitumen
6. 37-1 650°F+ Topped Cold Lake Bitumen
7. 6-CL-77 800°F+ Topped Cold Lake Bitumen
8. 3-LL-78 650°F+ Lloydminster Residue
9. 1-LL-78 760°F+ Lloydminster Residue
10. 4-AM-78 Amoco Feed
11. 91-1-1 60% Conversion Heavy End
12. 78-T-22 74.7% Conversion Heavy End
13. 78-T-23 80.1% Conversion Heavy End
14. 78-T-24 84.3% Conversion Heavy End
15. EMR Gas Oil

Samples 1 to 10 are the feedstocks of the CANMET Process. The Heavy Ends (samples 11-14) and the EMR Gas Oil are the products. The properties of the solvents 1-10, supplied by EMR, are listed in Tables 2 to 4 at the end of this section, along with those of a conventional crude oil

(47). Molecular weights of solvents 1, 2, 3, 5 and 14, determined by the Hydrocarbon Research Centre using the osmometric method, are given in Table 8.

The boiling point distributions of the solvents 4, 8, and 10 (adjusted to ASTM D 2892 atmospheric equivalent) are listed in Tables 5-7. The original Hempel distillation data for solvents 4, 8 and 10, supplied by EMR, are listed in Tables 48-50 of Appendix III. These data were not suitable for characterization of the bitumen feedstocks due to their very high residue contents.

Mesitylene was obtained from Eastman Organic Chemicals and had a boiling range of 160-163°C. Hydrogen was obtained from Linde in 6000 psi cylinders with reported purity of 99.995%, and hydrogen sulphide supplied by Matheson Gas Products was C.P grade with minimum purity of 99.6%. Sub-bituminous and Lignite coal samples (-200 mesh) were supplied by the Department of Energy, Mines and Resources, Ottawa.

3.2 Experimental Procedure

The equilibrium cell used was a 2 litre, 316 stainless steel Magnedrive autoclave (Model AF 2005) from Autoclave Engineers Inc. Equilibrium pressures were monitored with 0-340 bar and 0-1000 psi 316 stainless steel Heise Bourdon tube gauges which had been calibrated against a dead weight gauge. The temperature of the cell was measured with a type J iron-Constantan thermocouple inserted into a thermowell

TABLE 2

Properties of Cold Lake Bitumen and Conventional Oil

		Cold Lake Bitumen			Conv.
		(1-CL-77)	(37-1)	(6-CL-77)	Oil
Sp. Gravity	15/15°C	0.999	1.020	1.0333	0.84-0.9
Sulphur	wt %	4.30	4.80	5.54	0.1-2.0
Ash	wt %	0.03	0.076	0.073	nil
CCR	wt %	14.6	14.4	18.2	1-2
Vanadium	ppm (wt)	130	133	153	2-10
Nickel	ppm (wt)	92	-	-	total metals
Carbon	wt %	82.98	83.7	83.99	86
Hydrogen	wt %	10.05	10.34	10.25	13.5
Nitrogen	wt %	0.34	0.46	0.48	0.2
Viscosity at 99°C	cSt	94	309	2009	3-7
Pitch	wt %	48	-	-	-
H/C		0.121	0.124	0.122	0.157

TABLE 3

Properties of Athabasca Bitumen

		(4-AB-77)	(2-AB-77)	(36-1)
Sp. Gravity	15/15°C	1.009	1.023	1.042
Sulphur	wt %	4.48	4.97	5.49
Ash	wt %	0.59	0.66	0.73
CCR	wt %	13.3	15.0	19.6
Vanadium	ppm (wt)	213	184	193
Nickel	ppm (wt)	67	-	-
Carbon	wt %	83.36	83.32	82.49
Hydrogen	wt %	10.52	10.27	9.85
Nitrogen	wt %	0.43	0.44	-
Viscosity at 99°C	cSt	210	413	2237
Pitch	wt %	51.5	-	-
H/C		0.126	0.123	0.119

TABLE 4

Properties of Lloydminster Residue and Amoco Feed

		Lloydminster Residue			Amoco
		(3-LL-77)	(3-LL-78)	(1-LL-78)	Feed
Sp. Gravity	15/15°C	1.033	1.000	1.032	0.95
Sulphur	wt %	5.02	4.34	5.30	3.42
Ash	wt %	0.04	0.035	0.067	0.1
Vanadium	ppm (wt)	124	146	210	124
Nickel	ppm (wt)	-	66	92	37
Carbon	wt %	83.71	86.16	82.57	82.25
Hydrogen	wt %	9.91	10.57	10.11	11.37
Nitrogen	wt %	0.34	0.31	0.63	0.29
Viscosity at 99°C	cSt	3691	188	-	12
H/C		0.118	0.123	0.122	0.138

TABLE 5

Boiling Point Distribution for Topped Athabasca Bitumen (2-AB-77)

	Temperature °C									
	IBP-175	175-200	200-225	225-250	250-275	275-307	307-336	336-364	364-392	392-419	419+
% Vol	0.3	0.4	0.6	1.2	6.2	1.7	1.1	3.9	7.5	12.2	64.6
Sp Gr	.824	.824	.824	.838	.868	.881	.902	.927	.940	.957	1.058
S %	3.08	3.08	3.08	2.83	2.84	2.93	3.10	2.98	3.03	3.23	5.09
N %	.006	.006	.006	.008	.013	.018	.024	.062	.089	.132	.667

IBP 152°C

TABLE 6

Boiling Point Distribution for Lloydminster Residue (3-LL-78)

	Temperature °C								
	IBP-225	225-250	250-275	275-307	307-336	336-364	364-392	392-419	419+
% Vol	0.3	1.2	2.0	1.2	3.9	6.3	5.7	9.2	69.3

IBP 218°C

TABLE 7

Boiling Point Distribution for Amoco Feed (4-AM-78)

	Temperature °C									
	IBP-200	200-225	225-250	250-275	275-307	307-336	336-364	364-392	392-419	419+
% Vol	3.3	8.0	9.9	10.4	7.7	7.2	3.9	3.7	6.5	38.1
Sp Gr	.800	.820	.843	.859	.874	.889	.912	.935	.964	1.065
S %	<0.3	<0.3	<0.3	0.41	0.63	0.92	1.57	2.42	3.42	5.98
N %	trace	trace	.002	.004	.010	.017	.037	.073	.130	.710

IBP 176°C

TABLE 8

Molecular Weights of Selected Solvents

1-CL-77 Cold Lake Bitumen	515
4-AB-77 Athabasca Bitumen	522
3-LL-77 Lloydminster Residue	864
36-1 800°F+ Topped Athabasca Bitumen	732
78-T-24 84.3% Conversion Heavy End	332
EMR Gas Oil	250[1]

1 by API Method

extending into the liquid phase. The thermocouple was calibrated against a platinum resistance thermometer for use in the range 0° to 402°C. Temperatures were controlled to within ±0.5°C. The details of the apparatus are shown in Figure 2.

For each run, approximately 500 cc of solvent was charged into the autoclave and the system flushed with hydrogen. The reactor was brought to the desired temperature and the hydrogen pressure was set approximately by adjusting the cylinder delivery pressure. Stirring was commenced and maintained during the entire process at 600 rpm, except during sample withdrawal. Pressure declined as a result of hydrogen dissolution. The cell was left overnight to ensure equilibrium was achieved.

Samples of the vapor were withdrawn from the top of autoclave and analysed using a Hewlett-Packard Model 5710A gas chromatograph with a 1/4 inch O.D 2 metre long column containing Porapak QS, 50-80 mesh packing. The column was operated isothermally at 90°C with a high purity nitrogen carrier gas flowing at 25 ml/min. A thermal conductivity detector was used. Typical vapor analysis showed hydrogen concentration in excess of 99% by volume.

The stirrer was stopped before liquid samples were withdrawn from the cell into a weighed sampling flask. The gases evolved from the liquid were measured volumetrically by displacement of mercury from a calibrated burette. The amount of gas remaining in the bitumen at atmospheric

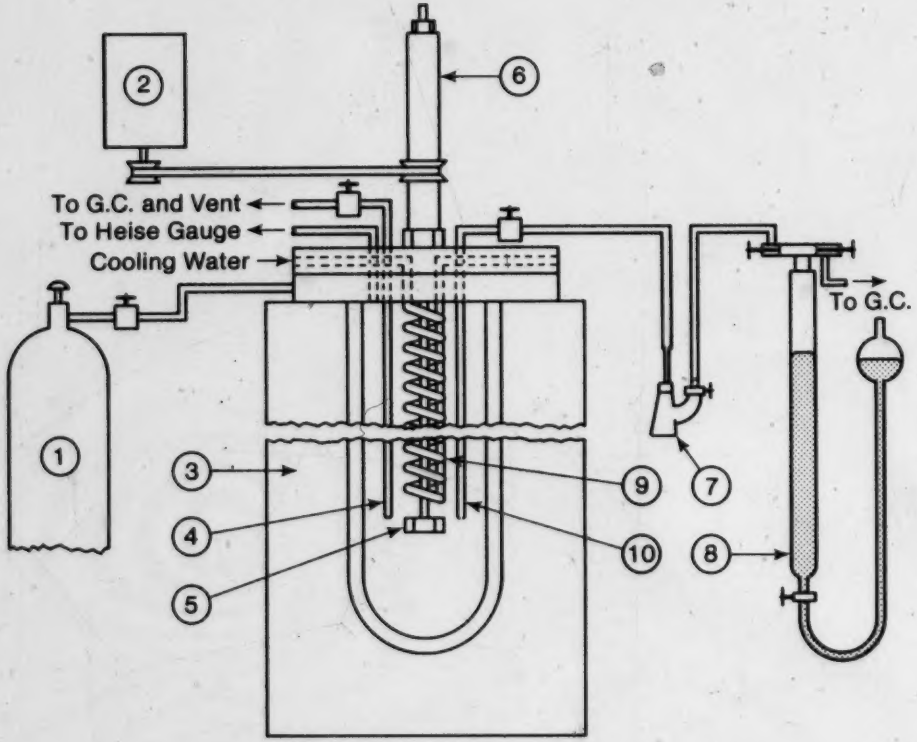

Legend

1. Gas cylinder
2. Stirrer motor
3. Heating jacket
4. Thermocouple well
5. Stirrer
6. Magnedrive
7. Liquid sample flask
8. Calibrated burette
9. Cooling coil
10. Liquid sample line

Figure 2 Schematic Diagram of the Apparatus

temperature and pressure was, at most, of the order of 1% of the total gas evolved. After volume measurement the gases were passed through a gas chromatograph for analysis. From this analysis, knowing the barometric pressure, ambient temperature, and total gas volume, the weight of hydrogen dissolved in the solvent was computed using the ideal gas law. By weighing the loaded sampling flask, the weight of the solvent was determined by difference, and the solubility calculated as grams hydrogen per gram solvent. From the molecular weights of the solvent and the solute gas, the solubility was converted to mole fraction.

A similar procedure was used to determine the solubility of hydrogen sulphide and carbon dioxide in these solvents. In the measurement of hydrogen solubility in slurries the stirrer was only slowed down during sampling to prevent coal particles from settling.

4. Results and Discussion

To confirm the sampling and analytical procedures, the solubility of hydrogen in mesitylene was determined at 200°C. The results are presented in Table 12 of Appendix I and are compared with data available in the literature (12,44) at 204°C in Figure 3. The data of Eakin and DeVaney (12) are for a ternary mixture containing hydrogen sulphide. The present results are in agreement with the literature values within a few percent.

4.1 Solubility of Hydrogen in Bitumens

Experimental data for the solubility of hydrogen in bitumens, hydrocracked products and EMR Gas Oil, reported as g hydrogen/g bitumen, are listed in Tables 13 to 27 of Appendix I. The results are plotted on Figures 4 to 15. Most of the data were obtained at 200° and 300°C; however a few points were measured at 100°, 250° and 370°C. For a particular sample, at a given pressure, the solubility of hydrogen increases with increasing temperature, an effect typical of hydrogen systems.

Comparisons of the solubility plots leads to the following observations:

1. The solubility of hydrogen in Athabasca and Cold Lake bitumens is essentially the same.
2. Results for the 650°F+ and 800°F+ topped bitumen products, with the exception of the 800°F+ Topped Cold Lake Bitumen (6-CL-77) at 200°C, support a conclusion

that hydrogen solubility decreases with increasing average molecular weight of the bitumen samples. The solubility in 6-CL-77 at 200°C is higher than expected. The solubility of hydrogen is essentially the same for the two 650°F+ products and for the two 800°F+ products except for the Cold Lake 800°F+ topped product at 200°C. The solubility in this topped Cold Lake product is approximately 15% higher than that in the topped Athabasca bitumen at 200°C.

3. The solubility of hydrogen in Lloydminster heavy oil is approximately 15% less than in Athabasca bitumen. However the solubility in the 650°F+ and 760°F+ Lloydminster residues is about the same as for the Athabasca Bitumen.
4. The solubility of hydrogen in Amoco feed is approximately 25% higher than in Athabasca Bitumen.
5. The solubility of hydrogen in EMR gas oil is approximately 10% higher than in Amoco Feed.
6. The solubility of hydrogen in 60% Conversion Heavy Ends is higher than in the 74.7% to 84.3% Conversion Heavy Ends at hydrogen partial pressures greater than approximately 8.0 MPa.

Significant cracking occurred for all samples investigated at 370°C; thus comparisons between samples of data obtained at this temperature are not valid.

The linear relationship between pressure and solubility enables one to estimate an apparent Henry's constant, H,

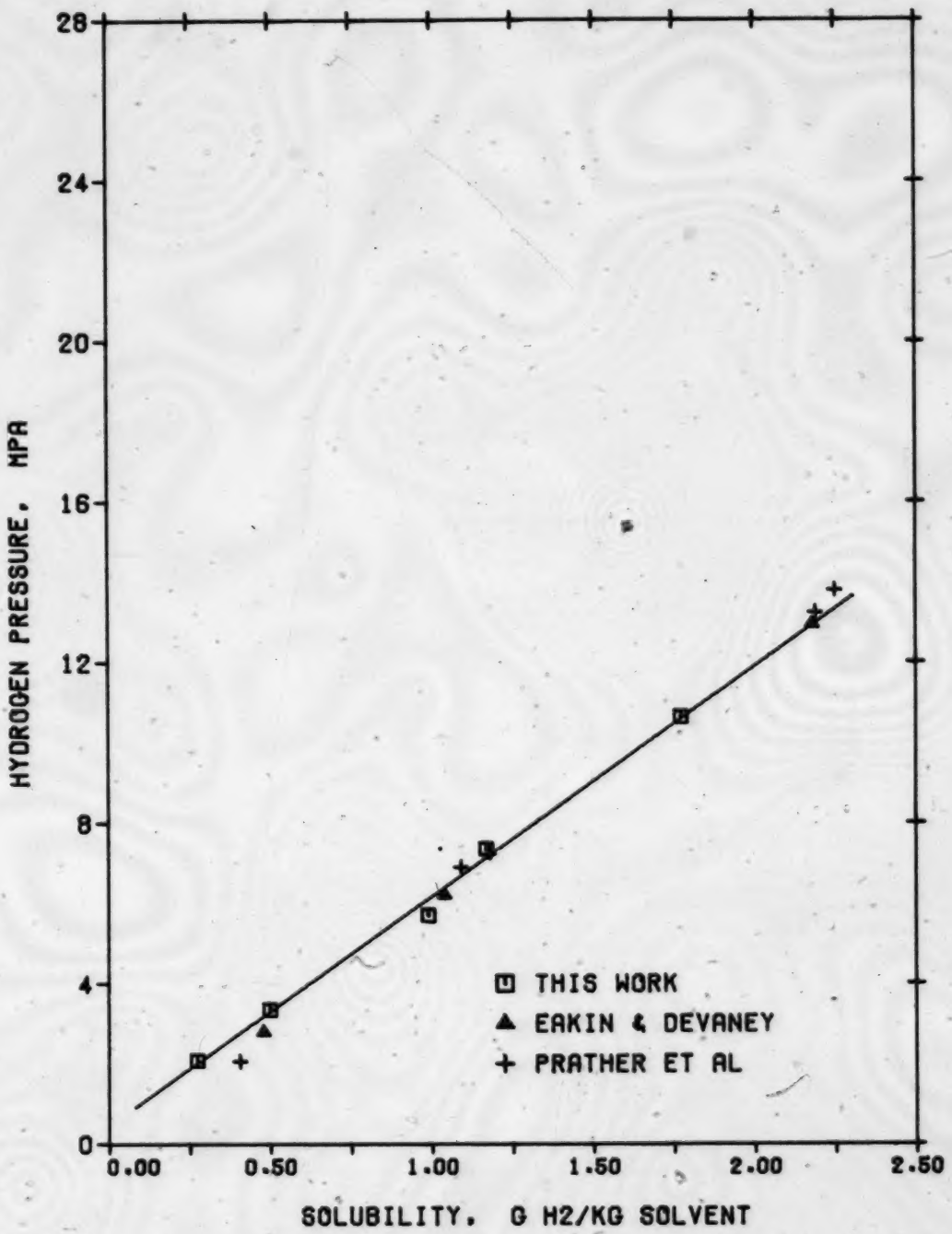

FIG 3 H2 SOLUBILITY IN MESITYLENE AT 204 C

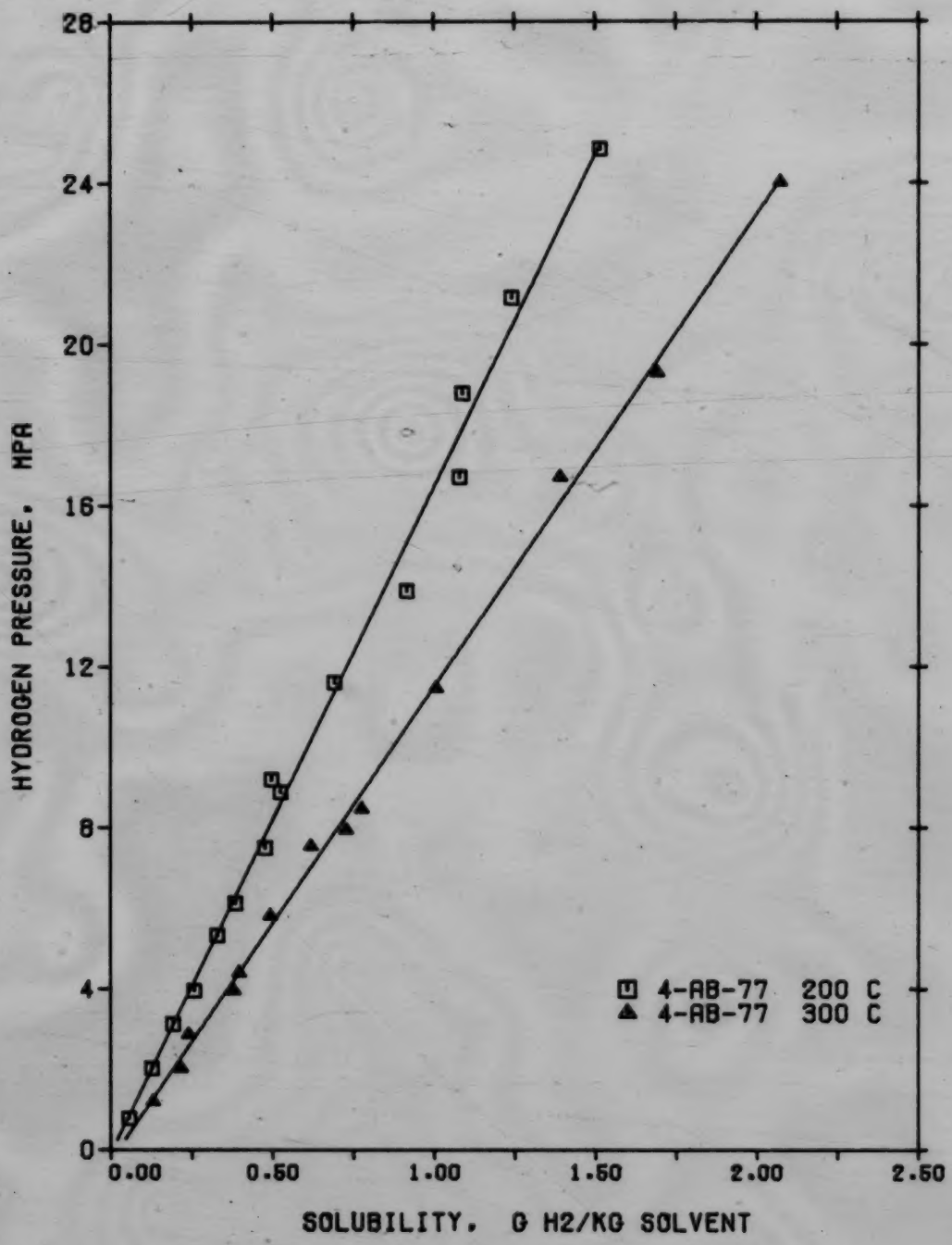

FIG 4 SOLUBILITY OF H2 IN ATHABASCA BITUMEN

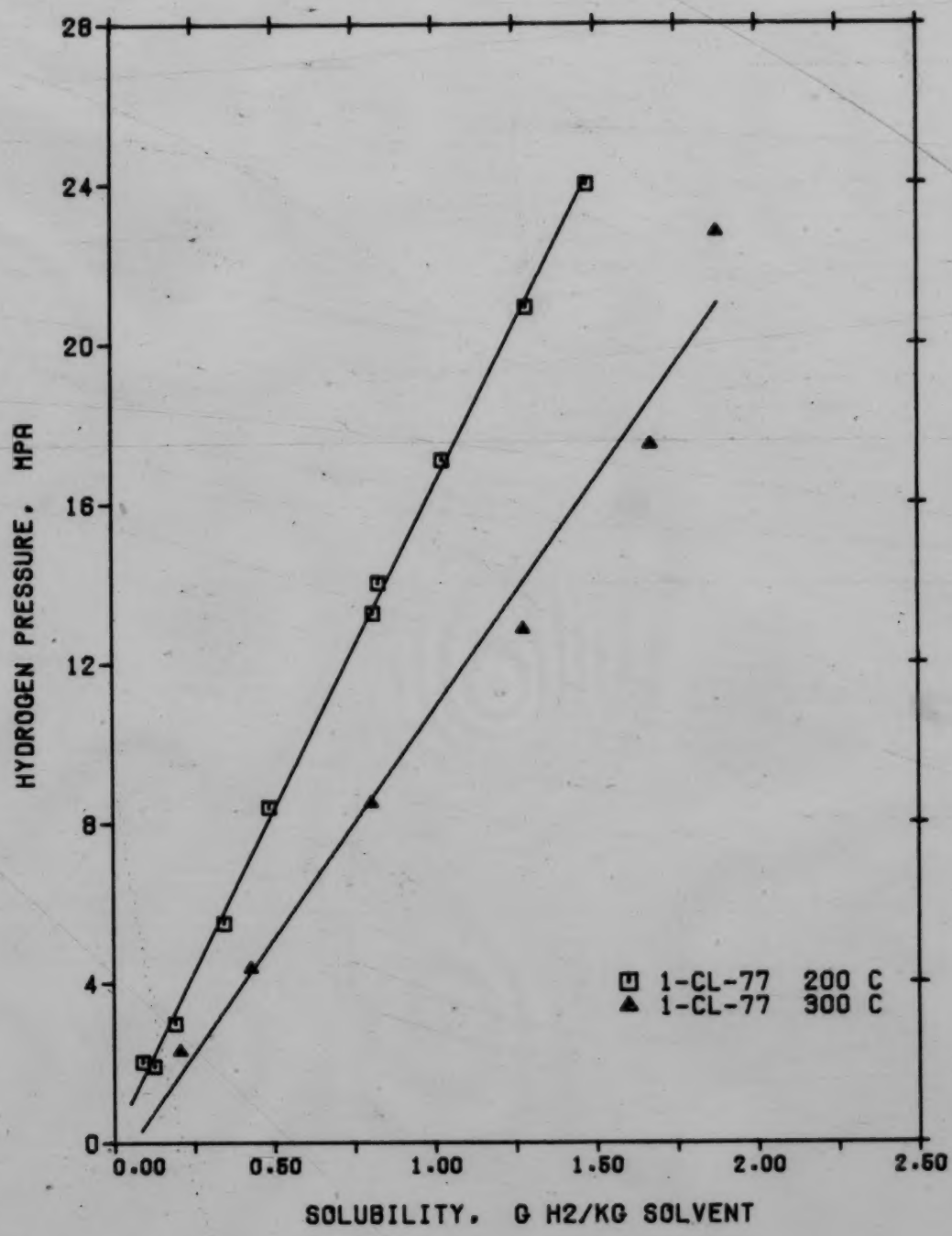

FIG 5 SOLUBILITY OF H2 IN COLD LAKE BITUMEN

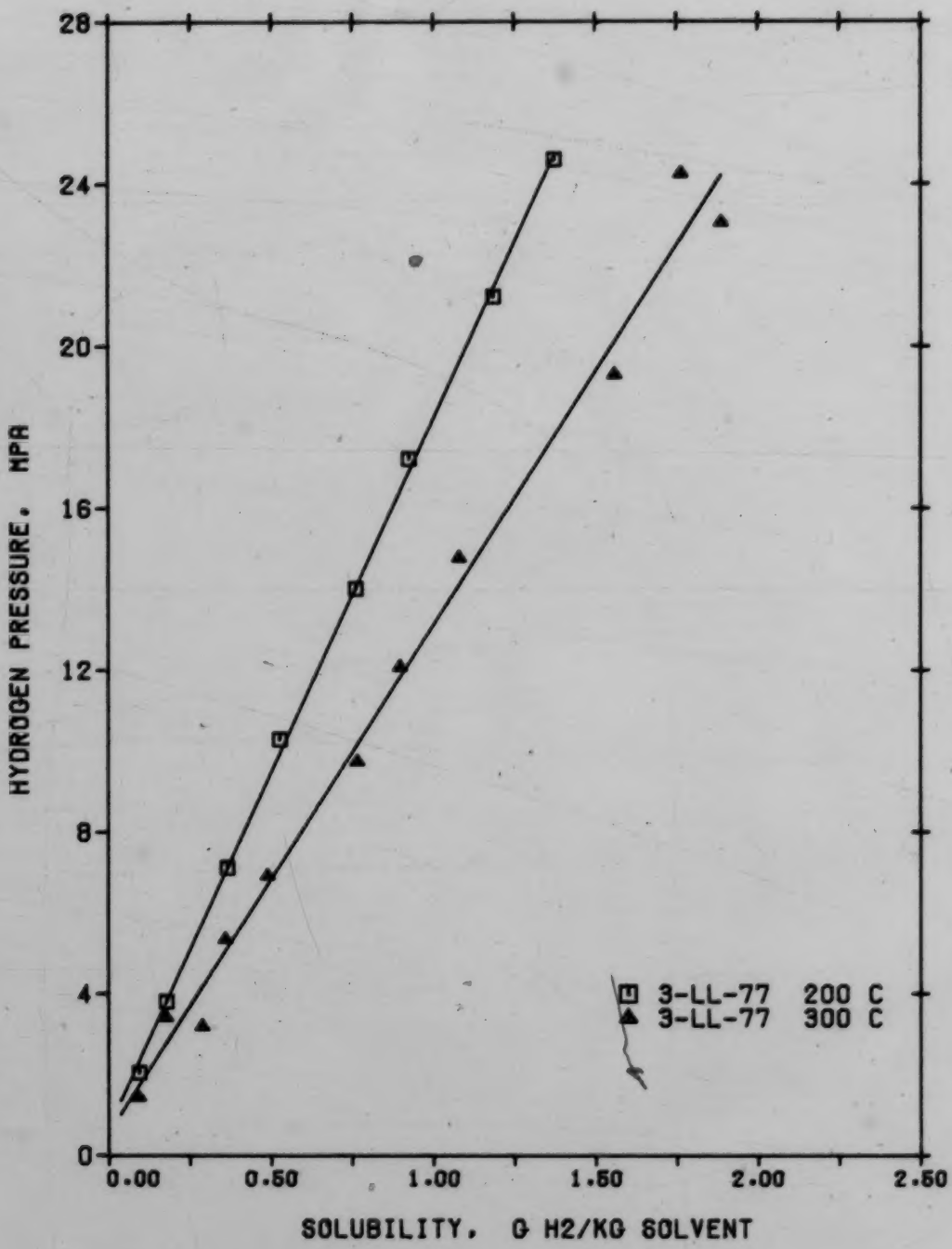

FIG 6 SOLUBILITY OF H2 IN LLOYDMINSTER RESIDUE

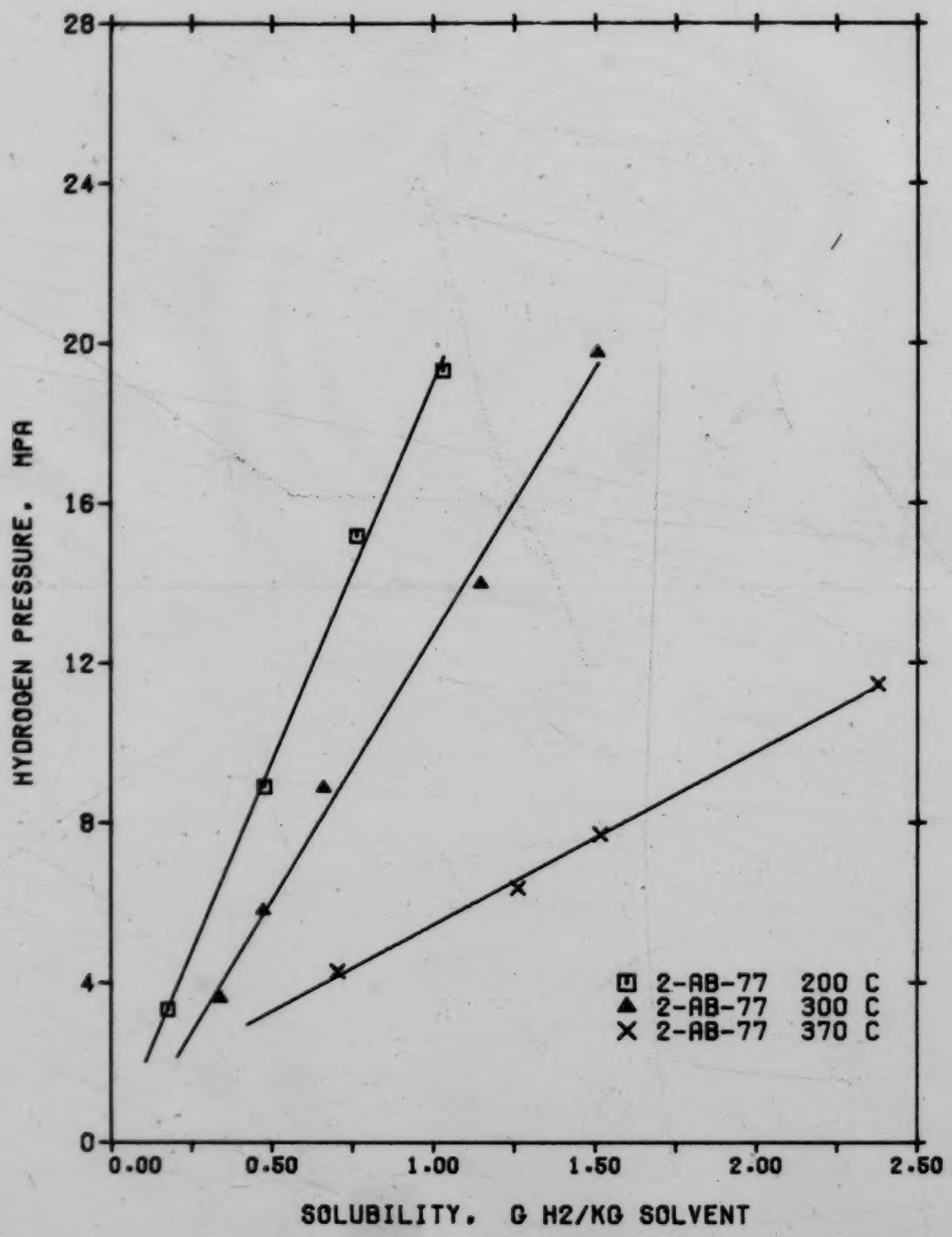

FIG 7 SOLUBILITY OF H2 IN 650 F+ TOPPED ATHABASCA BITUMEN

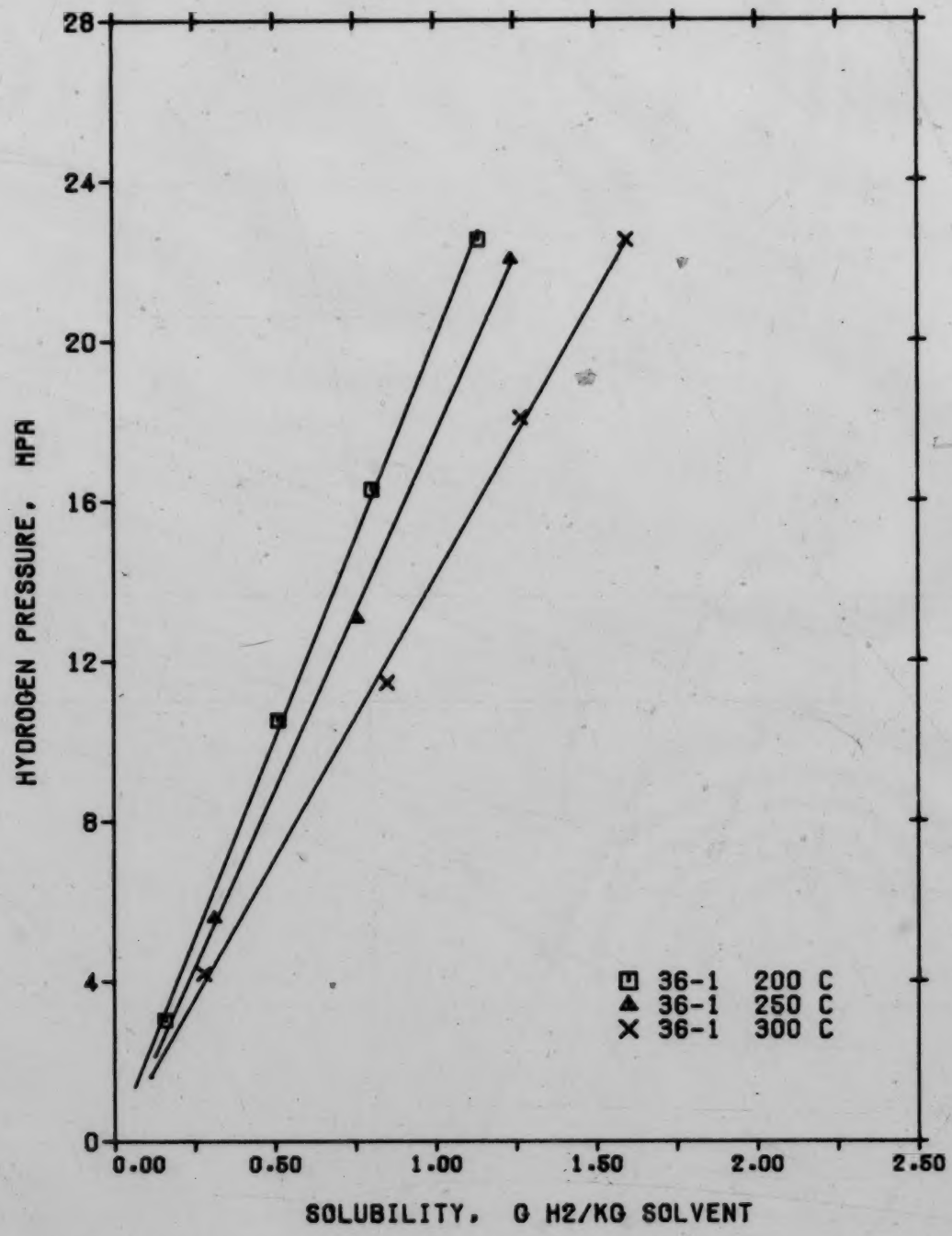

FIG 8 SOLUBILITY OF H2 IN 800 F+ TOPPED ATHABASCA BITUMEN

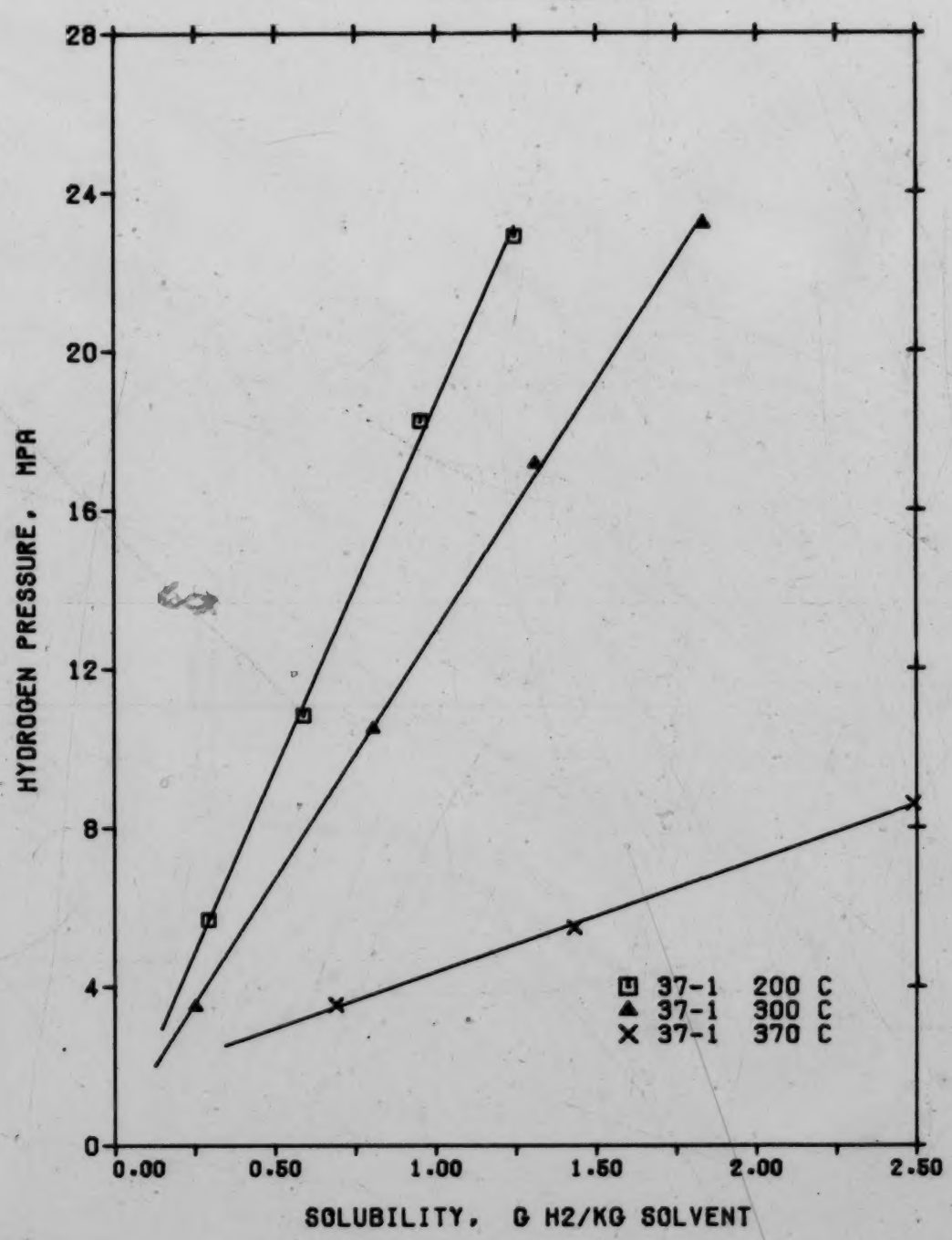

FIG 9 SOLUBILITY OF H2 IN 650 F+ TOPPED COLD LAKE BITUMEN

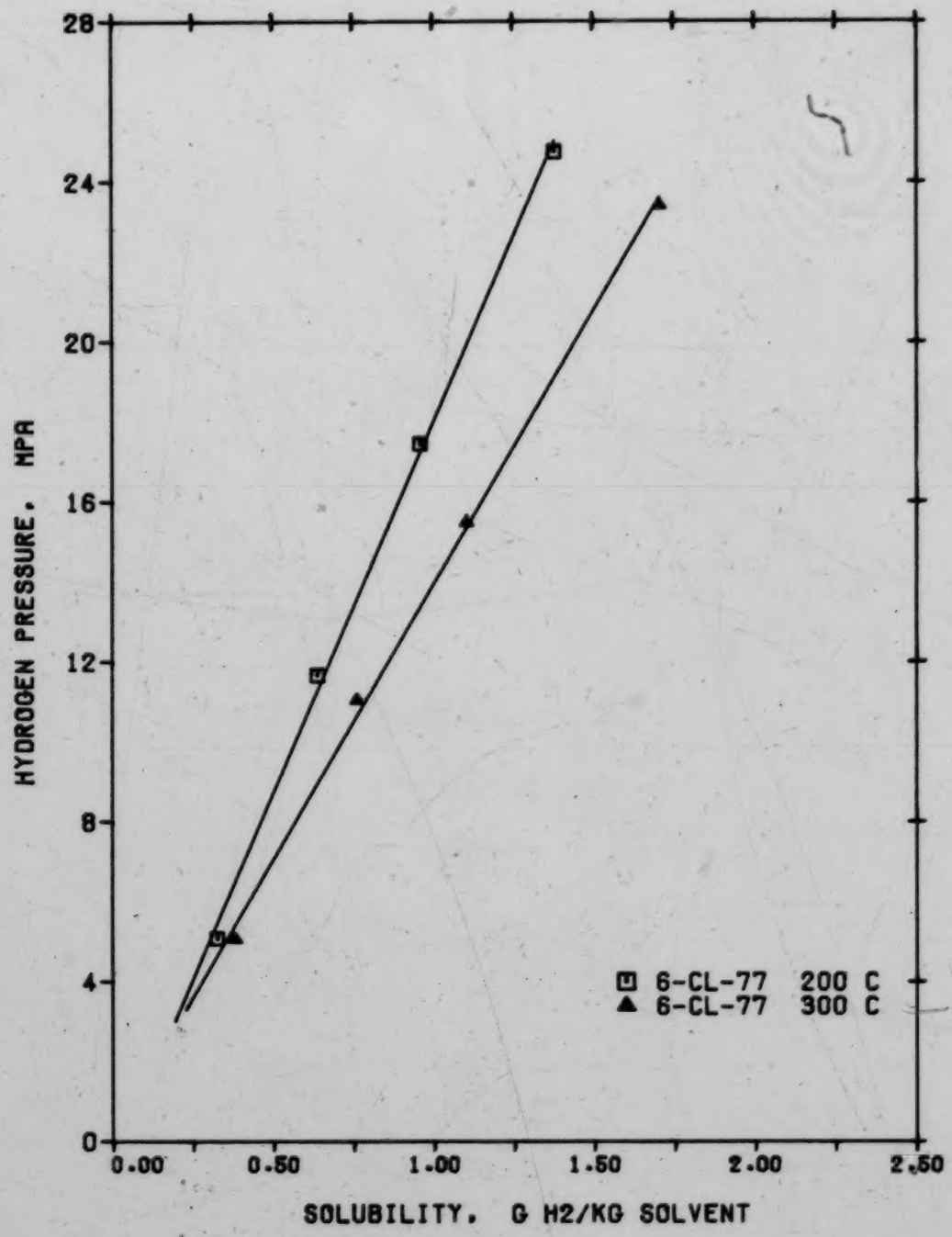

FIG 10 SOLUBILITY OF H2 IN 800 F+ TOPPED COLD LAKE BITUMEN

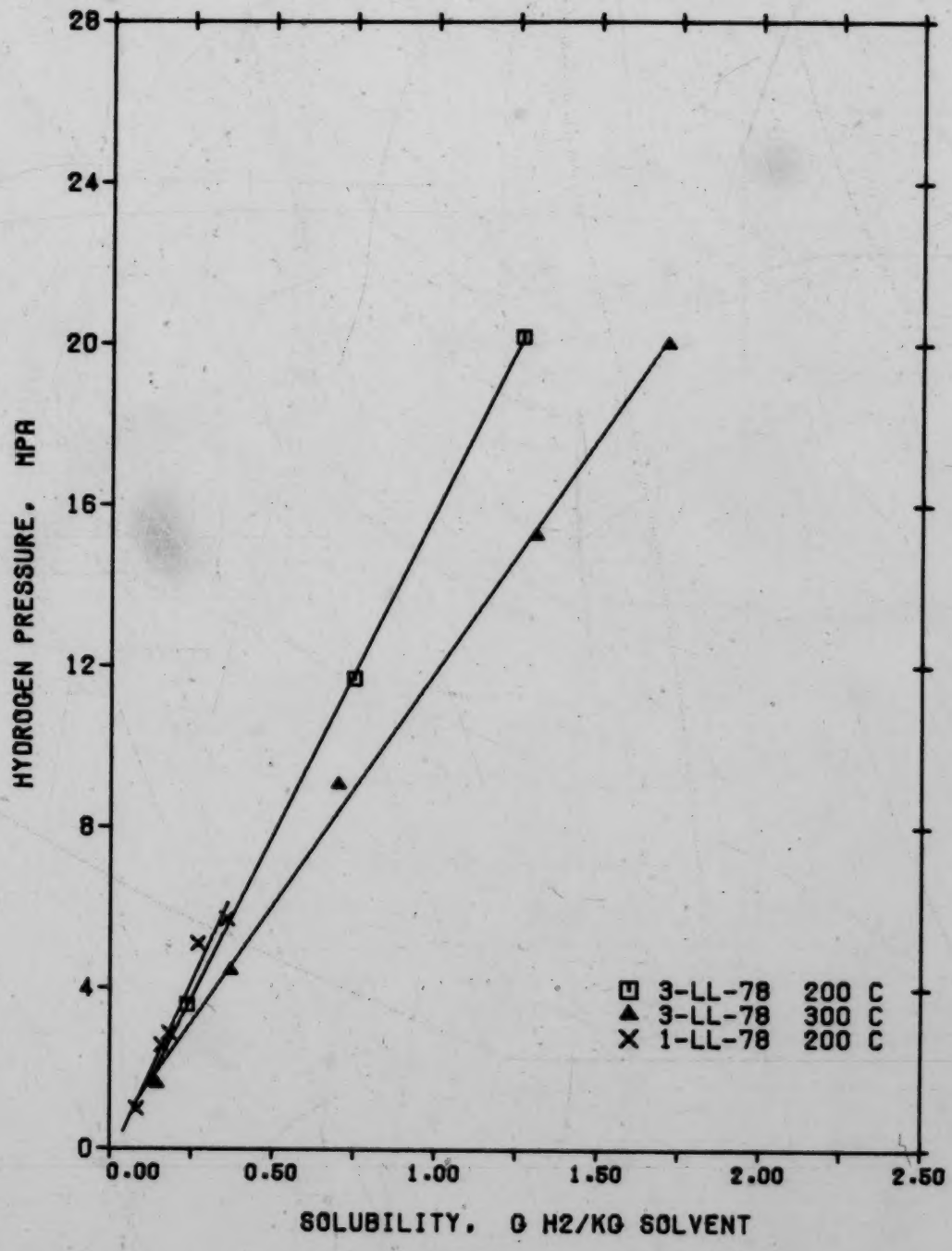

FIG 11 SOLUBILITY OF H2 IN LLOYDMINSTER RESIDUE

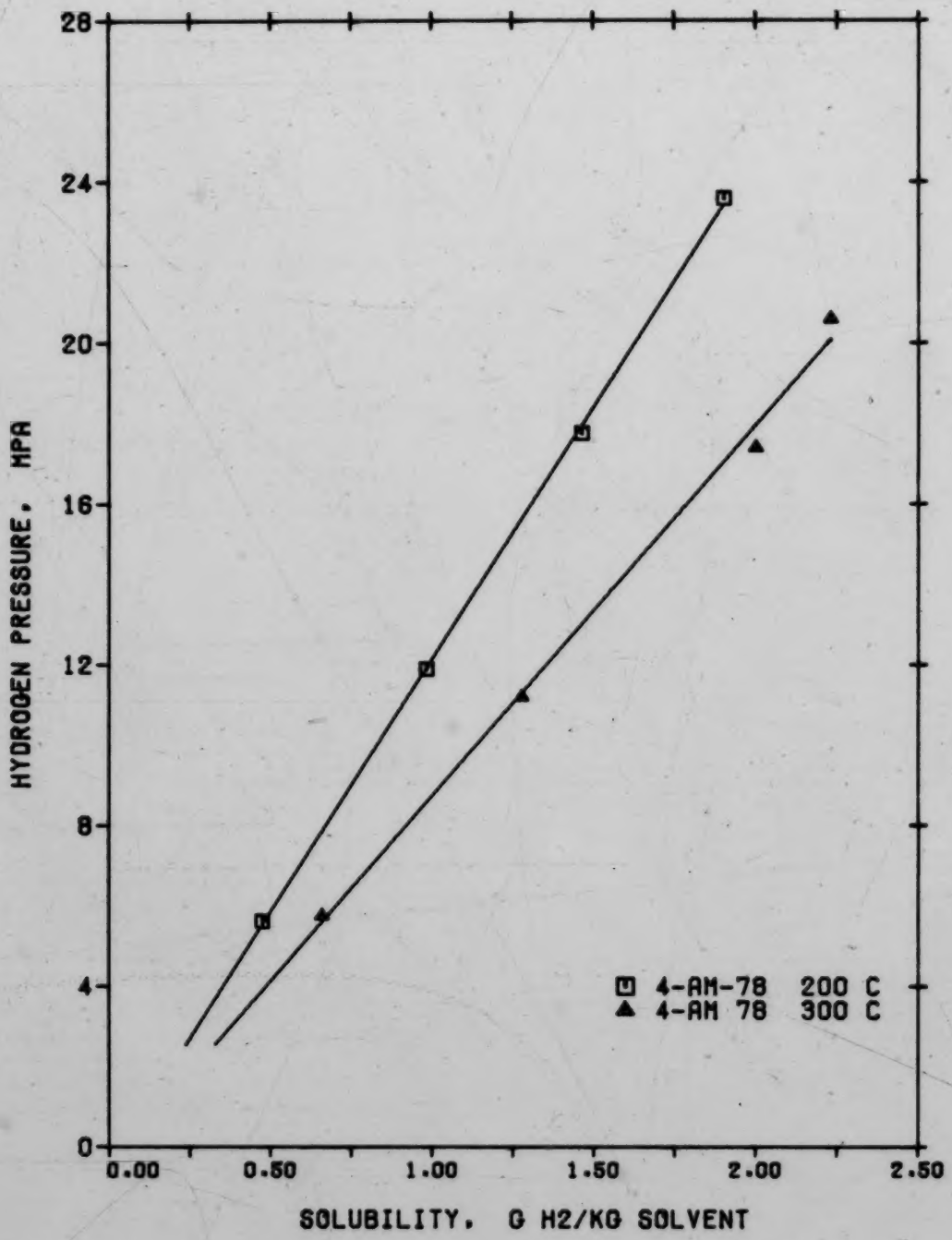

FIG 12 SOLUBILITY OF H2 IN AMOCO FEED

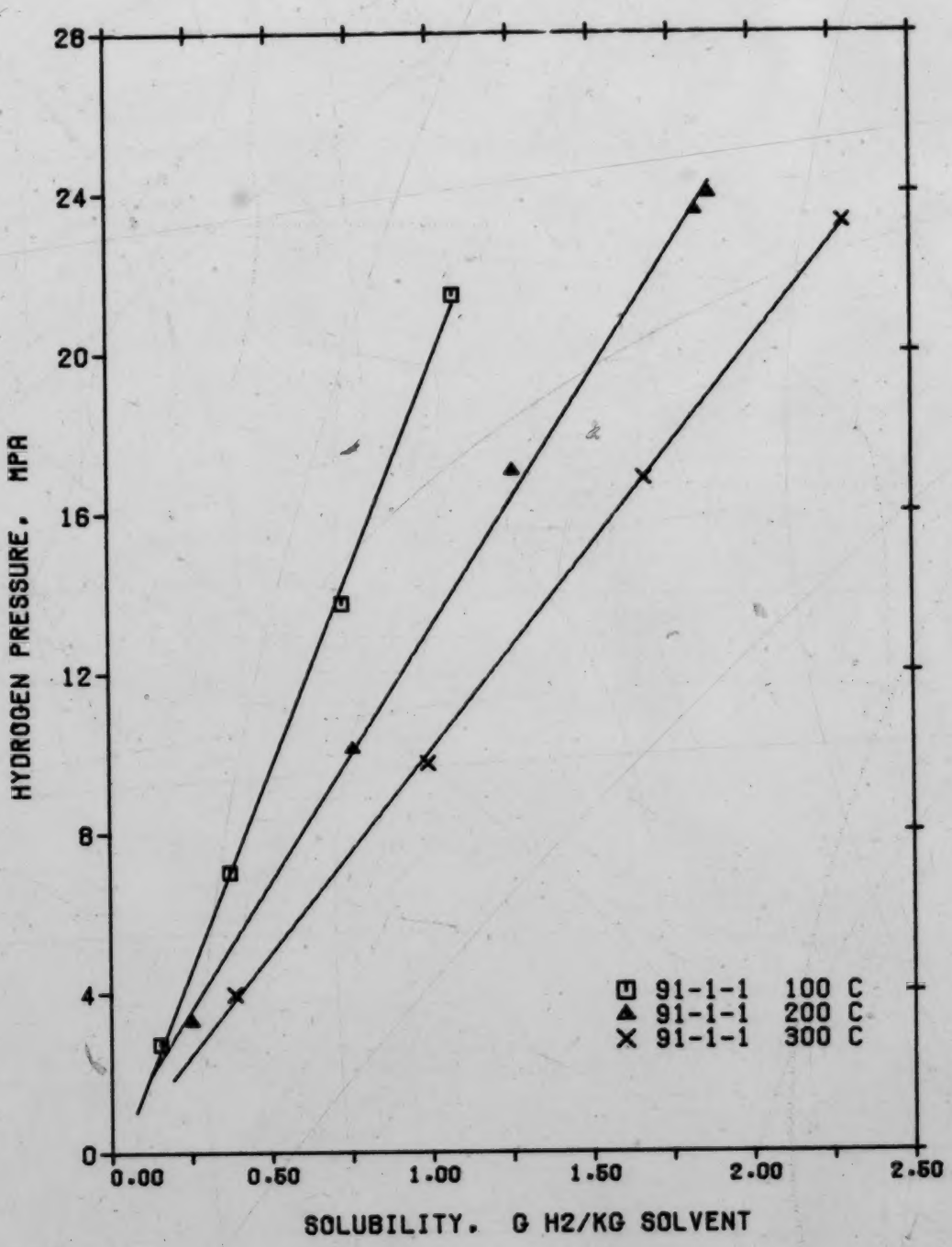

FIG 13 SOLUBILITY OF H2 IN 60% CONVERSION HEAVY END

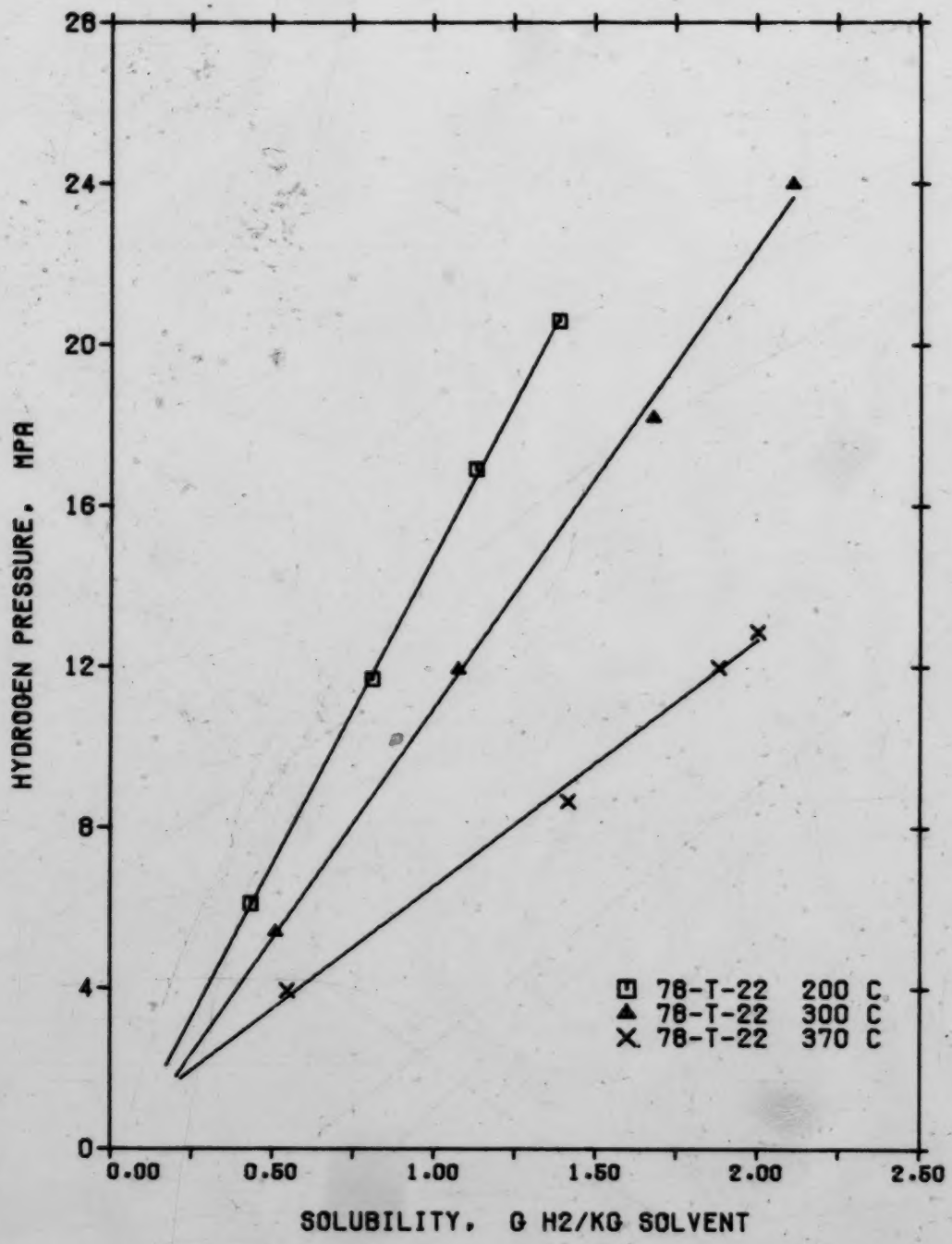

FIG 14 SOLUBILITY OF H2 IN 74.7% CONVERSION HEAVY END

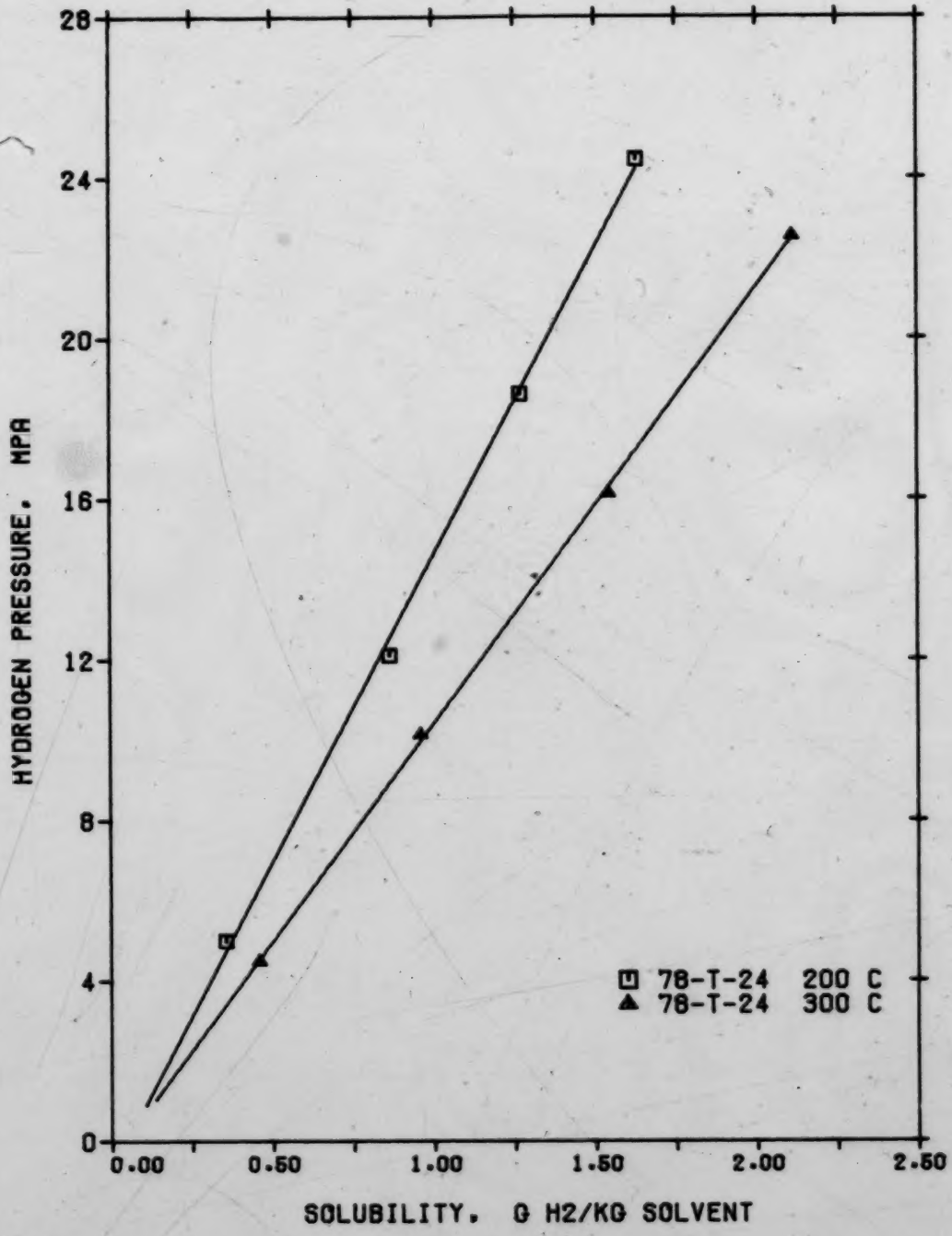

FIG 15 SOLUBILITY OF H2 IN 84.3% CONVERSION HEAVY END

equal to the slope of the pressure-solubility line. The lower the value of H, the higher is the solubility, and vice versa. From these data, the effect of solvent molecular weights on the solubility can be studied by plotting H against solvent molecular weight. Table 9 lists the solvent molecular weights and the Henry's constants, H, at 200° and 300°C. The plot of H versus molecular weight is shown on Figure 16. There is sharp increase in H up to molecular weight of 350 and then a slow increase above 350. Also, H increases with decrease in temperature, as expected.

4.2 Solubility of Hydrogen in Slurries

The results for the solubility of hydrogen at 200° and 300°C in a 10 wt.% sub-bituminous coal-90 wt.% Cold Lake bitumen slurry, reported as g hydrogen/g bitumen are given in Table 28. The results are plotted on Figure 17. The solubility is essentially the same as in the Cold Lake Bitumen. Results for 40 wt.% slurries of Cold Lake Bitumen and sub-bituminous and lignite coals respectively are given in Tables 29 and 30 and Figures 18 and 19 for temperatures of 200°, 250° and 300°C. The results are interesting and show a decrease in solubility with an increase in temperature up to a pressure of approximately 16.5 MPa and then an increasing solubility with increasing temperature at

TABLE 9

Effect of Molecular Weight on Apparent Henry's Constant

Mol Wt	Apparent Henry's Constant (MPa (kg bitumen/g H_2))	
	200°C	300°C
250	10.78	7.59
332	15.31	10.85
515	16.22	11.50
522	16.50	11.73
864	17.47	12.53

	(MPa (kg bitumen/g H_2S))	
	200°C	300°C
332	0.106	0.297
522	0.134	0.218

	(MPa (kg bitumen/g CO_2))	
	50°C	150°C
250	0.0638	0.1312
	50°C	300°C
522	0.0865	0.2052

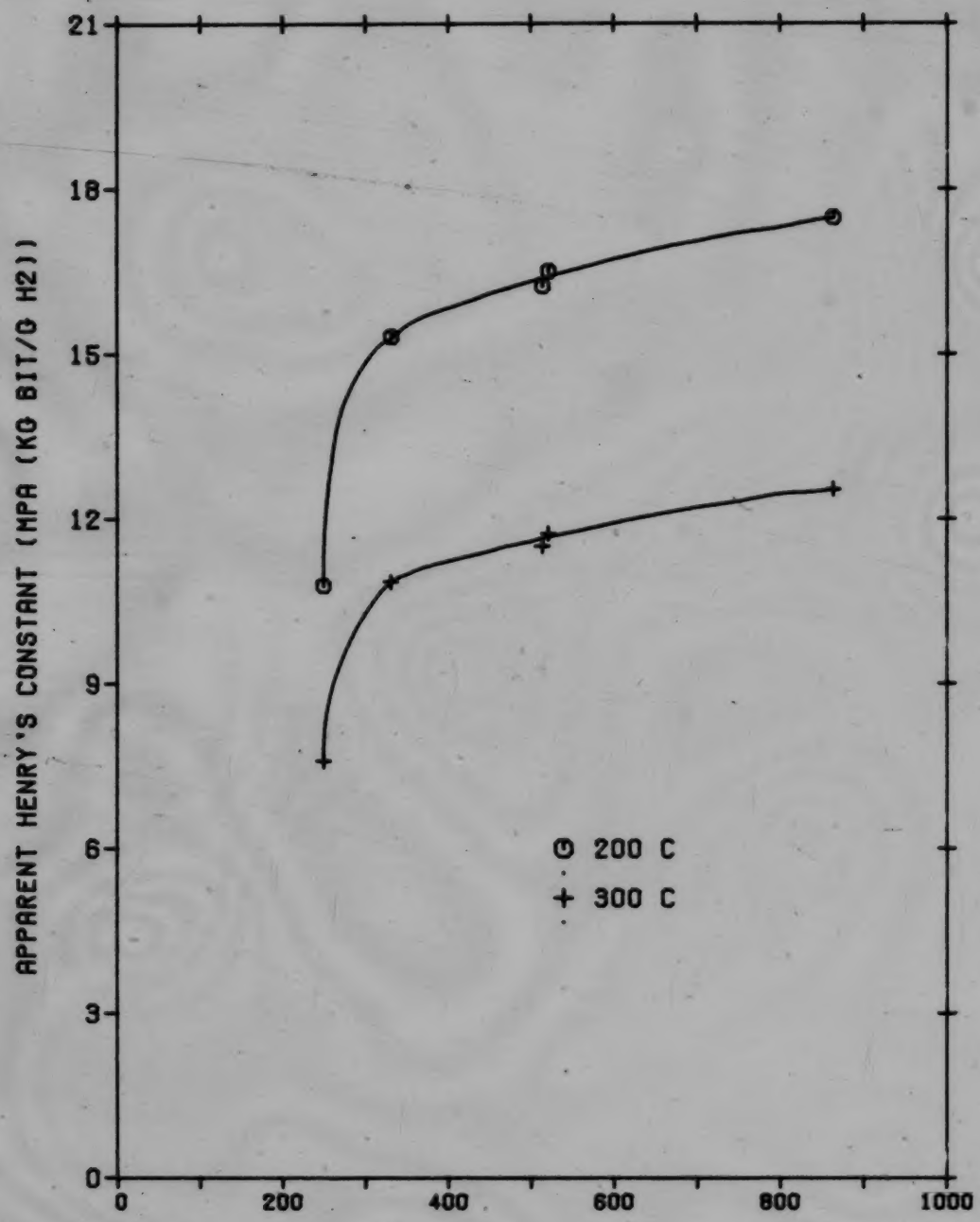

FIG 16 EFFECT OF SOLVENT MOLECULAR WEIGHT ON APPARENT HENRY'S CONSTANT

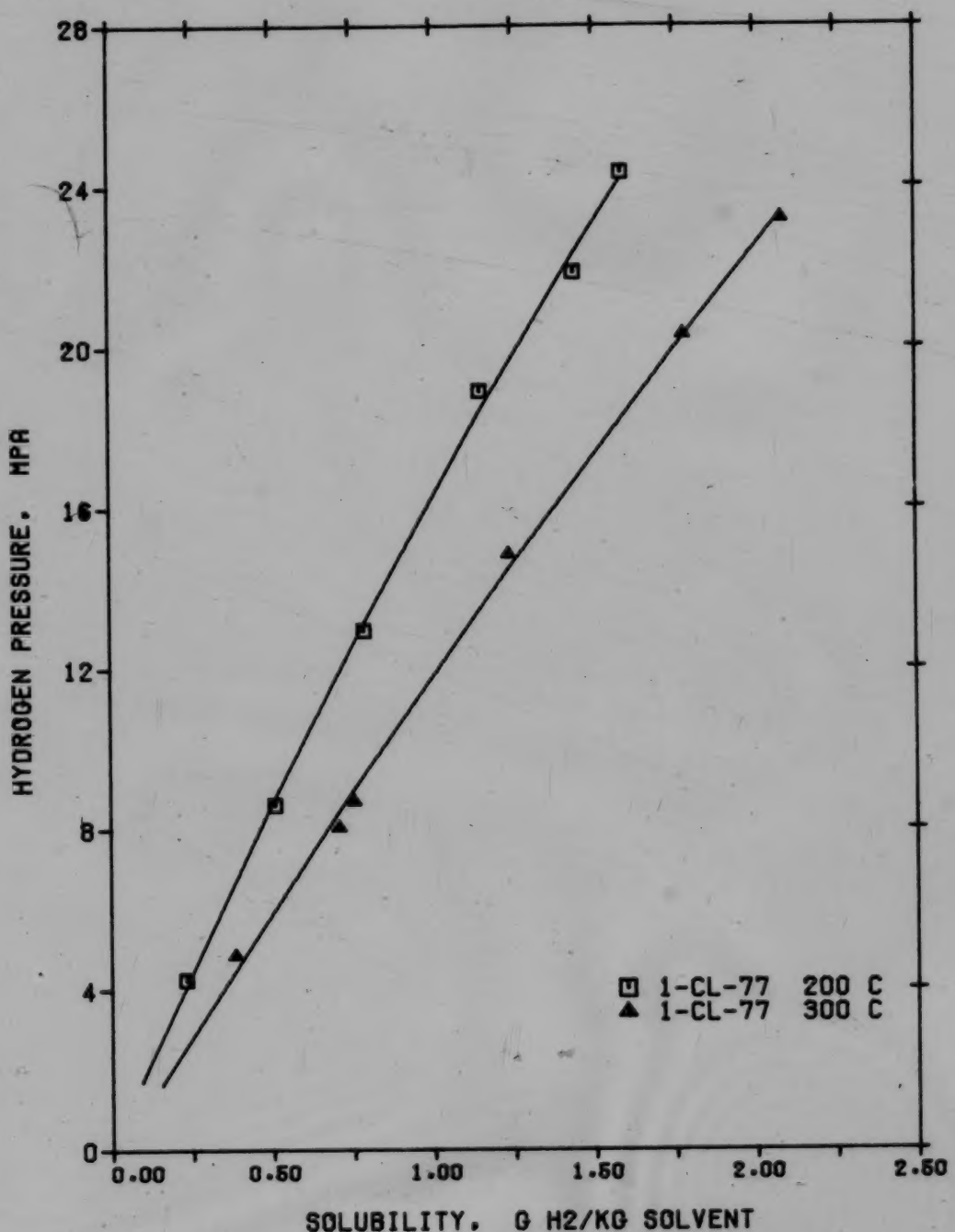

FIG 17 HYDROGEN SOLUBILITY IN 10 WT %
SUB-BITUMINOUS COAL/BITUMEN SLURRY

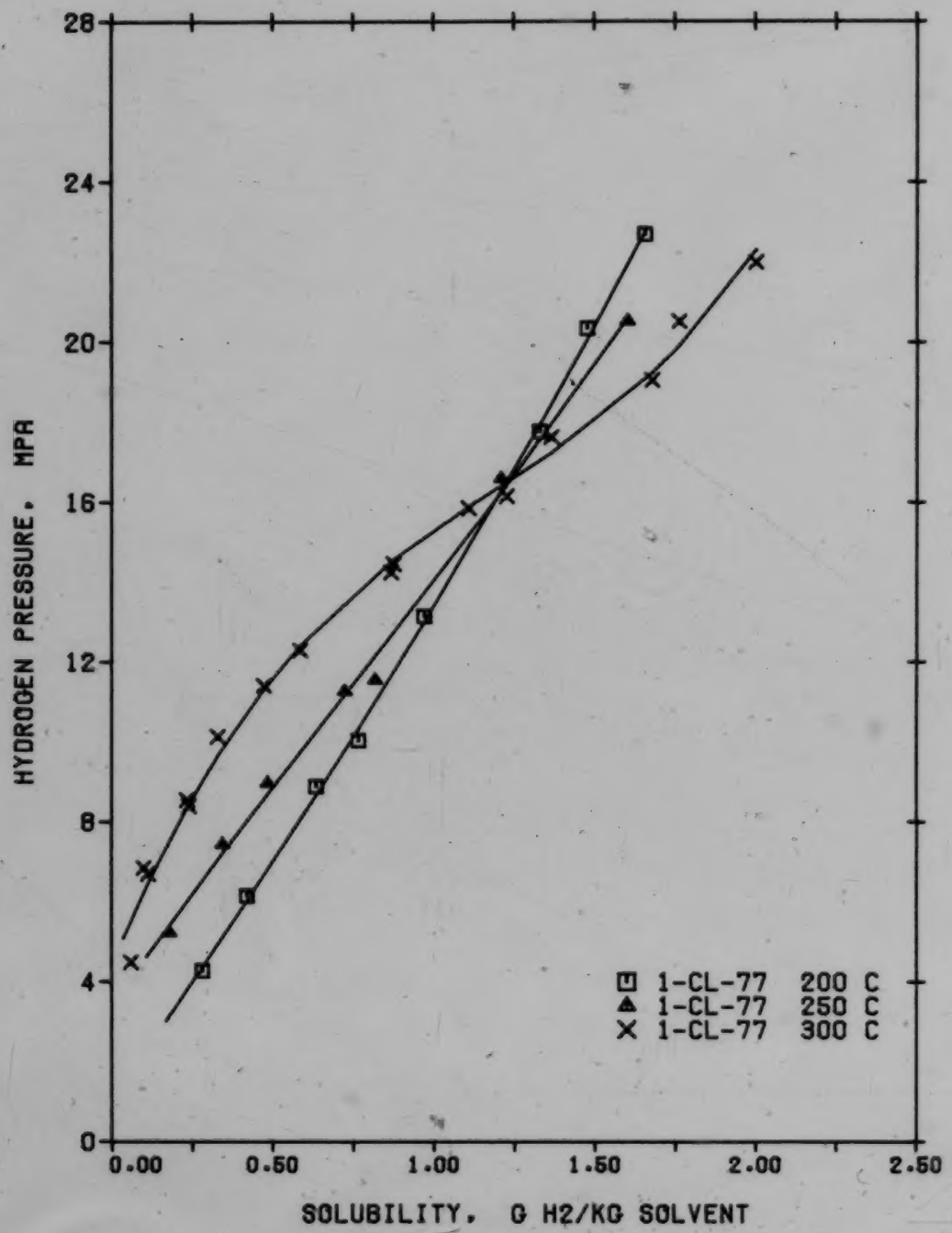

FIG 18 HYDROGEN SOLUBILITY IN 40 WT %
SUB-BITUMINOUS COAL/BITUMEN SLURRY

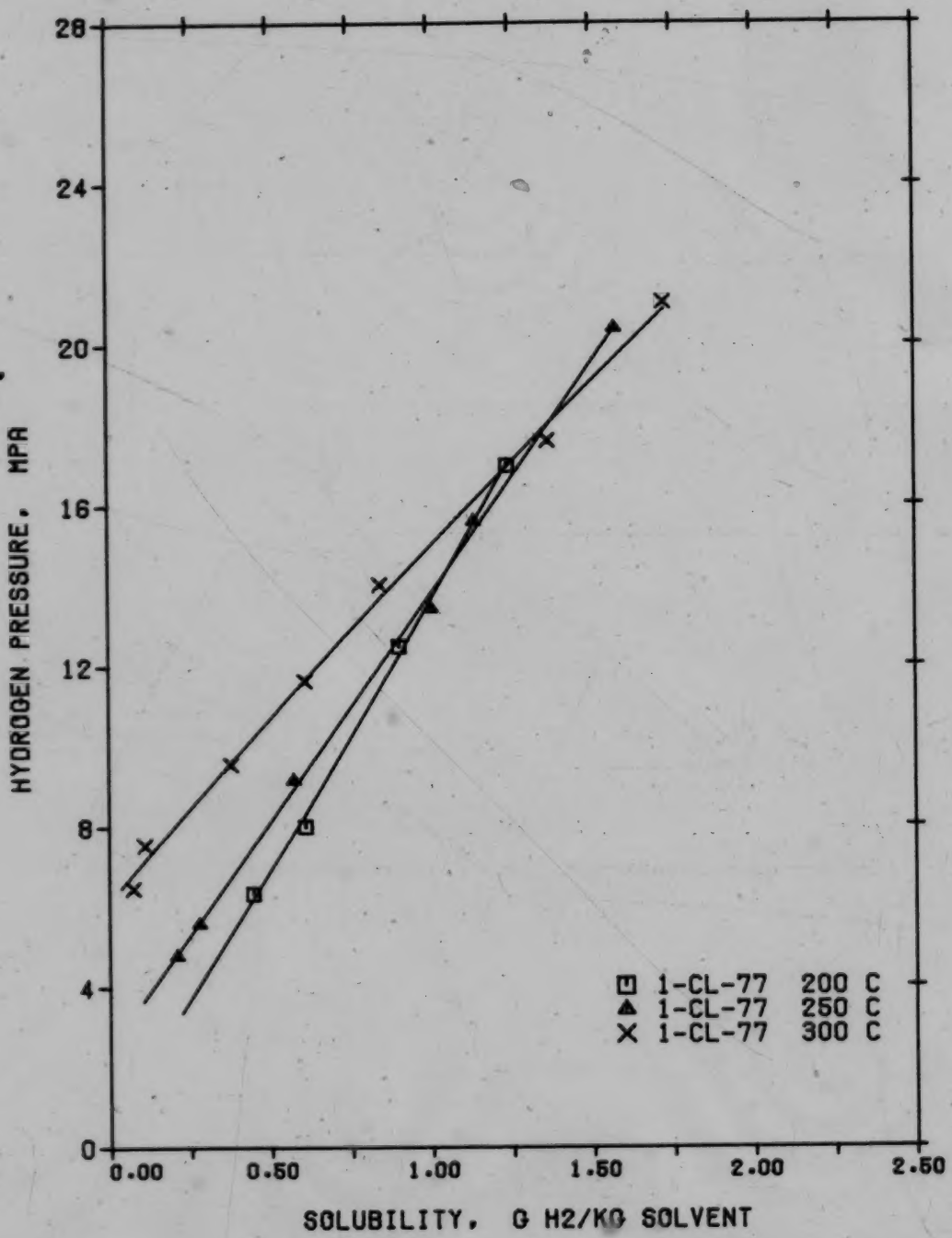

FIG 19 HYDROGEN SOLUBILITY IN 40 WT %
LIGNITE COAL/BITUMEN SLURRY

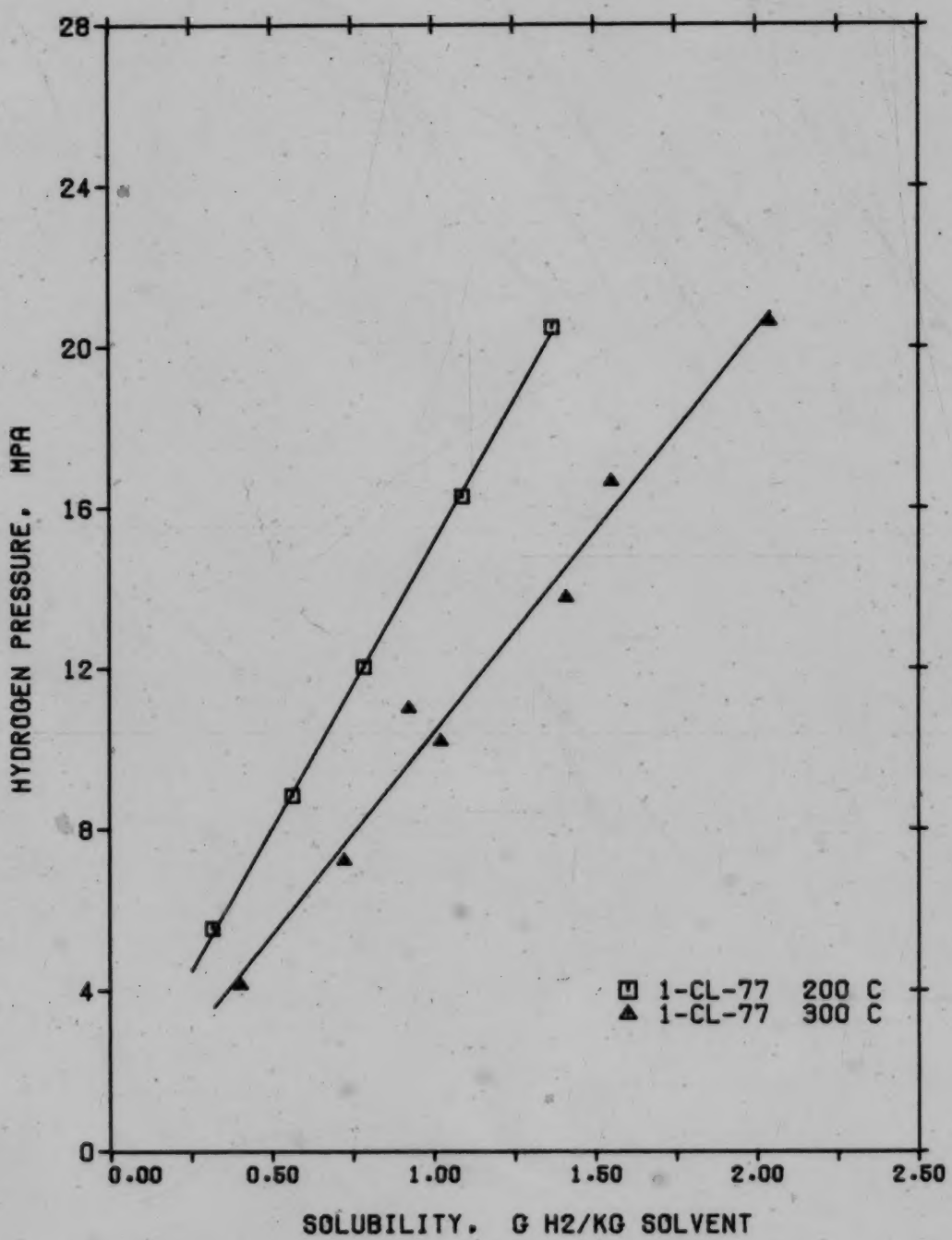

FIG 20 HYDROGEN SOLUBILITY IN 25 WT %
SUB-BITUMINOUS COAL/BITUMEN SLURRY

higher pressures. Measurements were made in a random order and with several different initial charges to confirm this result. The type of coal does not appear to have a significant effect on the hydrogen solubility. The solubility is higher in the slurry than in Cold Lake Bitumen at 200°C but lower at 300°C at hydrogen partial pressures up to 20.0 MPa. At higher partial pressures, at 300°C, the solubility appears to be the same as in Cold Lake Bitumen.

Data for a 25 wt.% slurry are given in Table 31 and are plotted on Figure 20. The solubility of hydrogen for this slurry increases with increasing temperature over the range of hydrogen partial pressures investigated and is higher than in Cold Lake bitumen.

4.3 Solubility of H_2S and CO_2 in Bitumens

Equilibrium solubility data for hydrogen sulphide in Athabasca Bitumen and Heavy End (78-T-24) are given in Tables 32 and 33 and are plotted on Figures 21 and 22. The solubility decreases with rising temperatures and is the same for both samples at 200°C. At 300°C, the solubility of hydrogen sulphide is higher in the Athabasca Bitumen. Solubility data for the EMR Gas Oil are given in Table 34 for 100°, 200° and 300°C. The data for 100° and 300°C are plotted on Figure 23. The solubility is higher in the EMR Gas Oil than in the heavier Athabasca Bitumen.

The apparent Henry's constants, H, for hydrogen sulphide are listed in Table 9. They are estimated at zero

solubilities. The values increase with increasing temperature.

Carbon dioxide solubility data in Athabasca Bitumen and EMR Gas Oil are listed in Tables 35 and 36, respectively. Temperatures range from 50° to 200°C, with pressures up to 6.4 MPa. The data are plotted on Figures 24 and 25. The solubility decreases with rising temperatures, as expected. It is higher in the EMR Gas Oil compared to that in the higher molecular weight Athabasca Bitumen.

The apparent Henry's constants, H, are listed in Table 9 for carbon dioxide in EMR Gas Oil at 50° and 150°C and in Athabasca Bitumen at 50° and 300°C. The values increase with increasing temperature and increasing solvent molecular weight.

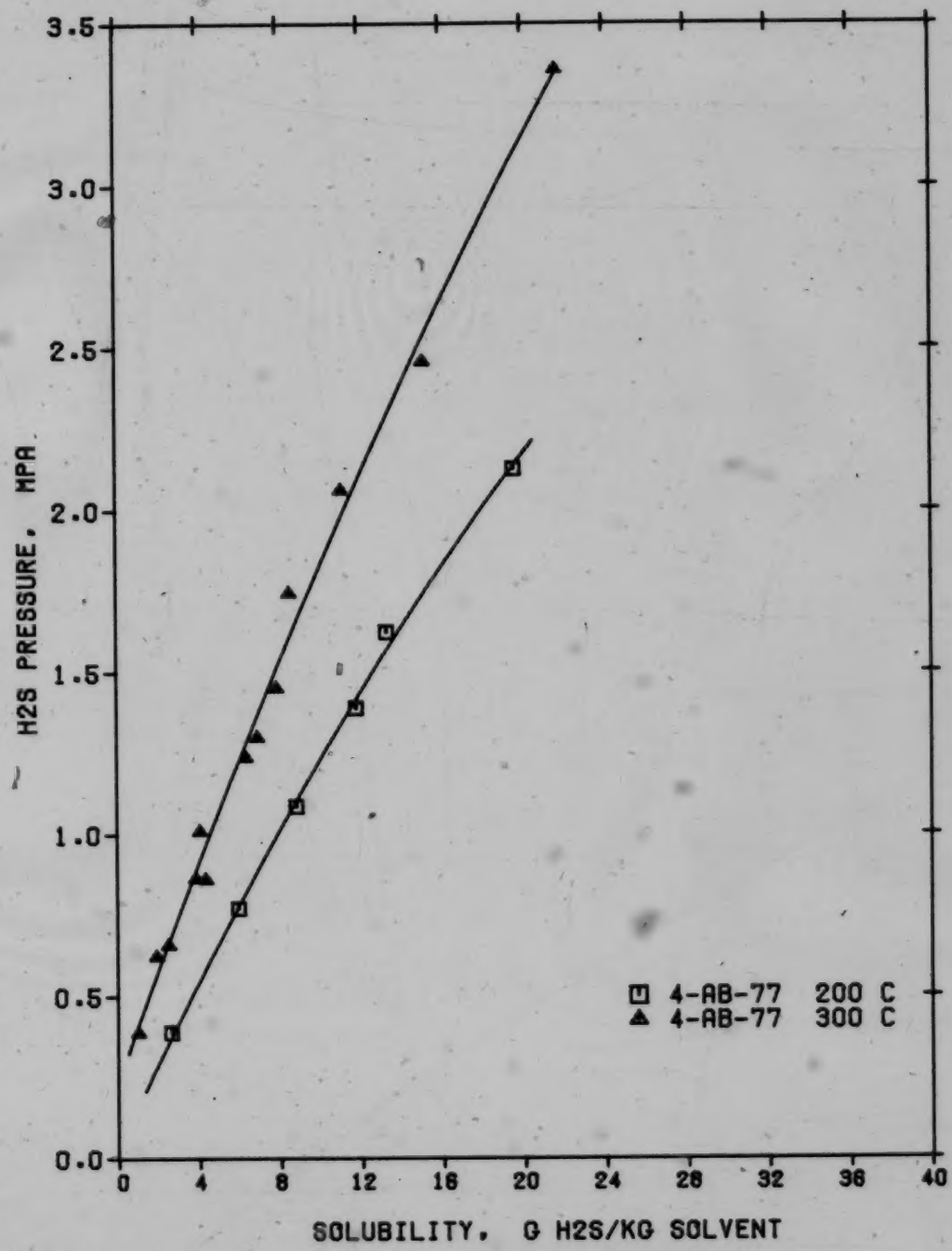

FIG 21 SOLUBILITY OF H2S IN ATHABASCA BITUMEN

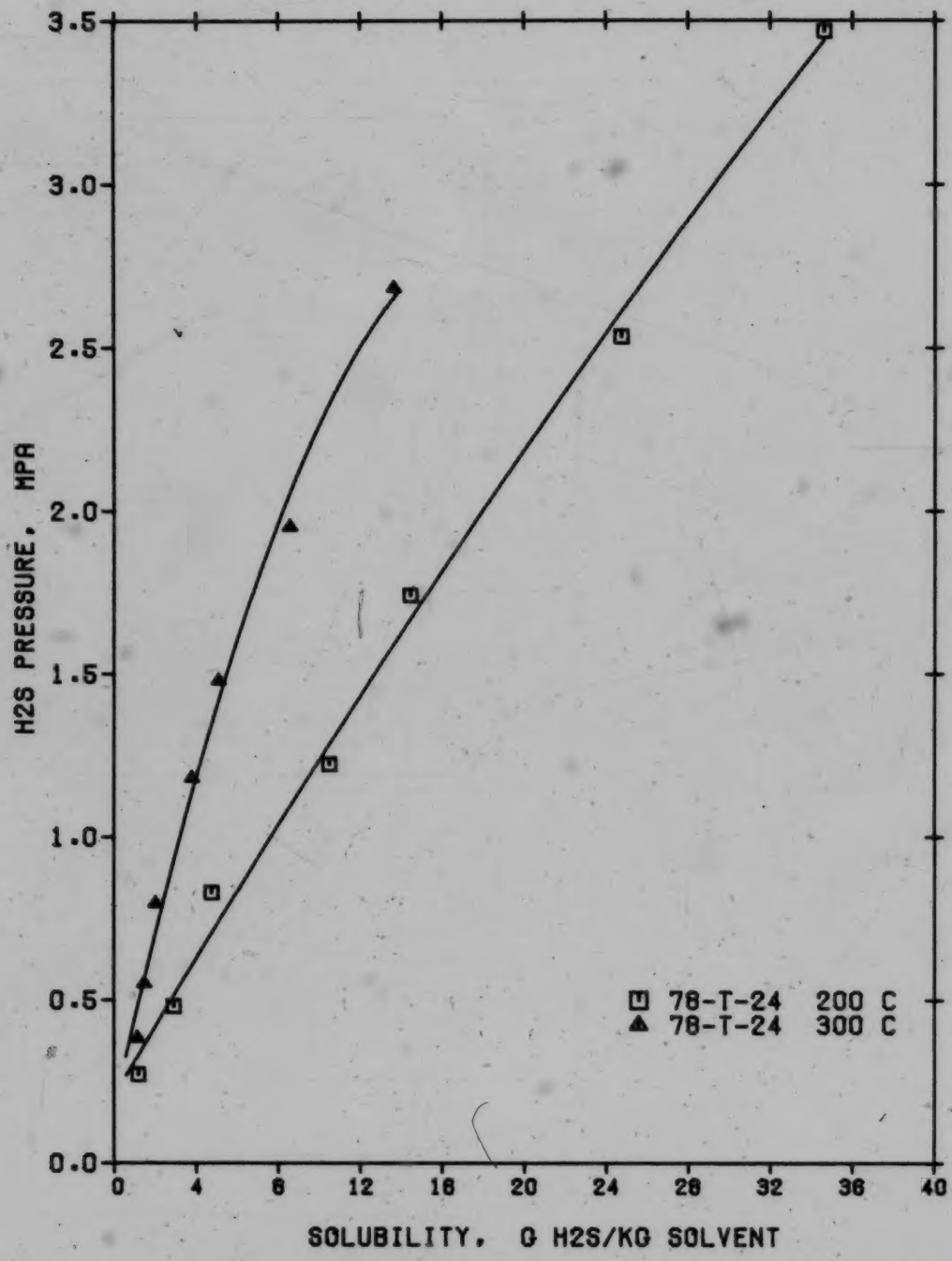

FIG 22 SOLUBILITY OF H2S IN 84.3% CONVERSION HEAVY END

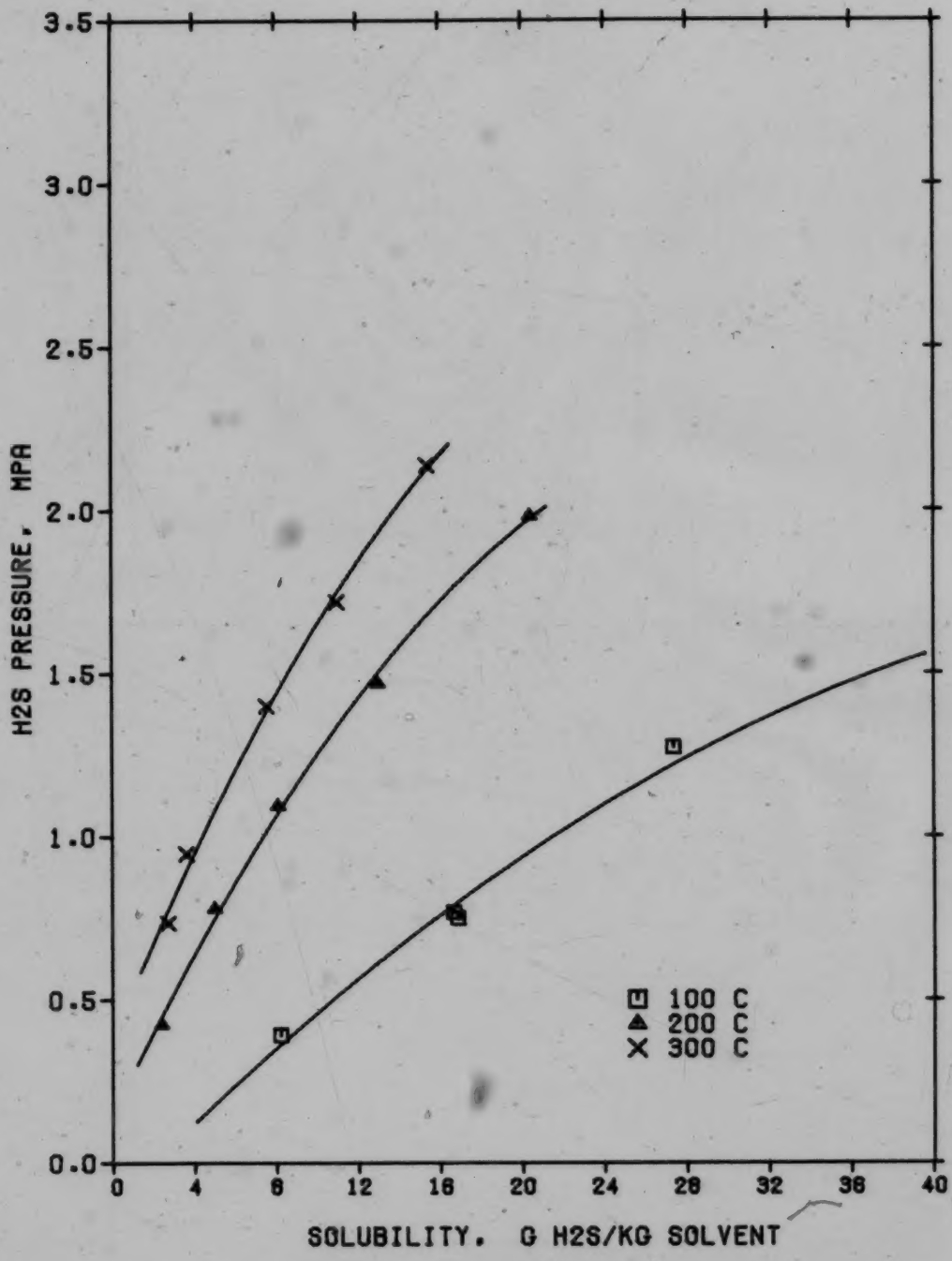

FIG 23 SOLUBILITY OF H2S IN EMR GAS OIL

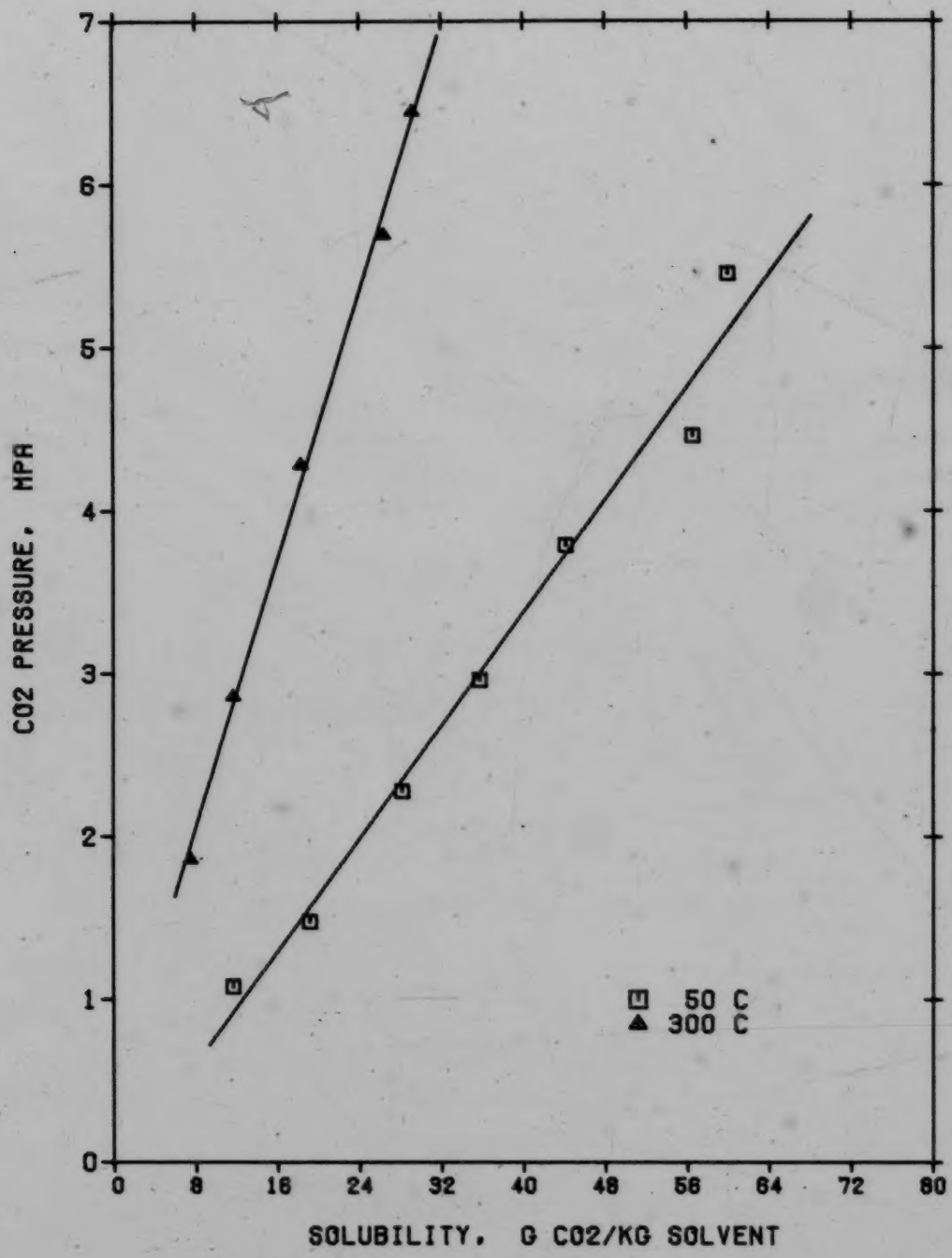

FIG 24 SOLUBILITY OF CO2 IN ATHABASCA BITUMEN

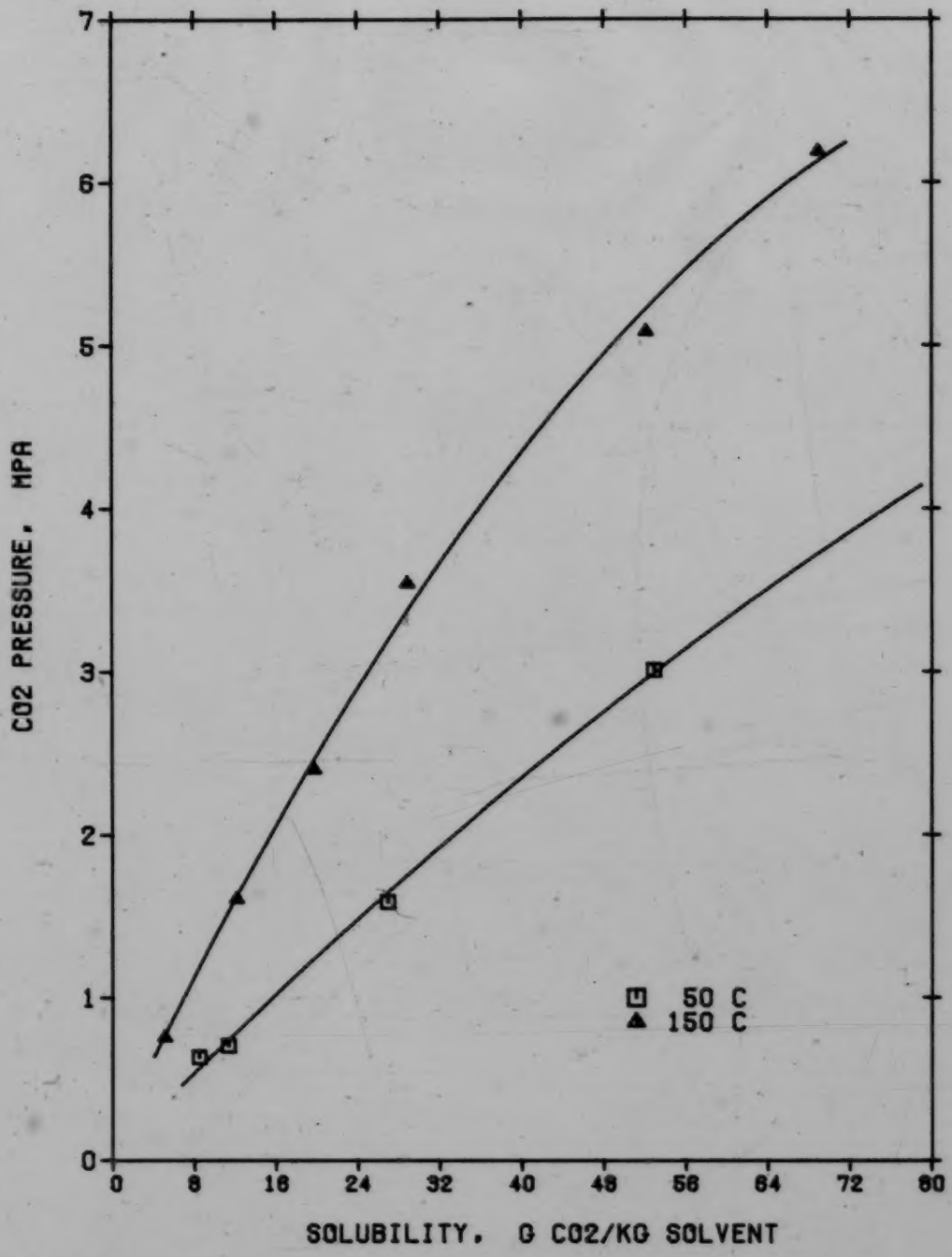

FIG 25 SOLUBILITY OF CO2 IN EMR GAS OIL

5. Correlation and Fraction Characterization

One of the useful applications of the experimental data is to test the validity of existing predictive methods, such as the methods of Chao-Seader, Grayson-Streed, Soave-Redlich-Kwong, modified Soave-Redlich-Kwong and Peng-Robinson. In practice, to do VLE calculations by any of these equations, the following procedures are implemented. An initial set of K-values are assumed and a flash calculation is performed to find the liquid and vapor compositions of each component. Using the calculated phase compositions, the equation of state can be solved for the fugacities of the liquid phase and the vapor phase. If the fugacities are not equal for all the components in both the phases, updated K-values are used and the flash calculation repeated until the fugacities match.

5.1 Results and Discussion

The presence of a light gas, like hydrogen, in hydrocarbon systems is not handled very well by the Chao-Seader and the SRK correlations at elevated temperatures and pressures. The high temperatures required in the hydrotreating processes exceed the upper limit value of 260°C set for hydrogen in the Chao-Seader method. To predict the VLE behavior of hydrogen-hydrocarbon systems by the SRK equation requires large interaction coefficients, C_{ij}. This, however, leads to physically meaningless values in the a term.

It is not immediately evident that an equation of state can successfully predict VLE properties of hydrogen-heavy hydrocarbon systems. The PR, modified SRK and the Grayson-Streed methods were used in this work to correlate experimental VLE data over wide ranges of temperature, pressure, and molecular weight of solvents. Toward that end, the experimental vapor and liquid compositions reported by Sebastian et al. (53,55,56), Simnick et al. (61,62,64), Yao et al. (72) and Nichols et al. (39) for hydrogen in heavy naphthenic and aromatic solvents, along with data obtained in this work for the EMR Gas Oil and the bitumens were compared with the values calculated by the three methods. Typical VLE calculation results are given in Tables 37-42 of Appendix II.

The experimental K-values of hydrogen in bitumens and EMR Gas Oil were approximated by 1/x (x is the hydrogen liquid phase composition), since the vapor phase was almost all hydrogen. The calculated K-values were derived from equation (2.5) for Grayson-Streed and equation (2.38) for the PR and modified SRK correlations. The critical properties and the acentric factors of the solvents used in the calculations were those reported in Reid et al. (50).

5.1.1 Modified Soave-Redlich-Kwong Method

The modified SRK method was used to correlate the VLE behavior of hydrogen in bicyclohexyl (56), tetralin (61), quinoline (53), diphenylmethane (62), m-cresol (64) and

Athabasca Bitumen at experimental temperatures and pressures. In all the cases tested, the characteristic constant, α, for hydrogen was calculated using equation (2.43) and those for the solvents were obtained using equation (2.13). The K-values of hydrogen were calculated using equation (2.38) and the liquid and vapor phase fugacity coefficients were obtained from equation (2.40). The interaction coefficient, $C_{i,j}$, was set at zero.

By adjusting the binary parameter E_{Hj} for each isotherm, very good agreement between the calculated and experimental hydrogen liquid phase compositions was obtained. To determine the optimum E_{Hj} for each isotherm the average absolute deviation (AAD) of the calculated hydrogen liquid phase compositions from experimental values was computed. The optimum E_{Hj} for an isotherm was one giving the minimum AAD. These are given in Table 10, and the average absolute deviations are given in Table 11.

Figure 26 shows the results for the K-values of hydrogen for hydrogen-bicyclohexyl system at 189° and 349°C. The E_{Hj} values used were 7.4 and 21.4, respectively, giving AAD of 2.2 % and 3.3 %. These low errors show the hydrogen-bicyclohexyl system is well represented by the modified SRK equation of state based on equation (2.39) with $C_{i,j}$ of zero. The VLE data are listed in Table 37.

Table 10 shows that the hydrogen-heavy hydrocarbon systems are well handled by the modified SRK equation.

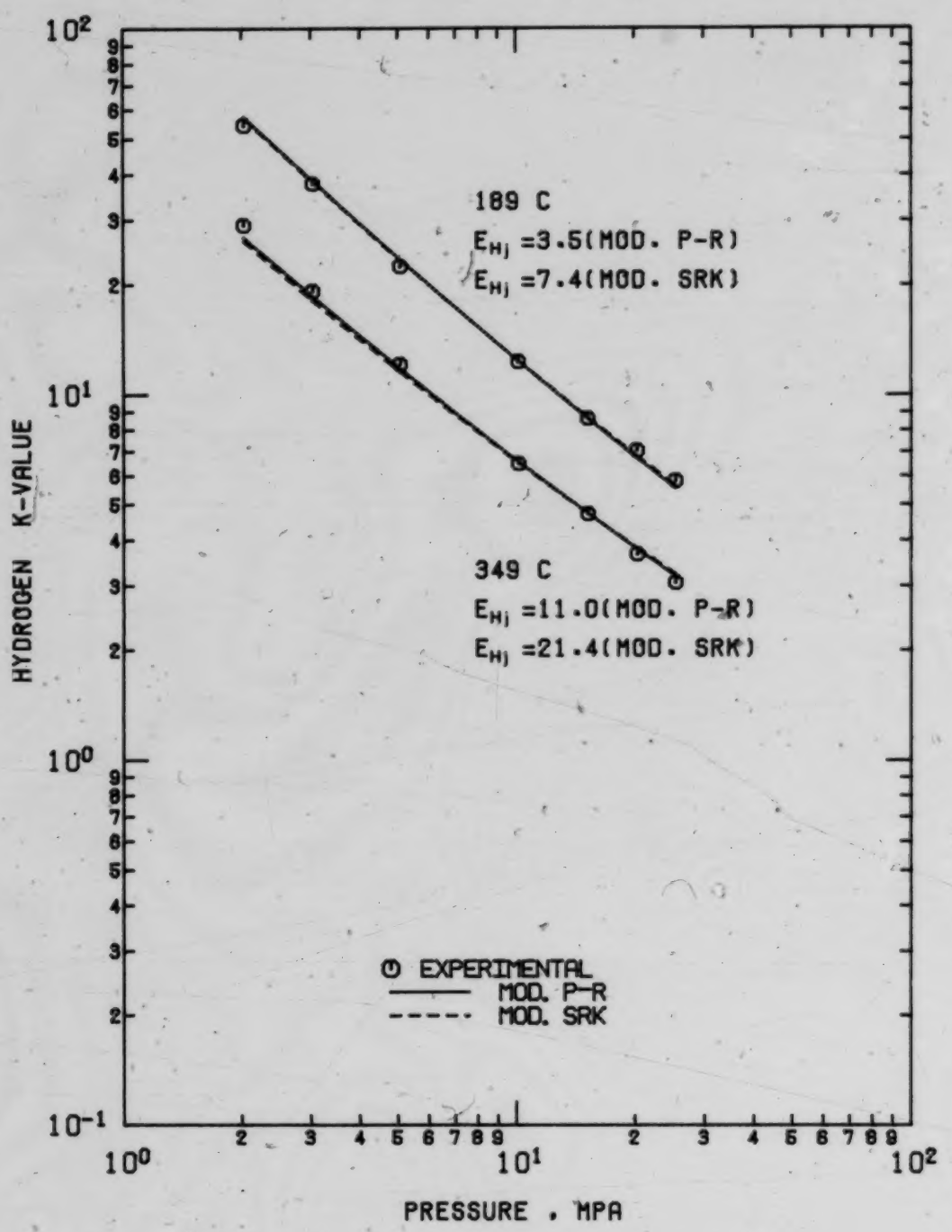

FIG 26 HYDROGEN K-VALUE VS PRESSURE FOR BICYCLOHEXYL (SEBASTIAN ET AL(56))

TABLE 10

INTERACTION PARAMETERS REQUIRED IN PR, MODIFIED PR AND MODIFIED SRK METHODS

SOLVENT	T (°C)	δ_{ij}	E_{Hj}(Mod PR)	E_{Hj}(Mod SRK)
BICYCLOHEXYL	189.0	-1.4	3.5	7.4
	268.7	-1.4	5.7	
	348.6	-1.4	11.0	21.4
	428.5	-1.4	33.0	
TETRALIN	189.6	-0.6	4.6	8.0
	268.7	-0.6	7.6	13.4
	348.6	-0.6	13.8	22.4
	389.1	-0.6	18.4	
QUINOLINE	189.3		-3.4	-2.9
	268.7		-5.0	-3.5
	348.6		-6.7	-4.1
	428.5		-8.8	-4.5
DIPHENYLMETHANE	189.6	-0.8	3.0	5.9
	268.7	-0.8	3.9	
	348.6	-0.8	6.8	15.7
	428.5	-0.8	16.7	

TABLE 10-Continued...

1-METHYLNAPHTHALENE	189.0	0.0	4.0	
	268.7	0.0	5.3	
	348.6	0.0	9.2	
	428.5	0.0	18.5	
THIANAPHTHENE	187.7	0.3	8.3	
	267.9	0.3	10.9	
	348.0	0.3	17.4	
	429.5	0.3	29.0	
m-CRESOL	188.9		2.7	4.7
	268.6		3.8	7.6
	348.3		7.4	14.5
n-HEXANE	4.4	-0.6	-1.0	
	37.8	-0.6		
	71.1	-0.6	1.5	
	137.8	-0.6	6.0	
	171.1	-0.6	11.1	
ATHABASCA BITUMEN	200.0	-4.6	-8.6	-4.1
	300.0	-4.6	-19.9	-12.0
COLD LAKE BITUMEN	200.0	-4.2	-6.6	
	300.0	-4.2	-21.1	
EMR GAS OIL	200.0	-3.2	-2.1	
	300.0	-3.2	0.1	

TABLE 11

COMPARISON OF AVERAGE ABSOLUTE DEVIATIONS

SOLVENT	T (°C)	PR	Mod PR	Mod SRK	GS
BICYCLOHEXYL	189	2.75	3.1	2.2	18.2
	268.7	8.6	0.6		23.9
	348.6	10.7	2.1	3.3	9.0
	428.5	9.2	7.4		12.9
TETRALIN	189.6	0.57	0.66	1.2	23.9
	268.7	1.4	1.8	1.5	32.8
	348.6	6.2	3.0	4.4	14.7
	389.1	6.4	3.7		8.7
QUINOLINE	189.3		1.6	1.9	
	268.7		0.65	0.85	
	348.6		1.1	1.7	
	428.5		0.36	0.37	
DIPHENYLMETHANE	189.6	1.4	0.33	1.0	16.9
	268.7	8.4	0.98		22.9
	348.6	7.9	1.3	1.5	20.5
	428.5	5.6	1.0		8.0
1-METHYLNAPHTHALENE	189.0	1.4	1.7		28.7
	268.7	1.1	1.3		38.3
	348.6	7.1	1.1		41.2
	428.5	12.1	2.3		29.9

TABLE 11 Continued...

THIANAPHTHENE	187.7	0.93	0.63		
	267.9	4.4	1.7		
	348.0	14.1	2.1		
	429.5	26.8	6.0		
m-CRESOL	188.9		0.48	0.8	
	268.6		0.77	1.4	
	348.3		1.4	2.6	
n-HEXANE	4.4	2.6	1.4		
	37.8	2.7			
	71.1	3.4	1.8		
	137.8		2.2		
	171.1		2.7		
ATHABASCA BITUMEN	200.0	1.7	0.34		13.3
	300.0	35.8	0.41		12.6
COLD LAKE BITUMEN	200.0	0.63	1.4		21.5
	300.0	37.8	1.6		12.7
GAS OIL	200.0	0.97	0.54		
	300.0	18.9	1.5		

Whereas the small values of E_{Hj} are physically credible, the large values of C_{ij} required in the original SRK are not. Except for hydrogen in quinoline and Athabasca Bitumen, the parameters are positive and increase with increase in temperature.

5.1.2 Peng-Robinson Method

The Peng-Robinson method was used to predict the VLE properties for hydrogen binaries in bicyclohexyl (56), tetralin (61), diphenylmethane (62), 1-methylnaphthalene (72), thianaphthene (55), *n*-hexane (39), Athabasca Bitumen, Cold Lake Bitumen and EMR Gas Oil at experimental temperatures and pressures. The characteristic constant, α, for hydrogen and the solvents was calculated from equation (2.35). The K-values of hydrogen were calculated using equation (2.38), and the liquid and vapor phase fugacity coefficients were obtained from equation (2.27). The optimum binary interaction coefficients, δ_{ij}, were determined by the same procedure used to find the optimum E_{Hj} in the modified SRK method.

No simple relationship between interaction coefficients and temperatures was observed. An overall interaction coefficient, optimized for the entire experimental temperature range, was determined for each binary. These are given in Table 10 and the AAD values are given in Table 11.

When optimum interaction coefficient values are used to calculate VLE data, a good agreement between the

experimental and calculated hydrogen liquid phase compositions exists at temperatures below 250°C. The deviations rise sharply above this temperature. For example, the hydrogen-bicyclohexyl system requires an overall interaction coefficient of -1.4 with AAD of 2.8% at 189°C and 10.7% at 349°C (cf. 2.2% and 3.3% for the modified SRK). The results for K-value of hydrogen are shown on Figure 27 at 189°C and 349°C. The VLE data are given in Table 38. Equation (2.38) calculates the K-values which agree reasonably well with experiments at 189°C but overpredicts for pressures above 10 MPa at 349°C.

Except for solutions of hydrogen in bicyclohexyl, Athabasca Bitumen, Cold Lake Bitumen and EMR Gas Oil the interaction coefficients lie in the range $-1 < \delta_{i,j} < +1$. More unrealistic interaction coefficient values are needed for hydrogen binaries in Athabasca Bitumen, Cold Lake Bitumen and EMR Gas Oil. If the critical properties and acentric factors of the solvents are determined by the Cavett's method, the binary interaction coefficients needed to handle the three systems by the PR correlation are -4.6 for the Athabasca Bitumen, -4.2 for the Cold Lake Bitumen and -3.2 for the EMR Gas Oil. At 200°C, the AAD values are low, being 1.7% for Athabasca Bitumen, 0.6% for Cold Lake Bitumen and 1.0% for EMR Gas Oil. However, at 300°C, the errors are large because the calculated VLE are not sensitive to large changes in the interaction coefficients (α for hydrogen equals zero at 289°C). The AAD values for 300°C are 36% for

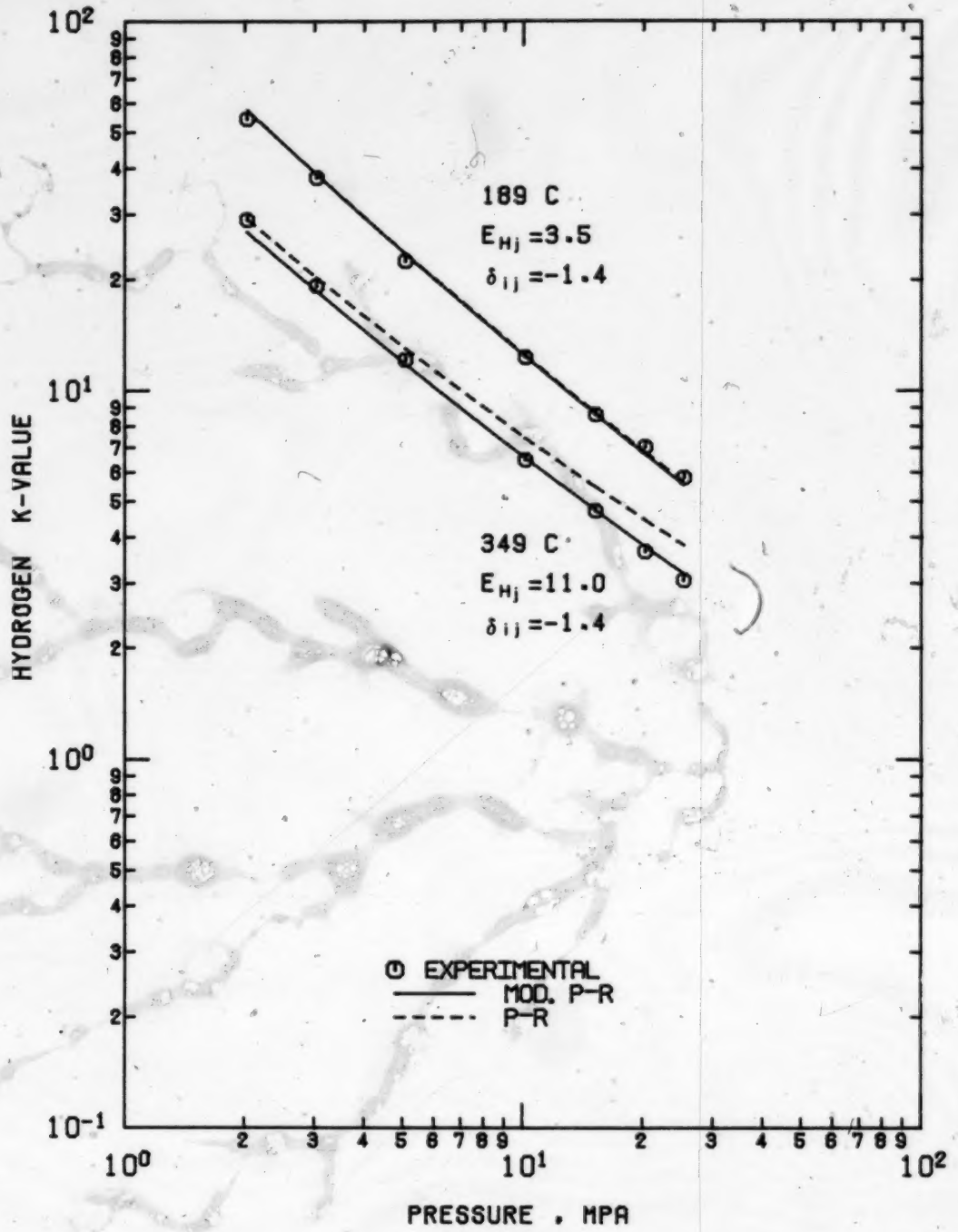

FIG 27 HYDROGEN K-VALUE VS PRESSURE FOR BICYCLOHEXYL (SEBASTIAN ET AL(56))

Athabasca Bitumen, 38% for Cold Lake Bitumen and 19% for EMR Gas Oil.

If the critical properties and the acentric factors of Athabasca Bitumen and Cold Lake Bitumen are determined by the PNA analysis, the interaction coefficients are still large and negative. The interaction coefficients are -2.7 for Athabasca Bitumen and -2.2 for Cold Lake Bitumen. The AAD values are 0.6% at 200°C and 20% at 300°C for Athabasca Bitumen, and 1.3% at 200°C and 22% at 300°C for Cold Lake Bitumen.

El-Twaty and Prausnitz (14) improved the SRK method by modifying the constant b in the repulsive term in the equation. For mixtures, they proposed equation (2.39):

$$b = \sum_i x_i b_i + x_H \sum_j x_j E_{Hj} \qquad (2.39)$$

They also changed the functional form of the dependence of the characteristic constant, α, on acentric factor and temperature by equation (2.43), whenever $T > T_c$. The PR equivalent of equation (2.43) is given by equation (4.1):

$$\alpha = \exp\{2\kappa(1 - \sqrt{T_r})\} \qquad (4.1)$$

These two changes produced significant improvement in the correlation of hydrogen-heavy hydrocarbons binary data over a wide range of temperatures and pressures; and at the same time requiring physically reasonable values of E_{ij}.

This approach was applied to the PR equation of state, equation (2.21). The new expression for the fugacity coefficient is then given by equation (4.2):

$$\ln \phi_i = \ln \phi_i^P + \frac{x_i}{b}\{(z-1) + \frac{A}{2\sqrt{2}B} \ln(\frac{z+2.414B}{z-2.414B})\} \quad (4.2)$$

where ϕ_i^P designates the fugacity coefficient found for the PR equation ; it is given by equation (2.27).

The modified PR method was used to predict VLE behavior of hydrogen in bicyclohexyl (56), tetralin (61), quinoline (53), diphenylmethane (62), 1-methynaphthalene (72), thianaphthene (55), *m*-cresol (64), *n*-hexane (39), Athabasca Bitumen, Cold Lake Bitumen and EMR Gas Oil. The characteristic constant, α, was determined by equation (4.1) for hydrogen and equation (2.35) for the solvents. The K-values of hydrogen were calculated using equation (2.38) and the liquid and vapor phase fugacity coefficients were obtained from equation (4.2).

The optimum E_{Hj} values required in (2.39) for each binary were determined by fitting experimental solubility data, following the same criterion to determine the optimum E_{Hj} in the modified SRK method and δ_{ij} in the PR method. These are given in Table 10. The AAD values are given in Table 11. The binary interaction coefficients were set equal to zero.

The use of E_{Hj} results in a good correlation of the hydrogen solubility data by the modified PR equation. The K-values of hydrogen plotted against pressure for the hydrogen-bicyclohexyl data of Sebastian et al. (56) are shown on Figures 26 and 27 for comparison with the modified SRK and the original PR methods (the VLE data are given in Table 38). At 189°C, best fit is achieved when E_{Hj} is set at 3.5, giving AAD of 3.1%. At 349°C, the optimum E_{Hj} is 11.0, with AAD of 2.1%. These experimental data are correlated equally well by the modified PR equation and the modified SRK method, as illustrated on Figure 26. Figure 27 compares the hydrogen K-values calculated by the modified PR and the original PR equations of state. At 349°C the experimental data are better correlated by the modified PR equation. This is further evident from the much lower AAD values reported in Table 11 for the modified PR equation.

In contrast to the results of El-Twaty and Prausnitz (14), negative values of E_{Hj} are found for some pure compounds (e.g. quinoline) and most complex mixtures. The results for the K-values of hydrogen in Athabasca Bitumen are shown on Figure 28 for 200° and 300°C (the VLE data are given in Table 41). A good agreement between the experimental and the calculated hydrogen K-values is obtained when E_{Hj} is set at -8.6 at 200°C and -19.9 at 300°C. The AAD values are as low as 0.3% at 200°C and 0.4% at 300°C. For hydrogen-Cold Lake Bitumen binary, E_{Hj} of -6.6 at 200°C and -21.1 at 300°C are found, giving AAD of 1.4%

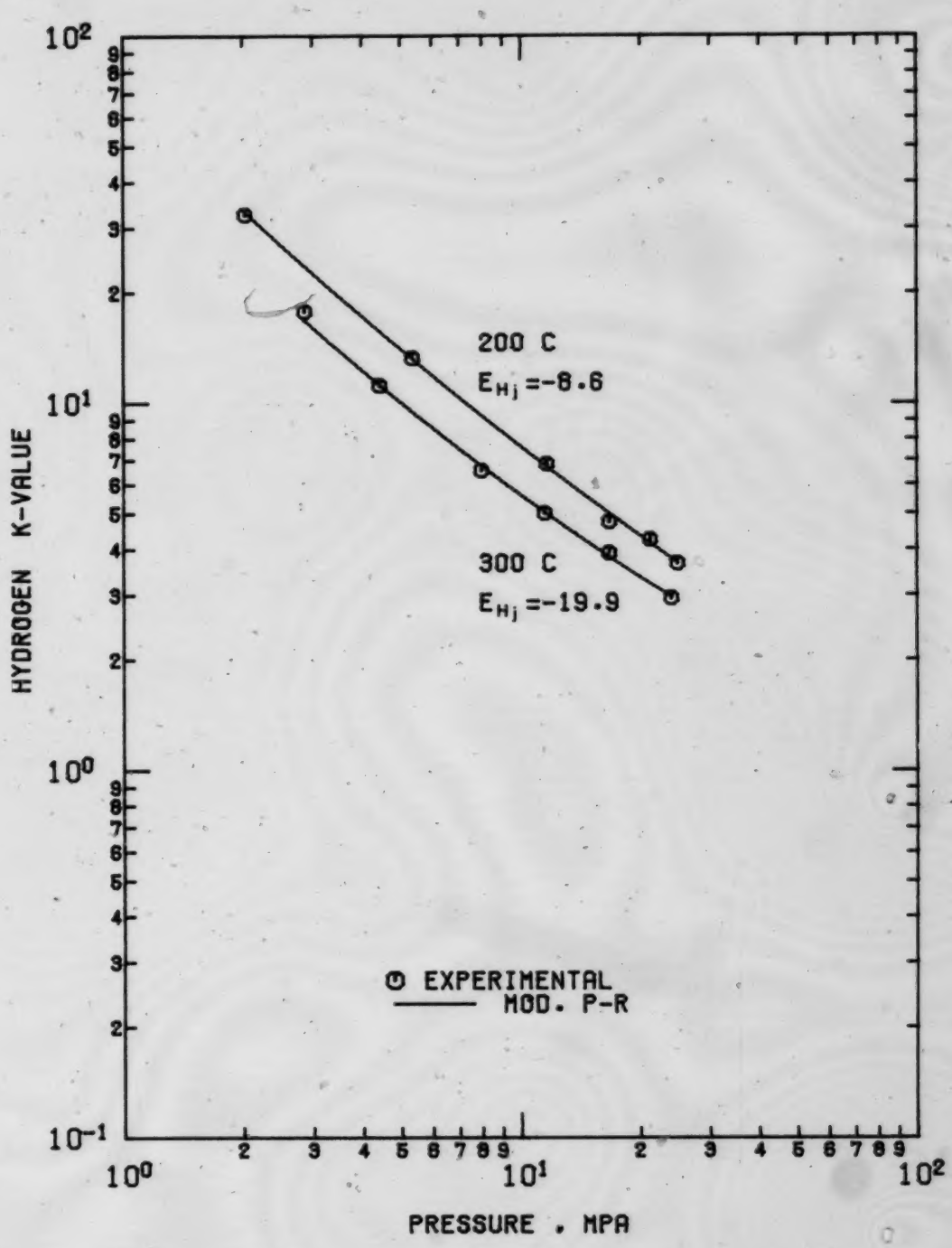

FIG 28 HYDROGEN K-VALUE VS PRESSURE FOR ATHABASCA BITUMEN

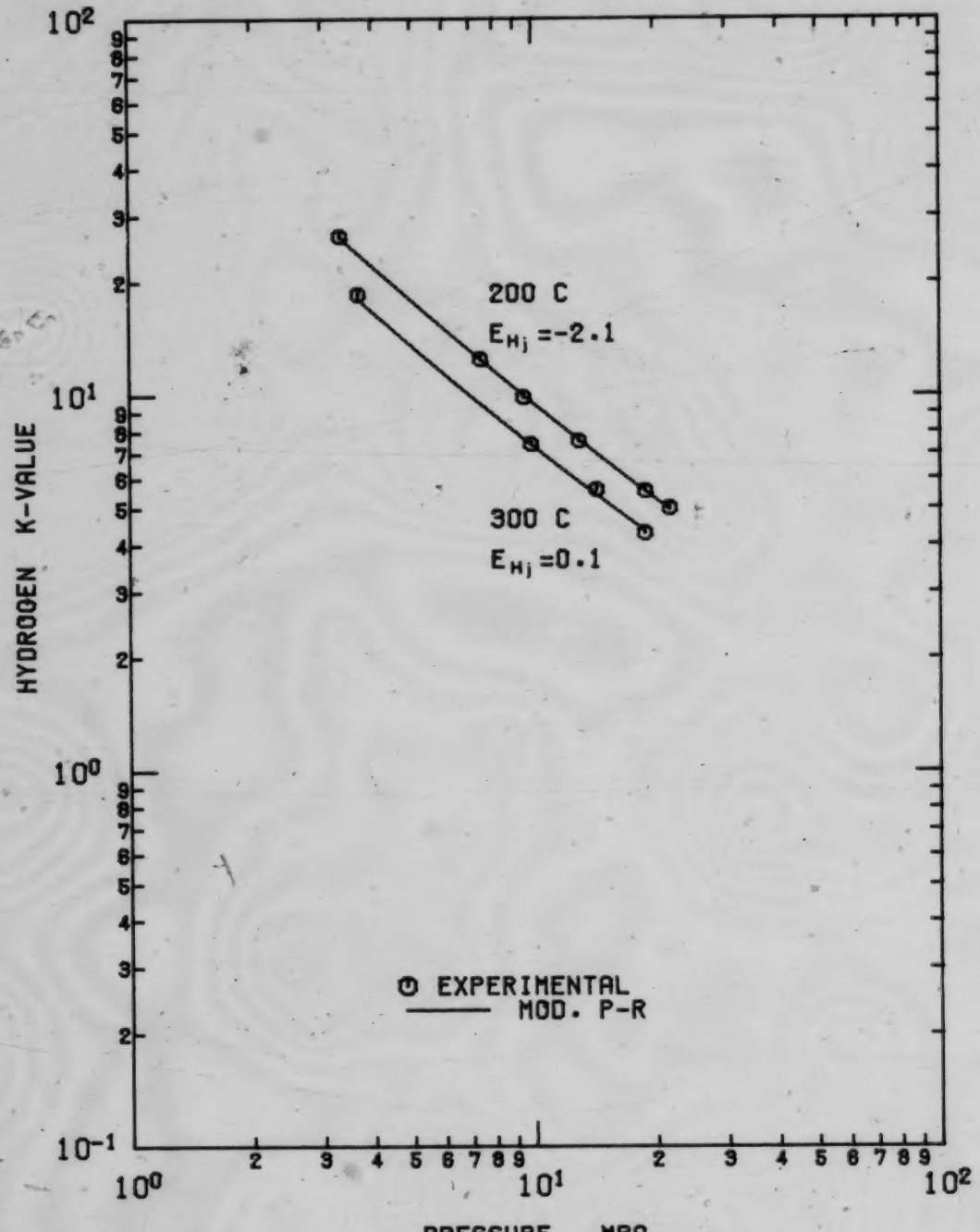

FIG 29 HYDROGEN K-VALUE VS PRESSURE FOR EMR GAS OIL

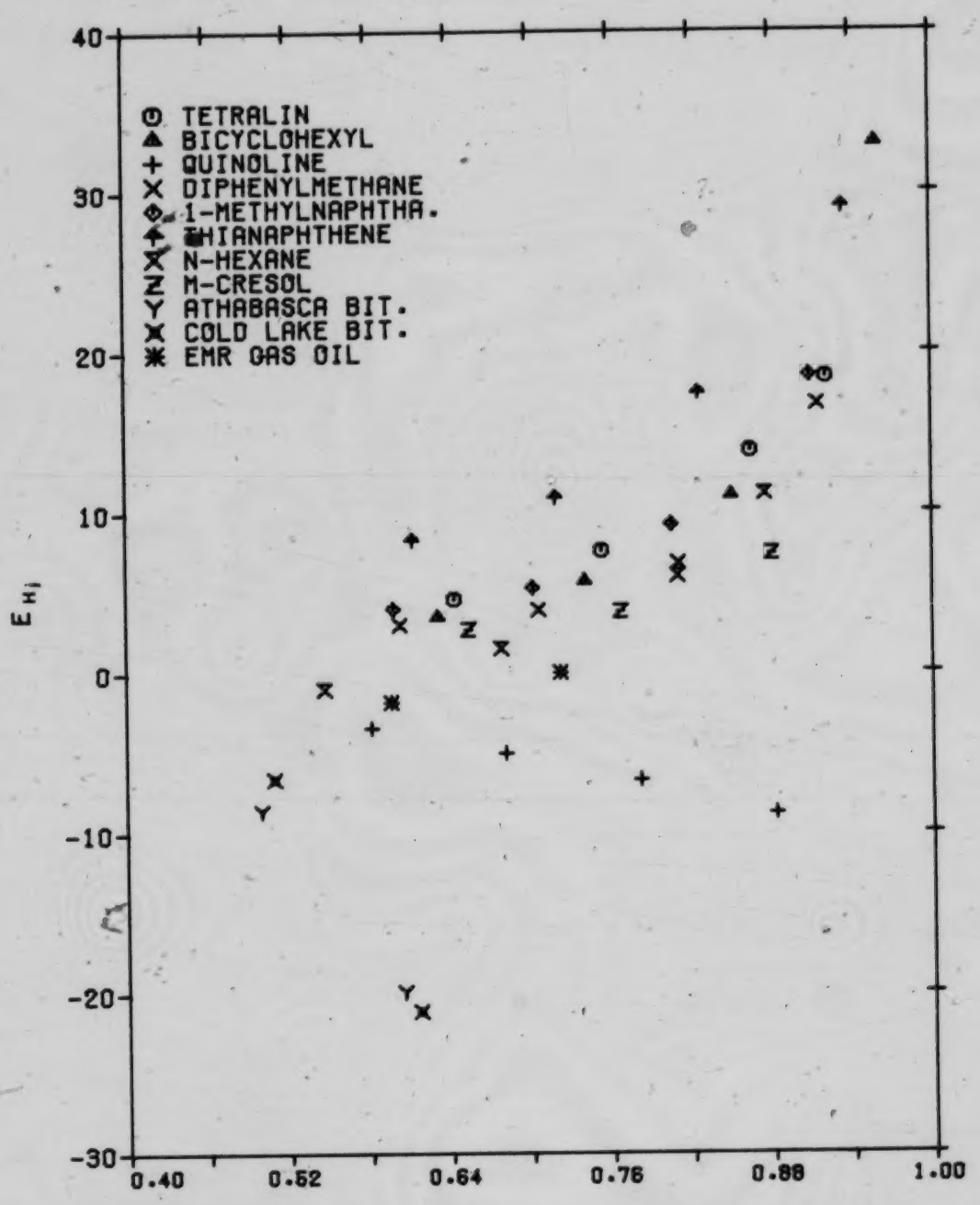

FIG 30 BINARY PARAMETER E_{Hj} IN MODIFIED PENG-ROBINSON EQUATION OF STATE

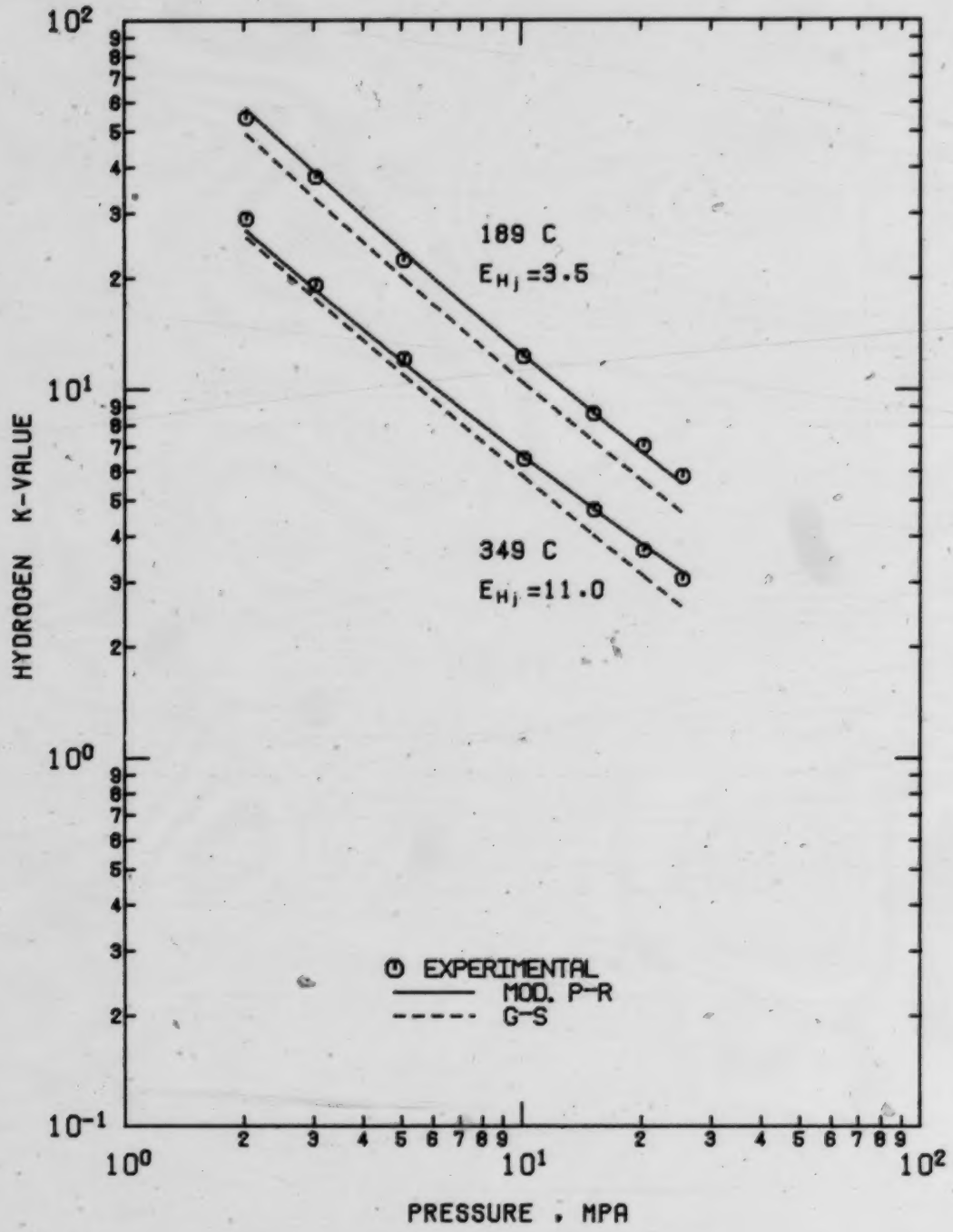

FIG 31 HYDROGEN K-VALUE VS PRESSURE FOR BICYCLOHEXYL (SEBASTIAN ET AL(56))

and 1.6%, respectively. The results for EMR Gas Oil are shown on Figure 29 (the VLE data are given in Table 42). The optimum E_{Hj} of -2.1 at 200°C (AAD of 0.5%) and 0.1 at 300°C (AAD of 1.5%) are found for this system.

In general, the values of E_{Hj} in the modified PR equation are always smaller than those in the modified SRK equation. All the binary parameters are shown on Figure 30 where E_{Hj} is plotted against solvent reduced temperature. The simple correlation found by El-Twaty and Prausnitz (14) for seven hydrocarbons does not apply to most of the systems studied here.

5.1.3 Grayson-Streed Method

The Grayson-Streed correlation was also applied to the bicyclohexyl (56), tetralin (61), diphenylmethane (62), 1-methylnaphthalene (72), *m*-cresol (64), Athabasca Bitumen and Cold Lake Bitumen systems. The results for the K-values of hydrogen for the hydrogen-bicyclohexyl system are shown on Figure 31 (the VLE data are given in Table 37). Despite a significant improvement in the correlation over the Chao-Seader method, the K-values are still consistently underpredicted. At 349°C, the AAD is as high as 24%. For the hydrogen-1-methylnaphthalene system, the average deviation is 41% at 349°C.

The consequence of an important assumption made in the development of the Chao-Seader and Grayson-Streed correlations explains, in part, the poor performance of GS

procedure for hydrogen-heavy hydrocarbon systems at elevated temperatures. Two distinct models are utilised in the development of the GS procedures; the 'regular' solution model is assumed for liquid solution, and the Redlich-Kwong equation of state is used to predict the properties of the vapor phase. At temperatures approaching the critical values the two phases approach a dense single phase. The two models will not necessarily match the properties for this phase.

5.1.4 Correlation of CO_2 and H_2S Systems

The solubility data for carbon dioxide in tetralin (57), Athabasca Bitumen and EMR Gas Oil were successfuly correlated by the PR equation for temperatures ranging from 50° to 392°C, and pressures up to 6.4 MPa. Unlike hydrogen systems, the phase compositions were strong functions of the binary interaction coefficients, $\delta_{i,j}$. For these systems it was possible to find a value of the interaction coefficient that reproduced the experimental data well and lay in the range $-1 < \delta_{i,j} < +1$. For the carbon dioxide-tetralin data of Sebastian et al. (57) the interaction coefficients were 0.14 at 189° and 270°C, 0.19 at 350°C, and 0.26 at 392°C. The results for the K-values of carbon dioxide are shown on Figure 32. The VLE data are given in Table 43 of Appendix II.

For the solubility of carbon dioxide in Athabasca Bitumen, the optimum binary interaction coefficients were found to be 0.09 at 50°, 0.07 at 100° and -0.04 at 300°C.

The AAD values were 4.8%, 2.9% and 1.1%, respectively. The results for the K-values of carbon dioxide at 50° and 300°C are shown on Figure 33. The VLE data are listed in Table 44 of Appendix II. For the EMR Gas Oil system the interaction coefficients were fairly constant at 0.13, 0.12 and 0.13 at 50°, 100° and 150°C, respectively. The results for the K-values of carbon dioxide are shown in Figure 34. The data are given in Table 45 of Appendix II.

Reliable and accurate phase equilibrium predictions for hydrogen sulphide systems were also possible by the PR equation. For the hydrogen sulphide-Athabasca Bitumen system, optimum interaction coefficients were -0.05 at 200°C and -0.055 at 300°C, with average deviation of 3.0% and 2.5%, respectively. The dependence of the K-values of hydrogen sulphide on pressure are shown on Figure 35. The data are given in Table 46 of Appendix II. For the EMR Gas Oil system, the interaction parameters were 0.05 at 100°C, and 0.18 at 200° and 300°C. The results for the K-values of hydrogen sulphide are shown on Figure 36. The data are given in Table 47 of Appendix II.

A reasonably good fit of the hydrogen sulphide-*n*-decane data of Reamer et al. (48) was possible by assigning a constant value of 0.04 for the interaction coefficient at 4°, 38°, 71°, 104°, 138° and 171°C, with an overall AAD of 4.3%. For the *n*-nonane data of Eakin and DeVaney (12) overall interaction coefficient of 0.04 was also required for data at 38°, 93° and 204°C.

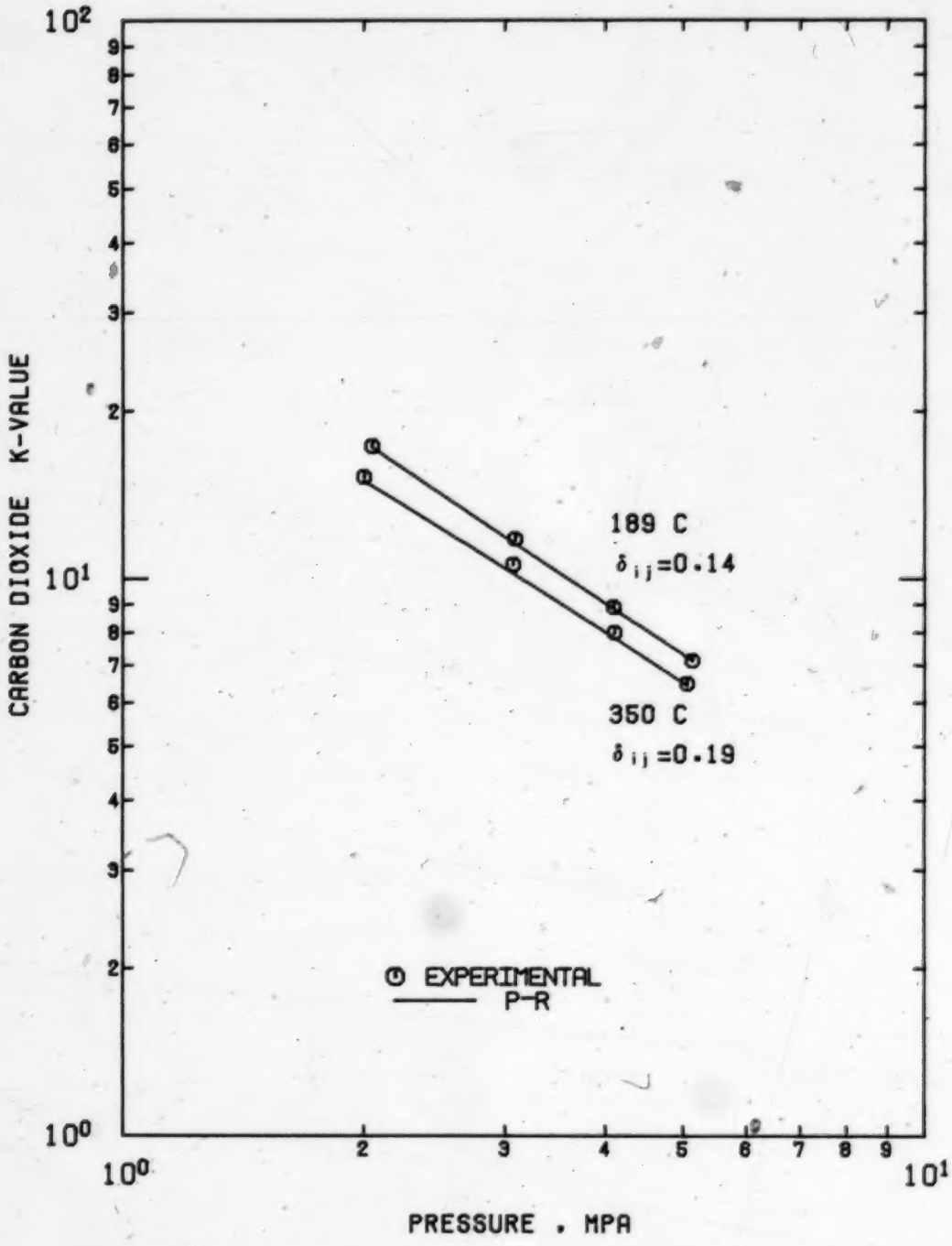

FIG 32 CARBON DIOXIDE K-VALUE VS PRESSURE FOR TETRALIN (SEBASTIAN ET AL(57))

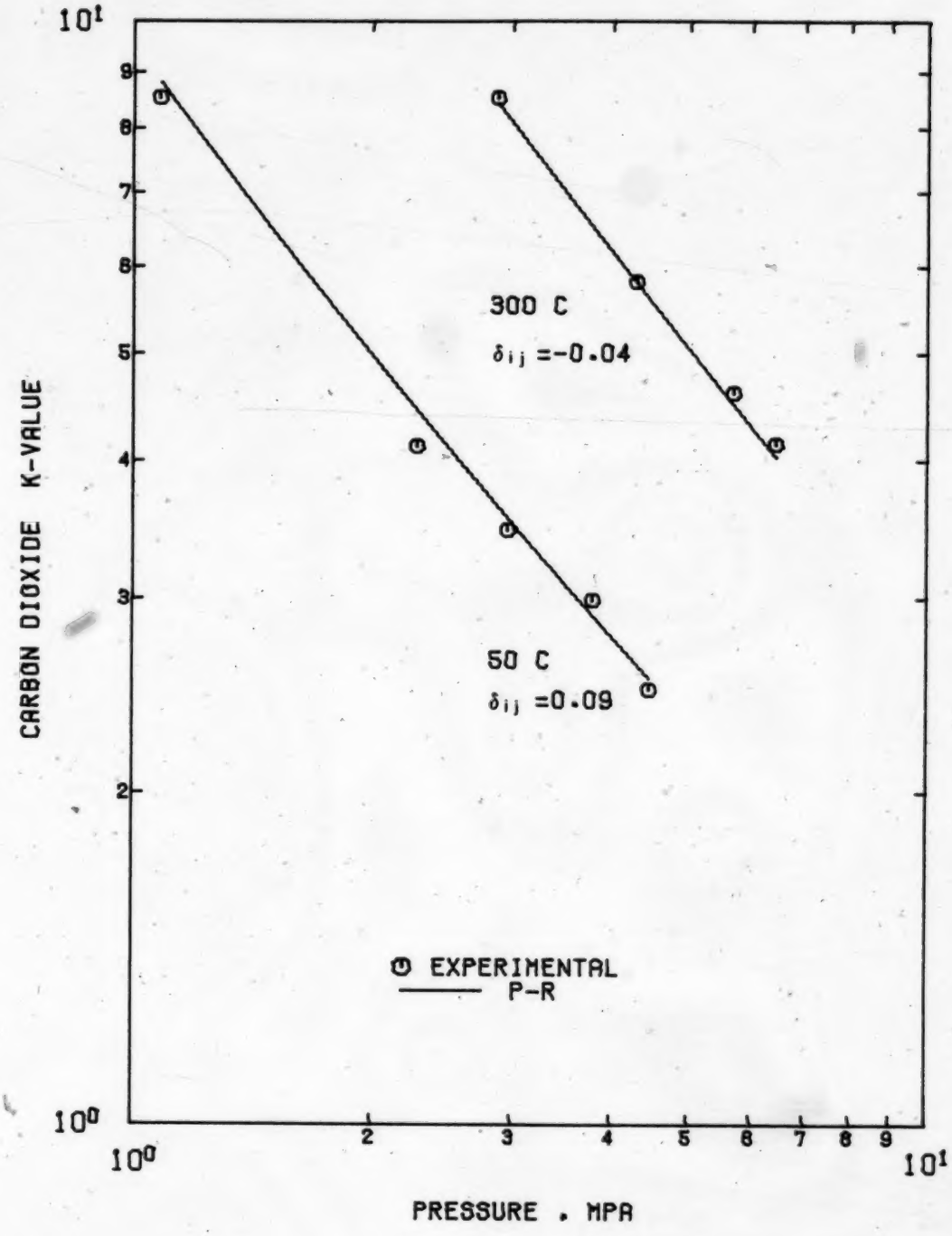

FIG 33 CARBON DIOXIDE K-VALUE VS PRESSURE FOR ATHABASCA BITUMEN

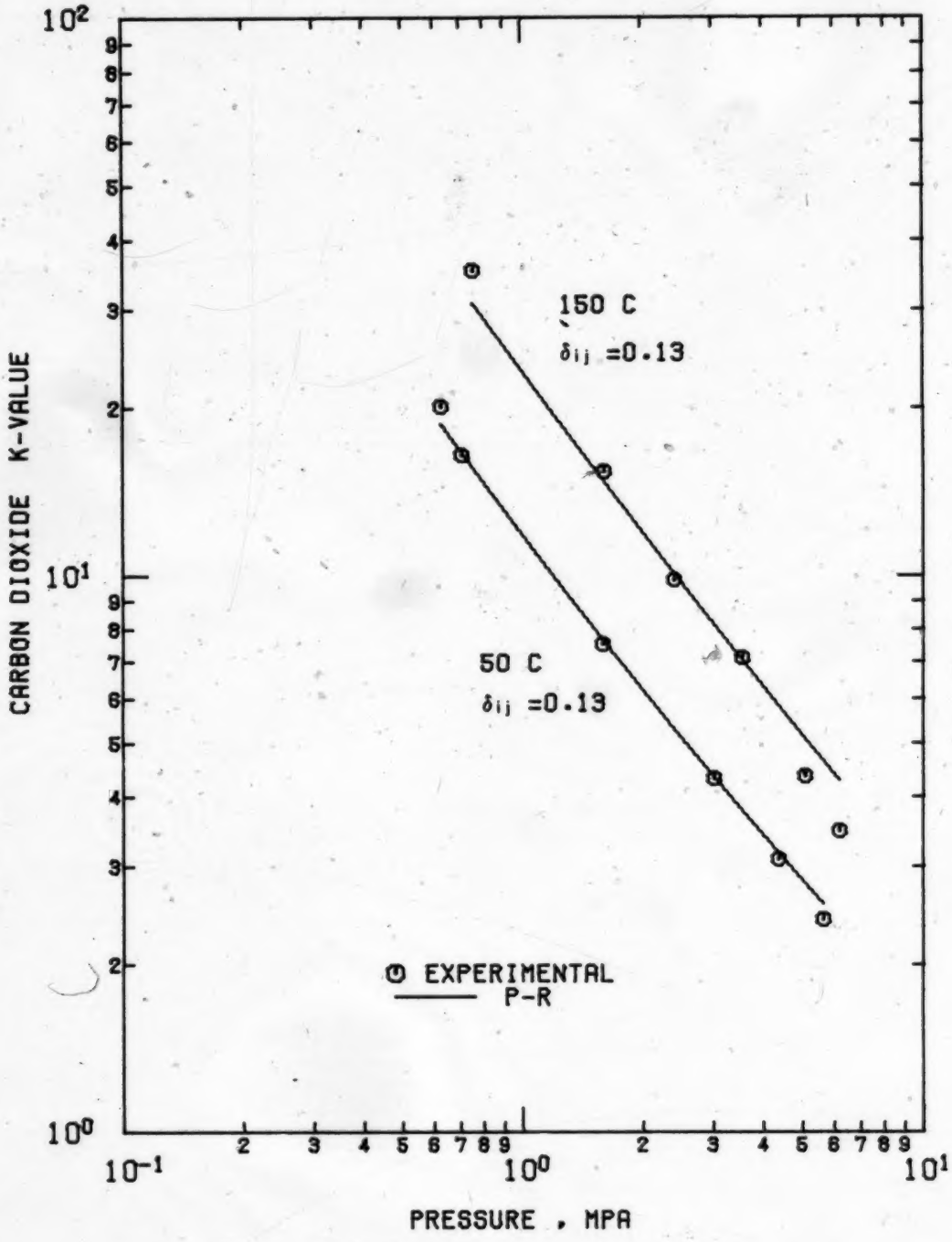

FIG 34 CARBON DIOXIDE K-VALUE VS PRESSURE FOR EMR GAS OIL

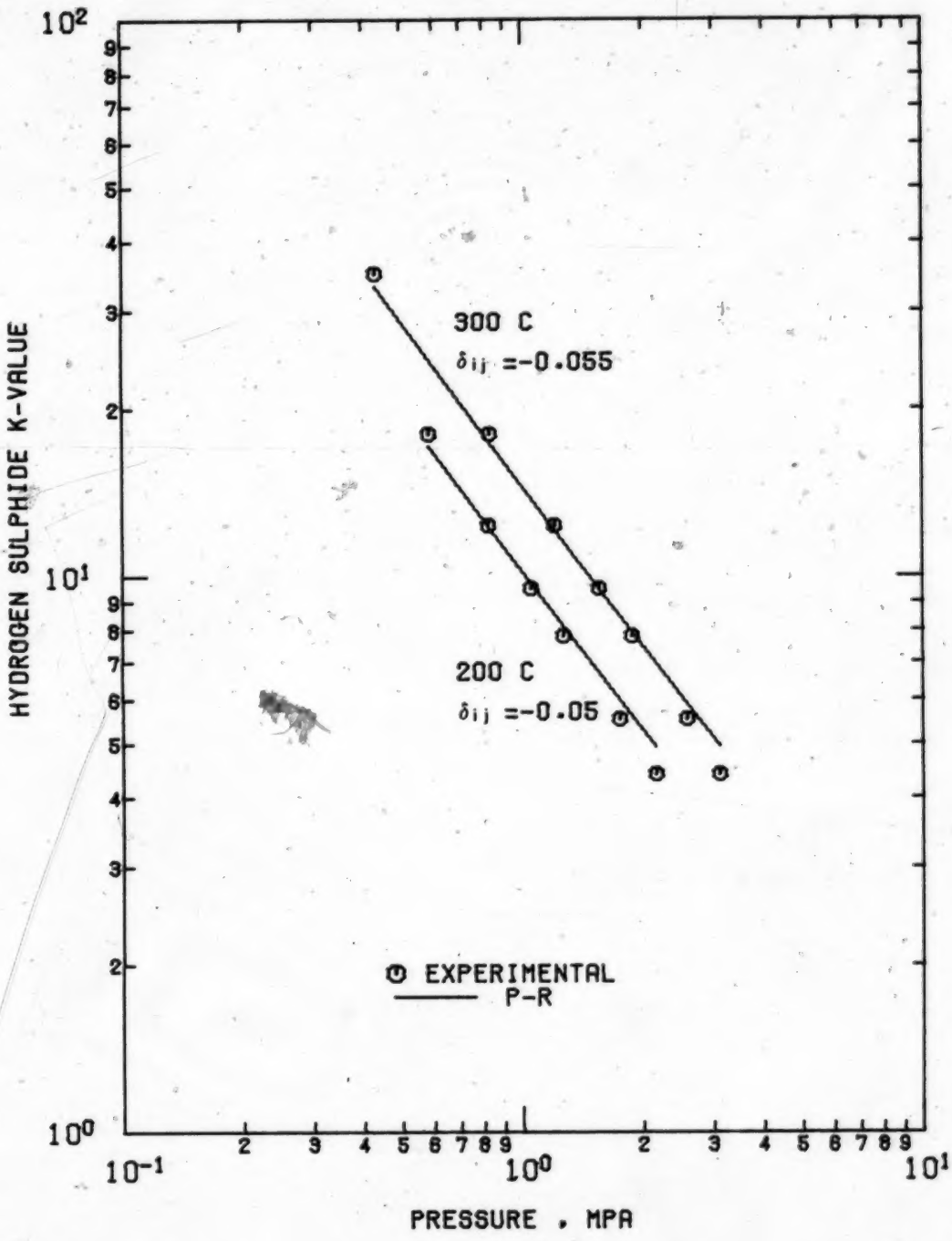

FIG 35 HYDROGEN SULPHIDE K-VALUE VS PRESSURE FOR ATHABASCA BITUMEN

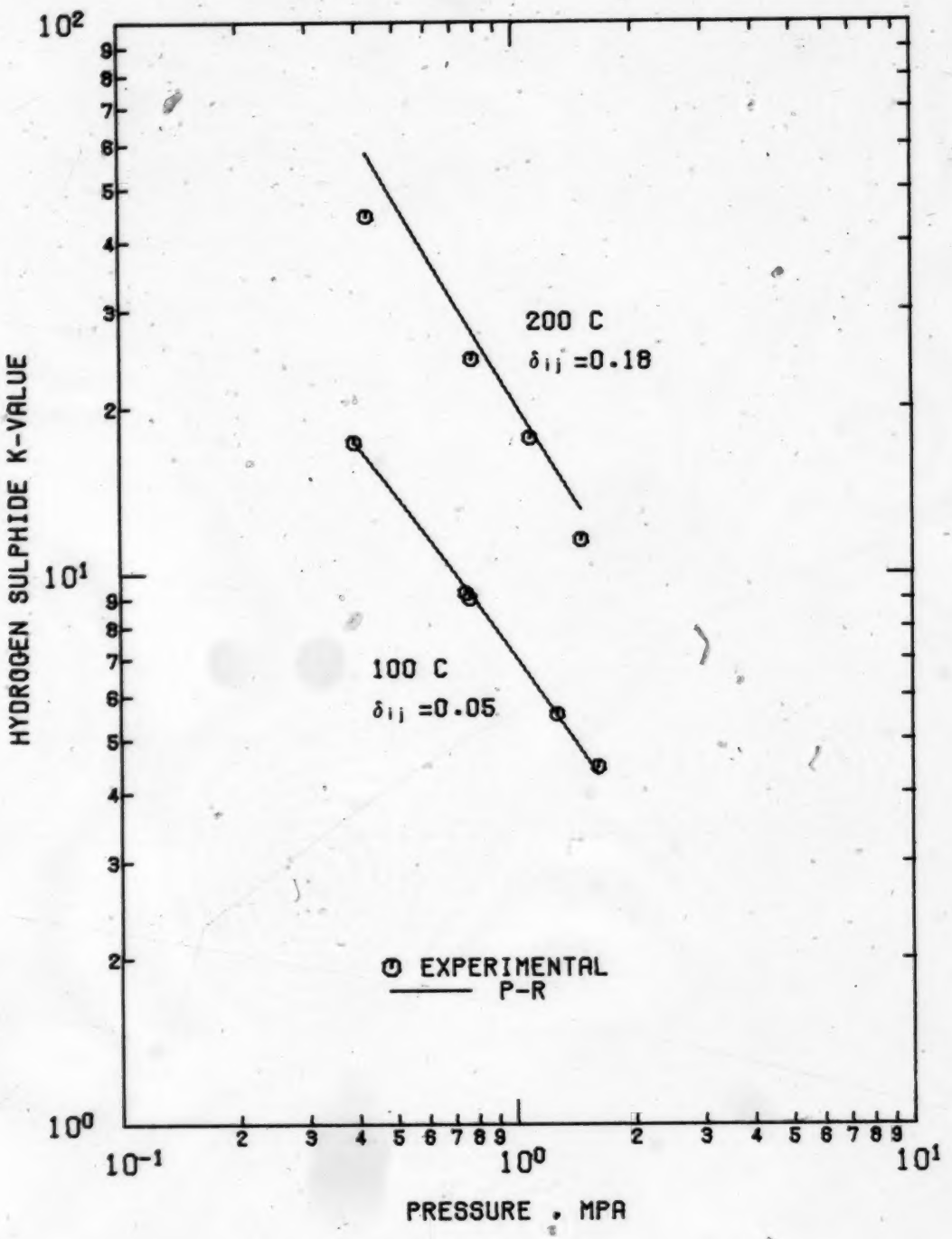

FIG 36 HYDROGEN SULPHIDE K-VALUE VS PRESSURE FOR EMR GAS OIL

It is apparent from the above results that the original PR equation is capable of handling carbon dioxide and hydrogen sulphide in a wide range of solvents and over a wide range of temperatures and pressures. The binary interaction coefficients are low and positive, with the exception for carbon dioxide in Athabasca Bitumen at 300°C and hydrogen sulphide in Athabasca Bitumen at 200° and 300°C.

5.1.5 Fraction Characterization

Table 1 compares the pure component properties required for the PR, SRK and the Grayson-Streed methods. It can be seen from this table that the PR and SRK (and their modifications discussed in this work) methods require fewer pure component properties than the Grayson-Streed correlation. However, the PR and SRK both require interaction coefficients for each binary pair present in the system.

For well-defined components the literature values of the parameters are utilised. In the cases of EMR Gas Oil and the bitumens, the method of Cavett (3) is used . This requires specification of normal boiling point and specific gravity for the component.

The boiling point curve for the EMR Gas Oil was obtained by simulated distillation and checked against the spinning-band distillation method. The molecular weight of this solvent was determined by the method outlined in the

API Data Handbook. The results for the EMR Gas Oil are listed below.

Molecular Weight	250
Specific Gravity	0.915
Critical Temperature, K	793
Critical Pressure, psia	263.9
Acentric Factor	0.630
Solubility Parameter $(cal/cc)^{0.5}$	7.98

A boiling point curve was not available for the bitumens and consequently characterization of these heavy hydrocarbons was difficult. Molecular weights of 500 for Athabasca Bitumen and 475 for Cold Lake Bitumen were estimated from the works of Selucky et al. (58). Specific gravities were 1.002 and 1.00 for Athabasca and Cold Lake Bitumen, respectively. Cavett's method was then used to derive the other parameters, assuming a boiling point of 500°C for Athabasca Bitumen and 475°C for Cold Lake Bitumen. The results are listed below.

	Athabasca	Cold Lake
Molecular Weight	500	475
Specific Gravity	1.002	1.00
Critical Temperature, K	947	929
Critical Pressure, psia	158.5	171.7
Acentric Factor	0.963	0.893

Solubility Parameter $(cal/cc)^{0.5}$ 7.365 7.318

The critical constants and the acentric factors of hydrogen, hydrogen sulphide and carbon dioxide are listed below.

	H_2	H_2S	CO_2
Critical Pressure, psia	305	1297	1070
Critical Temperature, K	41.67	373.2	304.2
Acentric Factor	0.0	0.100	0.225

The properties of hydrogen sulphide and carbon dioxide are obtained from Reid et al. (50). The effective critical properties of hydrogen are obtained from Graboski and Daubert (17).

6. Summary and Conclusions

1. A batch - type autoclave was installed and tested for measurement of hydrogen solubility in heavy oils and coal - bitumen slurries. Solubility data for hydrogen in bitumens, cracked fractions, heavy gas oil and coal - bitumen slurries were obtained mainly at 200° and 300°C, and pressures up to 24.8 MPa. Limited carbon dioxide and hydrogen sulphide solubility measurements were also made.
2. The solubility of hydrogen in pure solvents increased linearly with pressure, and increased with rising temperatures. The solubility decreased with increase in solvent molecular weight.
3. The solubility in the 10 wt% coal - bitumen slurry was essentially the same as in the bitumen. Increase in solubility was observed in the 25 wt% coal - bitumen slurry, and in the 40 wt% coal - bitumen slurry at 200° and 250°C. The solubility in the 40 wt% coal-bitumen slurry at 300°C was lower than that in the bitumen. There is no explanation available for this phenomenon. The type of coal did not have an appreciable effect on the hydrogen solubility.
4. Carbon dioxide and hydrogen sulphide solubility decreased with increase in temperature and with increase in solvent molecular weight.
5. The prediction and correlation of the solubility data by the Peng-Robinson equation and the Grayson-Streed method

were attempted. The use of the Peng-Robinson equation led to unrealistically large negative values of the interaction coefficient for some of the hydrogen - hydrocarbon systems. The Grayson-Streed method consistently underpredicted the K-values of hydrogen. The best result for the correlation of hydrogen solubility data was obtained with the use of either a modified Peng-Robinson or a modified Soave-Redlich-Kwong equation of state, which introduced an interaction parameter in the covolume factor, b.

6. The Peng-Robinson equation was suitable for the correlation of carbon dioxide and hydrogen sulphide solubility data.

7. In summary, the modified PR and the modified SRK equations of state work equally well in the prediction of hydrogen-hydrocarbon VLE. When no E_{Hj} values are available, then Figure 30 can be used to provide an estimate of these for use in the modified PR equation of state. Very little information on the hydrogen sulphide and carbon dioxide systems is available to make estimates of δ_{ij} for these gases in other solvents. The results show that non-zero values have to be assigned for accurate prediction of VLE of these systems by the PR equation of state.

7. References

1 American Petroleum Institute, "Technical Data Book - Petroleum Refining", 2nd Ed., Washington, D.C., 1970

2 Benedict,M.,Webb,G.B.,Rubin,L.C.,J. Chem. Phys., 8, 334(1940)

3 Cavett,R.H., Proc. Am. Pet. Inst., Sect.III, 42, 351(1962)

4 Chao,K.C., Seader,J.D., A.I.Ch.E.J., 7, 598(1961)

5 Chappelow,III,C.C., Prausnitz,J.M., A.I.Ch.E.J., 20, 1097(1974)

6 Chueh,P.L., Prausnitz,P.M., Ind. Eng. Chem., 60, 34(1968)

7 Conrard,P.G., Gravier,J.F., The Oil and Gas J., 78, (16), 77(1980)

8 Cook,M.W., Hanson,D.N., Adler,B.J.,J. Chem. Phys., 26, 748(1957)

9 Cukor,P.M., Prausnitz,J.M., J. Phys. Chem., 76, 598(1972)

10 Davidson,D., Eggleton,P., Foggie,P., Quart. J. Exptl. Physiol., 37, 91(1952)

11 Dean,M.R., Tooke,J.W., Ind. Eng. Chem., 38, 389(1946)

12 Eakin,B.E., DeVaney,W.E., A.I.Ch.E. Symposium Series, 70, (140), 80(1974)

13 Edmister,W.E., Petrol. Refiner, 37(4), 173(1958)

14 El-Twaty,A.I., Prausnitz,J.M., Chem. Eng. Sci., 35, 1765(1980)

15 Frolich, P.K., Tauch,E.J., Hogan,J.J.,Peer,A.A., Ind. Eng. Chem., 23, 548(1931); 24, 823(1932)

16 Gjaldbaek,J.Chr., Acta Chem. Scand., 6, 623(1952)

17 Graboski,M.S., Daubert,T.E., Ind. Eng. Chem. Process Des. Dev., 17, 443(1978a); 17, 448(1978b); 18, 300(1979)

18 Grayson,H.G., Streed,C.W., Sixth World Petroleum Congress, Frankfurt am Main, VII, Paper 20-PD7, 233(1963)

19 Grove,N.H., Whitby,F.J., Woolmer,R.N., J. Appl. Chem., 10, 101(1960)

20 Hopke,S.W., Lin,C.J., Proc. Gas Processors Ass., 53rd Annual Convention, 1974, 63-74

21 Ipatieff,Jr.,V., Teodorovich,V.P., Levine,I.M.,The Oil and Gas J., 32, (20), 14(1933)

22 Jacoby,R.H.,Rzasa,M.J., Trans. AIME, 195, 99(1952)

23 Kay,W.B., Chem. Rev., 29, 501(1941)

24 King,M.B., Al-Najjar,H., Chem. Eng. Sci., 32, 1241(1977)

25 King,M.B., Kassim,K., Al-Najjar,H., Chem. Eng. Sci., 32, 1247(1977)

26 Lachowicz,S.K, Newitt,D.M., Weale,K.E., Trans. Faraday Soc., 51, 1198(1955)

27 Laugier,S., Richon,D., Renon,H., J. Chem. Eng. Data, 25, 274(1980)

28 Lee,B.I., Kesler, M.G., A.I.Ch.E.J., 21 , 510(1975)

29 Lin,H.M.,Ind. Eng. Chem. Process Des. Dev., 19, 501(1980)

30 Lin,H.M., Sebastian,H.M., Chao,K.C., Fluid Phase Equilibria, 4, 321(1980)

31 Lunin,G., Silva,A.E., Denis,J.M., Paper presented at at the 30th Canadian Chemical Engineering Conference, Oct. 1980, Edmonton, Alberta.

32 Lydersen,A.L., Eng. Experimental Station Report 3, University of Wisconsin, Madison, April, 1955

33 McCulloch,D.C.,Roeder,R.A., Hydrocarbon Processing, 55 (2), 81(1976)

34 Merrill,W.H., Logie,R.B., Denis.J.M., Research Report R-281, Dept. of Energy, Mines and Resources, Ottawa. Dec. 1973

35 Moreland,C., Can. J. Chem. Eng., 41, 24(1963)

36 Mulliken,C.A., Sandler,S.I., Ind. Eng. Chem. Process Des. Dev., 19, 709(1980)

37 Nandi,B.N., Belinko,K., Ciavaglia,L.A., Fuel, 58, 247(1979)

38 Nasir,P., Martin, R.J., Kobayashi,R., Fluid Phase Equilibria, 5, 279(1981)

39 Nichols,W.B., Reamer,H.H., Sage,B.H., A.I.Ch.E.J., 3, 262(1957)

40 Oliphant,J.L., Lin,H.M., Chao,K.C., Fluid Phase Equilibria, 3, 35(1979)

41 Peng,D.Y., Robinson,D.B., Ind. Eng. Chem. Fundam., 15, 59(1976)

42 Peng,D.Y., Robinson,D.B., Gas Processors Association Research Report RR-28, March 1978

43 Peng,D.Y., Robinson.D.B., GPA Peng-Robinson Programs, Gas Processors Association, Tulsa, Oklahoma.

44 Prather,J.W., Ahangar,A.M., Pitts,W.S., Henley,J.P., Tarrer,A.R., Guin,J.A., Ind. Eng. Chem. Process Des. Dev., 16, 267(1977)

45 Prausnitz,J.M., "Molecular Thermodynamics of Fluid Phase Equilibrium", Prentice - Hall, Englewood Cliffs, N.J., 1969

46 Prausnitz,J.M., Benson,P.R., A.I.Ch.E.J., 5, 161(1959)

47 Ranganathan,R., Patmore,D., Belinko, K.,Khulbe,C.P., Tscheng,J., Logie,R.B., Denis,J.M., Paper presented at the 63rd Canadian Chemical Conference, June 1980, Ottawa, Ontario

48 Reamer,H.H., Sage,B.H., Lacey,W.N., Ind. Eng. Chem., 45, 1805(1953), 45, 1810(1953)

49 Redlich,O., Kwong,J.N.S., Chem. Rev., 44, 233(1949)

50 Reid,R.C., Prausnitz,J.M., Sherwood,T.K., "The Properties of Gases and Liquids", 3rd Ed., McGraw - Hill, N.Y., 1977

51 Sagara,H., Arai,Y., Saita,S., J. of Chem. Eng. of Japan, 5, 339(1972)

52 Schaffer,P.S., Haller,H.S., Oil and Soap, 20, 161(1943)

53 Sebastian,H.M., Simnick,J.J., Lin,H.M., Chao,K.C., J. Chem. Eng. Data, 23, 305(1978a); 24, 149(1979)

54 Sebastian,H.M., Lin,H.M., Chao,K.C., A.I.Ch.E.J., 27, 138(1981)

55 Sebastian,H.M., Simnick,J.J., Lin,H.M., Chao,K.C., Can. J. Chem. Eng., 56, 743(1978b)

56 Sebastian,H.M., Yao,J., Lin,H.M., Chao,K.C., J. Chem. Eng. Data, 23, 167(1978c)

57 Sebastian, H.M., Nageshwar,G.D., Lin,H.M., Chao,K.C., Fluid Phase Equilibria, 4, 257(1980)

58 Selucky,M.L., Chu,Y., Ruo,T., Strausz,O.P., Fuel, 56, 369(1977); 57, 9(1978)

59 Sherwood,A.E., Prausnitz,J.M., A.I.Ch.E.J., 8, 519(1962)

60 Sim,W.J., Daubert,T.E., Ind. Eng. Chem. Process Des. Dev., 19, 386(1980)

61 Simnick,J.J., Lawson,C.C., Lin,H.M., Chao,K.C., A.I.Ch.E.J., 23, 469(1977)

62 Simnick,J.J., Liu,K.D., Lin,H.M., Chao,K.C., Ind. Eng. Chem. Process Des. Dev., 17, 204(1978a)

63 Simnick,J.J., Sebastian,H.M., Lin,H.M., Chao,K.C., J. Chem. Eng. Data, 23, 339(1978b); 24, 239(1979a)

64 Simnick,J.J., Sebastian,H.M., Lin,H.M., Chao,K.C., J. Chem. Thermodyn., 11, 331(1979b)

65 Simnick,J.J., Sebastian,H.M., Lin,H.M., Chao,K.C., Fluid Phase Equilibria, 3, 145(1979c)

66 Simon,R., Graue,D.J., Jour. Pet. Tech., 17, 102(1965)

67 Soave,G., Chem. Eng. Sci., 27, 1197(1972)

68 Strausz,O.P., Jha,K.N., Montgomery,D.S., Fuel, 56, 114(1977)

69 Tremper,K.K., Prausnitz,J.M., J. Chem. Eng. Data, 21, 295(1976)

70 Tsonopoulos,C., Prausnitz,J.M., Cryogenics, 9, 315(1969)

71 Wilson,G.M., Johnston,R.H., Hwang,S. - C., Tsonopoulos,C.,Ind. Eng. Chem. Process Des., Dev., 20, 94(1981)

72 Yao,J., Sebastian,H.M., Lin,H.M., Chao,K.C., Fluid Phase Equilibria, 1, 293(1977/1978)

73 Yarborough,L., J. Chem. Eng. Data, 17, 129(1972)

74 Zudkevitch,D., Joffe,J., A.I.Ch.E.J., 16, 112(1970)

8. Appendix I

TABLE 12

SOLUBILITY OF H_2 IN MESITYLENE

T (° C)	P (kPa)	S (g H_2/g Solvent) x10⁴
200	1668	2.74
	2082	3.33
	3358	5.00
	5702	9.90
	10632	17.73

TABLE 13

SOLUBILITY OF H_2 IN ATHABASCA BITUMEN (4-AB-77)

T (° C)	P (kPa)	S (g H_2/g Solvent) x10^4
200	783	0.574
	2024	1.28
	3127	1.93
	3955	2.59
	5334	3.30
	6127	3.86
	7506	4.78
	8884	5.26
	9195	4.98
	11607	6.94
	13883	9.18
	16710	10.81
	18779	10.90
	21158	12.43
	24845	15.17

TABLE 13 continued...

300	1187	1.31
	2024	2.17
	2852	2.41
	3954	3.80
	4402	3.97
	5815	4.94
	7539	6.20
	7953	7.29
	8469	7.77
	11470	10.08
	16710	13.92
	19295	16.93
	24018	20.75

TABLE 14

SOLUBILITY OF H_2 IN COLD LAKE BITUMEN (1-CL-77)

T (° C)	P (kPa)	S (g H_2/g Solvent) x10^4
200	1920	1.25
	2037	0.89
	2988	1.92
	5506	3.36
	8402	4.88
	13261	8.13
	14021	8.30
	17089	10.29
	20916	12.89
	23983	14.77
300	2300	2.06
	4367	4.28
	8505	8.04
	12849	12.76
	17468	16.73
	22776	18.80

TABLE 15

SOLUBILITY OF H_2 IN LLOYDMINSTER RESIDUE (3-LL-77)

T (° C)	P (kPa)	S (g H_2/g Solvent) x10⁴
200	2058	0.94
	3815	1.79
	7125	3.67
	10298	5.29
	14020	7.64
	17227	9.28
	21226	11.88
	24603	13.75
300	1440	0.92
	3196	2.89
	3417	1.77
	5354	3.60
	6919	4.90
	9746	7.67
	12086	8.99
	14778	10.81
	19295	15.60
	23052	18.88
	24259	17.64

TABLE 16

SOLUBILITY OF H_2 IN 650° F+ TOPPED ATHABASCA BITUMEN (2-AB-77)

T (° C)	P (kpa)	S (g H_2/g Solvent) x10⁴
200	3334	1.77
	8905	4.79
	15179	7.64
	19316	10.30
300	3610	3.40
	5808	4.74
	8878	6.62
	13980	11.48
	19757	15.08
370	4293	7.05
	6381	12.63
	7706	15.18
	11470	23.79
	13165	29.02

TABLE 17

SOLUBILITY OF H_2 IN 800° F+ TOPPED ATHABASCA BITUMEN (36-1)

T (° C)	P (kPa)	S (g H_2/g Solvent) x10⁴
200	3044	1.58
	10534	5.12
	16294	8.06
	22534	11.39
300	5594	3.12
	13074	7.59
	22034	12.41
370	4204	2.79
	11463	8.52
	18084	12.70
	22513	16.00

TABLE 18

SOLUBILITY OF H_2 IN 650° F+ TOPPED COLD LAKE BITUMEN (37-1)

T (° C)	P (kPa)	S (g H_2/g Solvent) x10⁴
200	5693	2.94
	10834	5.91
	18294	9.55
	22894	12.47
300	3504	2.53
	10493	8.06
	17154	13.11
	23192	18.37
370	3543	6.90
	5483	14.32
	8593	25.01
	11564	36.69

TABLE 19

SOLUBILITY OF H_2 IN 800° F+ TOPPED COLD LAKE BITUMEN (6-CL-77)

T (° C)	P (kPa)	S (g H_2/g Solvent) x10⁴
200	5084	3.26
	11663	6.40
	17444	9.61
	24744	13.81
300	5064	3.88
	11043	7.63
	15494	11.05
	23403	17.07

TABLE 20

SOLUBILITY OF H_2 IN 650° F+

LLOYDMINSTER RESIDUE (3-LL-78)

T (° C)	P (kPa)	S (g H_2/g Solvent) x10⁴
200	3596	2.39
	11697	7.50
	20191	12.63
300	1611	1.46
	4437	3.72
	9058	7.02
	15263	13.07
	20021	17.12

TABLE 21

SOLUBILITY OF H_2 IN 760° F+

LLOYDMINSTER RESIDUE (1-LL-78)

T (° C)	P (kPa)	S (g H_2/g Solvent) x10⁴
200	991	0.83
	2575	1.60
	2886	1.83
	5099	2.71
	5713	3.61

TABLE 22

SOLUBILITY OF H_2 IN AMOCO FEED (4-AM-78)

T (° C)	P (kPa)	S (g H_2/g Solvent) x10^4
200	5614	4.76
	11893	9.87
	17753	14.67
	23594	19.04
300	5744	6.61
	11194	12.79
	17394	20.00
	20594	22.31

TABLE 23

SOLUBILITY OF H_2 IN EMR GAS OIL

T (° C)	P (kPa)	S (g H_2/g Solvent) x10^4
200	3333	3.16
	7403	7.03
	9452	9.08
	12935	12.31
	18843	17.71
	21643	20.15
300	3694	4.60
	9844	12.60
	14293	17.56
	18814	24.52

TABLE 24

SOLUBILITY OF H_2 IN HEAVY ENDS (91-1-1)

T (° C)	P (kPa)	S (g H_2/g Solvent) x10^4
100	2733	1.54
	7033	3.74
	13743	7.27
	21453	10.77
200	3294	2.53
	10114	7.58
	17044	12.59
	23544	18.33
	23954	18.77
300	3974	3.87
	9744	9.92
	16864	16.68
	23264	22.92

TABLE 25

SOLUBILITY OF H_2 IN HEAVY ENDS (78-T-22)

T (° C)	P (kPa)	S (g H_2/g Solvent) x10⁴
370	3941	5.48
	8659	14.18
	11981	18.82
	12879	20.02
	18116	27.35

TABLE 26

SOLUBILITY OF H_2 IN HEAVY ENDS (78-T-23)

T (° C)	P (kPa)	S (g H_2/g Solvent) x10⁴
200	6114	4.35
	11694	8.12
	16914	11.33
	20594	13.90
300	5402	5.12
	11933	10.78
	18193	16.80
	23993	21.11

TABLE 27

SOLUBILITY OF H_2 IN HEAVY ENDS (78-T-24)

T (° C)	P (kPa)	S (g H_2/g Solvent) x10^4
200	4993	3.56
	12103	8.66
	18604	12.69
	24444	16.29
300	4484	4.60
	10134	9.61
	16134	15.43
	22534	21.14

TABLE 28

SOLUBILITY OF H_2 IN COAL-BITUMEN SLURRY

10 WT % SUB-BITUMINOUS COAL

90 WT % COLD LAKE BITUMEN (1-CL-77)

T (° C)	P (kPa)	S (g H_2/g Solvent) x10⁴
200	4243	2.32
	8599	5.11
	12944	7.88
	18894	11.49
	21844	14.40
	24344	15.88
300	4844	3.86
	8043	7.09
	8683	7.56
	14833	12.36
	20303	17.79
	23182	20.86

TABLE 29

SOLUBILITY OF H_2 IN COAL-BITUMEN SLURRY

40 WT % SUB-BITUMINOUS COAL

60 WT % COLD LAKE BITUMEN (1-CL-77)

T (° C)	P (kPa)	S (g H_2/g Solvent) x10⁴
200	4284	2.82
	6154	4.22
	8888	6.37
	10044	7.68
	13143	9.73
	17773	13.32
	20343	14.78
	22694	16.57
250	5233	1.80
	7445	3.45
	8972	4.86
	11263	7.26
	11553	8.20
	16594	12.12
	20524	16.03

TABLE 29 continued...

300	4494	0.603
	6844	0.995
	6695	1.14
	8393	2.41
	8543	2.35
	10134	3.31
	11404	4.75
	12292	5.88
	14242	8.71
	14452	8.79
	15843	11.12
	16144	12.28
	17623	13.67
	19044	16.79
	20513	17.63
	21993	20.01

TABLE 30

SOLUBILITY OF H_2 IN COAL-BITUMEN SLURRY

40 WT % LIGNITE COAL

60 WT % COLD LAKE BITUMEN (1-CL-77)

T (° C)	P (kPa)	S (g H_2/g Solvent) x10⁴
200	6342	2.74
	7993	6.12
	12473	9.04
	16982	12.40
250	4793	2.09
	5584	2.79
	9154	5.75
	13424	10.03
	15585	11.36
	20394	15.75
300	6473	0.739
	7544	1.11
	9553	3.80
	11615	6.11
	14015	8.44
	17593	13.66
	21043	17.27

TABLE 31

SOLUBILITY OF H_2 IN COAL-BITUMEN SLURRY

25 WT % SUB:BITUMINOUS COAL

75 WT % COLD LAKE BITUMEN (1-CL-77)

T (° C)	P (kPa)	S (g H_2/g Solvent) x10⁴
200	5543	3.17
	8844	5.66
	12043	7.88
	16283	10.92
	20492	13.70
300	4144	4.03
	7225	7.25
	10195	10.24
	11013	9.25
	16653	15.52
	20623	20.42

TABLE 32

SOLUBILITY OF H_2S IN ATHABASCA BITUMEN (4-AB-77)

T (° C)	P (kPa)	S (g H_2S/g Solvent) x10^3
200	390.4	2.65
	773.0	5.99
	1087.0	8.85
	1390.0	11.80
	1624.0	13.30
	2127.0	19.57
300	389.7	0.99
	404.7	1.83
	624.1	1.91
	659.0	2.52
	865.7	3.87
	862.4	4.38
	1010.0	4.08
	1238.0	6.35
	1300.0	6.93
	1452.0	7.88
	1652.0	7.48
	1745.0	8.52
	1824.0	10.55

TABLE 32 continued...

2061.0	11.10
2068.0	13.48
2368.0	11.26
2458.0	15.14
3357.0	21.70

TABLE 33

SOLUBILITY OF H_2S in HEAVY ENDS (78-T-24)

T (° C)	P (kPa)	S (g H_2S/g Solvent) x10^3
200	273.5	1.20
	482.1	2.93
	831.1	4.77
	1224.3	10.52
	1741.9	14.48
	2534.9	24.78
	3468.6	34.63
300	384.3	1.46
	551.7	1.46
	797.2	2.02
	1180.1	3.79
	1480.1	5.11
	1952.7	8.60
	2582.9	14.64

TABLE 34

SOLUBILITY OF H_2S IN EMR GAS OIL

T (° C)	P (kPa)	S (g H_2S/g Solvent) x10^2
100	393.4	0.823
	750.4	1.69
	768.4	1.67
	1273	2.74
	1613	4.33
200	425.3	0.241
	780.4	0.502
	1094	0.811
	1469	1.30
	1982	2.04
300	735.5	0.274
	946.9	0.363
	1400	0.755
	1718	1.10
	2136	1.54

TABLE 35

SOLUBILITY OF CO_2 IN ATHABASCA BITUMEN (4-AB-77)

T (° C)	P (kPa)	S (g CO_2/g Solvent) x10^2
50	1079	1.17
	1479	1.92
	2279	2.82
	2962	3.58
	3788	4.42
	4461	5.66
	5453	6.00
100	1535	1.16
	3037	2.28
	3810	2.88
	4568	3.58
	5471	4.90
300	1858	0.750
	2859	1.17
	4279	1.83
	5689	2.64
	6444	2.92

TABLE 36

SOLUBILITY OF CO_2 IN EMR GAS OIL

T (° C)	P (kPa)	S (g CO_2/g Solvent) x10^2
50	635.0	0.853
	707.2	1.14
	1589	2.70
	3011	5.30
	4362	8.42
	5637	12.46
100	845.6	0.843
	2221	2.47
	3693	4.42
	4831	5.76
	5596	6.97
150	755.9	0.512
	1604	1.22
	2399	1.98
	3540	2.89
	5084	5.22
	6188	6.90

9. Appendix II

TABLE 37

VAPOR - LIQUID EQUILIBRIUM DATA

FOR H_2 - BICYCLOHEXYL (56)

	Liq. Comp. of H_2			Equil. Const. of H_2		
P(kPa)	Exp	Mod SRK	GS	Exp	Mod SRK	GS
189° C(E_{HJ}=7.4(Mod SRK))						
2027	0.0181	0.0174	0.0201	54.4	56.6	48.9
3041	0.0262	0.0240	0.0257	37.7	38.1	32.9
5068	0.0443	0.0425	0.0496	22.4	20.2	23.4
10135	0.1158	0.1157	0.1389	8.61	8.62	7.18
20270	0.1418	0.1473	0.1786	7.03	6.77	5.59
25338	0.1718	0.1761	0.2153	5.81	5.67	4.64
348° C(E_{HJ}=21.4(Mod SRK))						
2027	0.0211	0.0227	0.0230	29.0	26.0	25.6
3041	0.0382	0.0393	0.0404	19.16	18.17	17.61
5068	0.0686	0.0644	0.0691	12.09	11.60	10.95
10135	0.1398	0.1399	0.1559	6.48	6.45	5.77
15203	0.1975	0.1986	0.2327	4.71	4.69	4.00
20270	0.2578	0.2490	0.3056	3.66	3.79	3.11
25338	0.3112	0.2929	0.3752	3.06	3.26	2.57

TABLE 38

VAPOR - LIQUID EQUILIBRIUM DATA

FOR H_2 - BICYCLOHEXYL (56)

	Liq. Comp. of H_2			Equil. Const. of H_2		
P(kPa)	Exp	PR	Mod PR	Exp	PR	Mod PR
189° C(δ_{ij}=-1.4(PR), E_{Hj}=3.5(Mod PR))						
2027	0.0181	0.0172	0.0172	54.4	57.2	57.3
3041	0.0262	0.0257	0.0257	37.7	38.5	38.5
5068	0.0442	0.0420	0.0421	22.4	23.6	23.6
10135	0.0810	0.0804	0.0808	12.29	12.38	12.32
15203	0.1158	0.1153	0.1162	8.61	8.65	8.58
20270	0.1418	0.1470	0.1488	7.03	6.78	6.70
25338	0.1718	0.1762	0.1788	5.81	5.66	5.58
348° C(δ_{ij}=-1.4(PR), E_{Hj}=11.0(Mod PR))						
2027	0.0211	0.0207	0.0221	29.0	28.9	26.7
3041	0.0382	0.0356	0.0383	19.16	20.3	18.67
5068	0.0688	0.0635	0.0691	12.09	13.07	11.86
10135	0.1398	0.1240	0.1382	6.48	7.38	6.52
15203	0.1975	0.1740	0.1978	4.71	5.42	4.70
20270	0.2578	0.2159	0.2499	3.66	4.44	3.77
25338	0.3112	0.2517	0.2959	3.06	3.84	3.21

TABLE 39

VAPOR - LIQUID EQUILIBRIUM DATA

FOR H_2 - TETRALIN (61)

	Liq. Comp. of H_2			Equil. Const. of H_2		
P(kPa)	Exp	PR	Mod PR	Exp	PR	Mod PR
169.6° C (δ_{ij}=-0.6(PR), E_{Hj}=4.6(Mod PR))						
2027	0.0118	0.0119	0.0117	81.8	81.0	82.4
3041	0.0176	0.0179	0.0176	55.4	54.5	55.3
5068	0.0297	0.0296	0.0292	33.1	33.3	33.7
10135	0.0571	0.0570	0.0567	17.33	17.40	17.48
15203	0.0823	0.0822	0.0823	12.06	12.09	12.07
20270	0.1051	0.1055	0.1062	9.46	9.44	9.37
25338	0.1289	0.1270	0.1285	7.72	7.85	7.74
348.6° C (δ_{ij}=-0.6(PR), E_{Hj}=13.8(Mod PR))						
5068	0.0452	0.0487	0.0452	15.63	14.66	15.40
10135	0.0925	0.1019	0.0975	9.02	8.36	8.53
15203	0.1390	0.1467	0.1436	6.35	6.14	6.12
20270	0.1884	0.1849	0.1847	4.80	5.00	4.89
25338	0.2314	0.2179	0.2216	3.96	4.31	4.14

TABLE 40

VAPOR - LIQUID EQUILIBRIUM DATA

FOR H_2 - TETRALIN (61)

	Liq. Comp. of H_2			Equil. Const. of H_2		
P(kPa)	Exp	Mod SRK	GS	Exp	Mod SRK	GS
169.6° C(E_{Hj}=7.98(Mod SRK))						
2027	0.0118	0.0118	0.0145	81.8	81.9	66.7
3041	0.0176	0.0177	0.0218	55.4	55.1	44.8
5068	0.0297	0.0292	0.0362	33.1	33.7	27.2
10135	0.0571	0.0564	0.0705	17.33	17.59	14.05
15203	0.0823	0.0813	0.1027	12.06	12.23	9.68
20270	0.1051	0.1042	0.1326	9.46	9.55	7.50
25338	0.1289	0.1254	0.1605	7.72	7.94	6.21
348.6° C (E_{Hj}=22.4(Mod SRK))						
5068	0.0452	0.0465	0.0524	15.63	14.97	13.21
10135	0.0925	0.0991	0.1176	9.02	8.41	6.83
15203	0.1390	0.1446	0.1800	6.35	6.10	4.86
20270	0.1884	0.1841	0.2403	4.80	4.92	3.76
25338	0.2314	0.2188	0.2988	3.96	4.21	3.09

TABLE 41

VAPOR - LIQUID EQUILIBRIUM DATA FOR

H_2 - ATHABASCA BITUMEN (4-AB-77)

	Liq. Comp. of H_2		Equil. Const of H_2	
P(kPa)	Exp	Mod PR	Exp	Mod PR
------	---	------	---	------
		200° C (E_{Hj}=-8.6)		
2024	0.0307	0.0302	32.6	33.1
5334	0.0757	0.0755	13.21	13.24
11607	0.1468	0.1497	6.81	6.68
16710	0.2111	0.2010	4.74	4.98
21158	0.2356	0.2405	4.24	4.16
24845	0.2734	0.2701	3.66	3.70
		300° C (E_{Hj}=-19.9)		
2852	0.0564	0.0597	17.73	16.73
4402	0.0896	0.0889	11.16	11.25
7953	0.1531	0.1484	6.53	6.74
11470	0.2000	0.1993	5.00	5.02
16710	0.2566	0.2638	3.90	3.79
24018	0.3398	0.3369	2.94	2.97

TABLE 42

VAPOR - LIQUID EQUILIBRIUM DATA

FOR H_2 - EMR GAS OIL

	Liq. Comp. of H_2		Equil. Const of H_2	
P(kPa)	Exp.	Mod PR	Exp.	Mod PR
200° C (E_{HJ}=-3.2)				
3333	0.0377	0.0378	26.5	26.4
7403	0.0802	0.0801	12.47	12.47
9452	0.1012	0.0999	9.88	10.00
12935	0.1325	0.1316	7.55	7.59
18843	0.1801	0.1803	5.55	5.54
21643	0.1999	0.2014	5.00	4.96
300° C (E_{HJ}=0.1)				
3694	0.0540	0.0543	18.52	18.04
9844	0.1351	0.1340	7.40	7.40
14293	0.1788	0.1837	5.59	5.41
18814	0.2332	0.2286	4.29	4.35

TABLE 43

VAPOR - LIQUID EQUILIBRIUM DATA

CO_2 - TETRALIN (57)

	Liq. Comp. of CO_2		Equil. Const. of CO_2	
P(kPa)	Exp	PR	Exp	PR
189° C ($\delta_{i,j}$=0.14)				
2047	0.0555	0.0556	17.30	17.21
3085	0.0823	0.0836	11.79	11.57
4095	0.1095	0.1100	8.90	8.84
5128	0.1370	0.1364	7.13	7.15
270° C ($\delta_{i,j}$=0.14)				
2017	0.0429	0.0421	18.47	18.45
3055	0.0673	0.0679	12.64	12.36
4095	0.0931	0.0933	9.44	9.32
5098	0.1149	0.1172	7.77	7.56
350° C ($\delta_{i,j}$=0.19)				
1999	0.0229	0.0212	15.22	14.97
3069	0.0492	0.0494	10.61	10.21
4105	0.0764	0.0762	8.00	7.82
5057	0.1018	0.1009	6.49	6.43

TABLE 43 Continued...

392° C ($\delta_{i,j}$=0.26)

3118	0.0340	0.0338	7.85	7.30
4145	0.1174	0.1168	5.93	5.75
5108	0.0902	0.0932	4.99	4.79

TABLE 44

VAPOR - LIQUID EQUILIBRIUM DATA

FOR CO_2 - ATHABASCA BITUMEN

	Liq. Comp. of CO_2		Equil. Const. of CO_2	
P(kPa)	Exp	PR	Exp	PR
------	---	--	---	-
		50° C ($\delta_{i,j}$=0.09)		
1079	0.1174	0.1138	8.52	8.79
2279	0.2427	0.2256	4.12	4.43
2962	0.2892	0.2828	3.46	3.54
3788	0.3343	0.3461	2.99	2.89
4461	0.3914	0.3932	2.48	2.54
5453	0.4054	0.4556	2.47	2.20
		100° C ($\delta_{i,j}$=0.07)		
1535	0.1165	0.1093	8.58	9.15
3037	0.2058	0.2039	4.86	4.91
3810	0.2466	0.2481	4.06	4.03
4568	0.2892	0.2887	3.46	3.46
5471	0.3577	0.3339	2.80	3.00

TABLE 44 Continued...

300° C ($\delta_{i,j}$=-0.04)

1858	0.0785	0.0787	12.73	12.70
2859	0.1174	0.1185	8.52	8.43
4279	0.1722	0.1721	5.81	5.81
5689	0.2308	0.2222	4.61	4.50
6444	0.2491	0.2479	4.14	4.03

TABLE 45

VAPOR - LIQUID EQUILIBRIUM FOR

CO_2 - EMR GAS OIL

	Liq. Comp. of CO_2		Equil. Const. of CO_2	
P(kPa)	Exp	PR	Exp	PR
------	---	--	---	--
		50° C ($\delta_{i,j}$=0.13)		
635.0	0.0497	0.0540	20.1	18.53
707.2	0.0608	0.0599	16.44	16.68
1589	0.1329	0.1297	7.52	7.71
3011	0.2315	0.2313	4.32	4.32
4362	0.3237	0.3163	3.09	3.16
5637	0.4146	0.3865	2.41	2.59
		100° C ($\delta_{i,j}$=0.12)		
845.6	0.0456	0.0488	21.7	20.5
2221	0.1226	0.1225	8.07	8.16
3693	0.1986	0.1942	4.97	5.10
4831	0.2445	0.2448	4.07	4.08
5596	0.2808	0.2767	3.54	3.61

TABLE 45 Continued...

150° C ($\delta_{i,j}$=0.13)

755.9	0.0282	0.0326	35.2	30.7
1604	0.0649	0.0676	15.35	14.78
2399	0.1005	0.0991	9.82	10.08
3540	0.1400	0.1422	7.10	7.03
5084	0.2271	0.1966	4.36	5.09
6188	0.2790	0.2329	3.47	4.29

TABLE 46

VAPOR - LIQUID EQUILIBRIUM DATA FOR

H_2S - ATHABASCA BITUMEN (4-AB-77)

	Liq. Comp. of H_2S		Equil. Const. of H_2S	
P(kPa)	Exp	PR	Exp	PR
------	---	--	---	--
		200° C ($\delta_{i,j}$=-0.05)		
585.7	0.0556	0.0585	17.99	17.10
822.9	0.0811	0.0815	12.33	12.27
1049	0.1053	0.1031	9.50	9.70
1263	0.1282	0.1230	7.80	8.13
1746	0.1807	0.1667	5.53	6.00
2155	0.2273	0.2029	4.40	4.93
		300° C ($\delta_{i,j}$=-0.055)		
429.9	0.0286	0.0302	35.0	33.1
828.8	0.0556	0.0575	17.99	17.38
1202	0.0811	0.0825	12.33	12.11
1551	0.1053	0.1054	9.50	9.48
1874	0.1282	0.1262	7.80	7.92
2571	0.1807	0.1696	5.53	5.89
3109	0.2273	0.2020	4.40	4.95

TABLE 47

VAPOR - LIQUID EQUILIBRIUM DATA

FOR H_2S - EMR GAS OIL

	Liq. Comp. of H_2S		Equil. Const. of H_2S	
P(kPa)	Exp	PR	Exp	PR
100° C ($\delta_{i,j}$=0.05)				
393.4	0.0572	0.0579	17.27	17.48
750.4	0.1101	0.1086	9.21	9.08
768.4	0.1090	0.1111	9.00	9.17
1273	0.1678	0.1800	5.55	5.96
1613	0.2414	0.2247	4.45	4.14
200° C ($\delta_{i,j}$=0.18)				
425.2	0.0174	0.0233	44.5	57.5
780.4	0.0356	0.0406	24.5	28.1
1094	0.0563	0.0566	17.60	17.76
1469	0.0869	0.0753	11.51	13.23
1982	0.1304	0.1004	7.67	9.93
300° C ($\delta_{i,j}$=0.18)				
946.9	0.0260	0.0399	38.5	23.1
1397	0.0526	0.0597	19.01	15.79
1718	0.0748	0.0736	13.37	12.92
2136	0.1016	0.0915	9.84	10.48

10. Appendix III

TABLE 48

Hempel Distillation of Athabasca Topped Bitumen (2-AB-77)

Fraction	Cut ° C	Vol %	Sum %	Sp. Gravity 15/15° C
1	50			
2	75			
3	100			
4	125			
5	150			
6	175	0.3	0.3	0.824
7	200	0.4	0.7	0.824
8	225	0.6	1.3	0.824
9	250	1.2	2.5	0.838
10	275	6.2	8.7	0.868
Distillation at 40 mm Hg				
11	200	1.7	10.4	0.881
12	225	1.1	11.5	0.902
13	250	3.9	15.4	0.927
14	275	7.5	22.9	0.940
15	300	12.2	35.1	1.058
Residuum		64.6	99.7	1.058
Loss		0.3		

Initial Boiling Point 152° C

TABLE 49

Hempel Distillation of Lloydminster Residue (3-LL-78)

Fraction	Cut ° C	Vol %	Sum %	Sp. Gravity 15/15° C
1	50			
2	75			
3	100			
4	125			
5	150			
6	175			
7	200			
8	225	0.3	0.3	-
9	250	1.2	1.5	-
	275	3.0	4.5	-
Distillation at 40 mm Hg				
11	200	1.2	5.7	-
12	225	3.9	9.6	-
13	250	6.3	15.9	-
14	275	5.7	21.6	-
15	300	9.2	30.8	-
Residuum %		69.3	100.1	
Gain		0.1		

Initiial Boiling Point 218° C

TABLE 50

Hempel Distillation of Amoco Feed

Fraction	Cut ° C	Vol %	Sum %	Sp. Gravity 15/15° C
1	50			
2	75			
3	100			
4	125			
5	150			
6	175			
7	200	3.3	3.3	0.800
8	225	8.0	11.3	0.820
9	250	9.9	21.2	0.843
10	275	10.4	31.6	0.859
Distillation at 40 mm Hg				
11	200	7.7	39.3	0.874
12	225	7.2	46.5	0.889
13	250	3.9	50.4	0.912
14	275	3.7	54.1	0.935
15	300	6.5	60.6	0.964
Residuum %		38.1	98.7	
Loss		1.3		

Initial Boiling Point 176° C